MICROSTRUCTURES IN AROMATIC POLYIMIDES STUDIED WITH INTERMOLECULAR CHARGE-TRANSFER FLUORESCENCE

（分子間電荷移動螢光による芳香族ポリイミドのミクロ構造の研究）

Masatoshi Hasegawa

MICROSTRUCTURES IN AROMATIC POLYIMIDES STUDIED WITH INTERMOLECULAR CHARGE-TRANSFER FLUORESCENCE

Thesis submitted to The University of Tokyo
for the degree of Doctor of Engineering

Masatoshi Hasegawa

(December 1990)

CONTENTS

GENERAL INTRODUCTION

About 30 years ago, aromatic polyimides (PIs) were invented during a heated space race between U.S.S.R and U.S.A. In Japan at present, they are mainly used as an electric insulator by taking advantage of excellent thermal stability. Recently, many investigators are interesting in photo and electron beam resists[1,2] and low dielectric constant[3] in PIs. A large number of data for chemical and physical heat resistances, mechanical properties, and kinetics of polycondensation and thermal imidization of polyimide precursors have been accumulated to obtain aerospace materials by several research groups.[4-6] Although the overall studies on PIs in Japan is inferior to those of U.S.A. and U.S.S.R., several researchers in Japan studied the relationship between chemical structures and expansion coefficients[7] and the improvement of thermal stability by modifying chemical structure of PIs.[8]

As known well, since aromatic polyimides are generally infusible and insoluble to common organic solvents, they are synthesized by thermal or chemical cyclodehydration of soluble prepolymer, poly(amic acid)(PAA).[4-6] Manufacturing of PAAs such as uni[9,10] or biaxial stretching[11] makes possible to control physical properties of PIs because most of rigid aromatic PIs are brittle so that it is difficult to stretch such PI films. Therefore it is very important to know not only physical properties of final PIs but also those of PAAs and imidization process. At present, there are important problems for PAAs. The first is about non-equilibrium nature in final PIs which changes due to the condition of thermal imidization of PAAs.[12] The second is the influence of amide exchange reaction between PAAs in solution[13,14] and during thermal imidization.[15] The third is about the miscibility[16,17] of a PAA with other PAA (characterization and theory) although it remains insolved even in simpler systems such as vinyl polymers,[18] and the last is the problem on liquid crystalline (LC) PAAs.[19]

However PIs prepared from PAAs have a limit that a block of PI can not be formed by molding because residual solvents (e.g., DMAc) connected by hydrogen bonding[20] with PAA and water generated by imidization remain in the system. Thermoplastic PIs such as LARC-TPI and ULTEM are allowed to produce PI blocks by compression molding of PI powders.[21] Therefore the studies on PAAs become important only in film state less than 100 μ m thick.

One of the problems in fully cured PIs is concerned with intra and intermolecular charge-transfer complex (CTC).[22,23] It is necessary to explore the CTC in PIs for the mechanisms of photoconductivity.[24] Several

workers dealing with aromatic PIs accept that color of PIs is due to either intra or intermolecular CTC or both.[25-27] Also if intermolecular CTC presents in PIs, it may play a role as a physical crosslinking points.[28]

It appears that solution of the problems mentioned above for PAAs and PIs is closely related to the control of molecular aggregation of final PIs. Then the author's concern was first focused to the characterization of molecular aggregation of PIs. Although for the studies on the molecular aggregation of PIs wide-angle x-ray diffraction (WAXD)[29-32] has been so far used, it may be not so suitable to PIs because the most of PIs prepared from isotropic PAA are amorphous. Small-angle x-ray scattering (SAXS)[33-35] which can observe middle-range order is rather suitable than WAXD. The presence of the LC like ordered structure was observed by SAXS.[33]

In principle, photoluminescence and photoreactive probe method, which has been mainly developed in the fields of biochemistry, are suitable to observe microstructures in solid polymers. Several photo-probes were used for observation of molecular motions of polymer chains and microstructures including molecular packing, short-range order, polymer-polymer miscibility and free volume distribution in solid polymers.[36,37] For examples, twisted intramolecular CT (TICT)[38] and molecular rotor[39,40] are sensitive to local viscosity and the dimension of free volume in a surrounding medium. Hydrophobic probes such as DNS and TNS is useful for detection of the change in hydrophobicity.[41] Since energy transfer systems such as naphthalene-anthracene provide information on the distance between different probes, it can be used to evaluate the miscibility of polymer blends.[42] So excimer probes such as dipyrenyl propane are sensitive to local viscosity,[43] they are used for monitoring the bulk polymerization and crosslinking reaction (for example, in epoxy resins). Molecular motions of polymer chains with long relaxation time can be examined using phosphorescence probes such as benzophenone,[44] which is used as a photoreactive probe.[45] Free volume distribution is studied using photoisomerization in photochromic molecules such as azo compounds.[46] The cure process in epoxy resins are monitored by using as a hardner a fluorescent azo compound.[47] These probes are called as "external probe". The works using "internal" probes (intrinsic chromophores in polymer units) on molecular aggregation in solid polymers are not many. For examples, molecular aggregation of polystyrene (PS),[48] Poly(ethylene-2,6-naphthalenedicarboxylate) (2,6-PEN),[49] poly(p-xylylene) (PPX),[50] poly(ethylene terephthalate) (PET),[51] thermotropic LC poly(ethylene terephthalate-co-hydoxybenzoate)(X-7G)[52] and polymer-polymer miscibility of blends of poly(vinyl naphthalene) (PVNp) with other vinyl polymers was

examined.[83] Although internal probe method can not be applied to various polymer materials unlike external probe method, it has several advantages as follows. First, there is no deterioration due to introduction of external probes and no apprehension that the environment surrounding an external probe may be different from that of neat polymers. Second, unexpected aggregation and evaporation as for free probes are avoidable, and third, it is especially useful when suitable external probe can not be nominated due to the intrinsic strong electronic absorption. However only one disadvantage in the internal probe method is that luminescences from an aimed polymer have to be assigned and characterized before use, which requires a great effort. Electronic conjugation between chromophores in polymer chains makes it difficult. Accordingly, the application of the method has significant meaning when the aimed polymers are of high performance as in the case of aromatic PIs for example.

The purposes of this thesis is to assign and characterize the luminescence of aromatic PIs first and then to apply it to the examination of molecular aggregation of PIs.

In chapter 1, the natures of fluorescence in PIs and the characterization of higher-order structure by using the fluorescence are discussed. In section 1.1 fluorescences in a series of aromatic PIs are assigned and the effects of heat treatment and uniaxial orientation on PI's luminescence are studied. In section 1.2 emission mechanism and the intermolecular interaction in PI are discussed from absorption and emission spectra. Excitation energy transfer behavior is closely related to the increase in the fluorescence intensity.

In chapter 2 reactions of PAAs in solution and solid state are discussed. The intrinsic photoluminescence in a PI is used for monitoring of molecular packing during isothermal imidization in section 2.1. The relation between reaction rates and chain rigidity increasing during the reaction, and non-equilibrium state are discussed. In section 2.2 the presence of amide exchange reaction in PAA solution is elucidated. This study was carried out to support the result in chapter 3 where physical blends of PIs are concerned with.

In chapter 3 the miscibility of rigid PI/PI blends is evaluated with the intrinsic luminescence of a PI. This method is compared with common techniques for the evaluation of miscibility, and the availability of fluorescence technique is discussed.

This work was carried out as a graduate-course study at Research Center for Advanced Science and Technology of the University of Tokyo.

References

1. "Photoreactive Polymers" (Ed. Reiser), Wiley Interscience, N.Y. (1989).
2. "Photopolymer Technology" (Ed. GT.Nagamatsu and T.Yamaoka) Nikkan Kogyo, Japan, (1988).
3. T.Kikuchi, T.Saito and H.Sato, Chemisrty (in Japanease), 45, 411 (1990).
4. "Polyimides" (Ed. K.L.Mittal), Vol 1,2, Plenum Press, N.Y. (1984).
5. "Polyimides" (Ed. M.I.Bessonov, M.M.Koton, V.V.Kuryavtsev and L.A.Laius), Plenum Press, N.Y. (1987).
6. "Polyimides: Materials, Chemistry and Characterization" (Ed. C.Feger, M.M.Khojasteh and J.E.McGrath, Elsevier, p.379 (1989).
7. S.Numata, K.Fujisaki and N.Kinjyo, Polymer, 28, 2282 (1987).
8. "High Performance Aromatic Polymer Materials" (Ed. Y.Imai et al.) Maruzen, (1990).
9. M.Kochi, T.Uruji, T.Iizuka, I.Mita and R.Yokota, J.Polym.Sci., C, 25, 441 (1987).
10. T.Yonezawa, I.Mita, M.Kochi and R.Yokota, Polym.Pre.Jpn., 39, 2412(1990).
11. G.Elsner, J.Appl.Polym.Sci., 34, 815 (1987).
12. M.Hasegawa, H.Arai, I.Mita and R.Yokota, Polym.J., 22, 875 (1990).
13. M.Ree, D.Y.Yoon and W.Volksen, ACS spring Conf., Polym.Mat. and Sci.Eng., 60, 179 (1989).
14. M.Hasegawa, Y.Shindo, T.Sugimura, R.Yokota, K.Horie and I.Mita, J.Polym.Sci., A, submitted.
15. M.I.Tsapovetsky and L.A.Laius, in "Polyimides: Materials, Chemistry and Characterization" (Ed. C.Feger, M.M.Khojasteh and J.E.McGrath, Elsevier, p.379 (1989).
16. R.Yokota, R.Horiuchi, M.Kochi, H.Soma and I.Mita, J.Polym.Sci., C, 26, 215 (1988).
17. M.Hasegawa, M.Kochi, I.Mita and R.Yokota, Polymer, in press.
18. "Polymer Blends" (in Japanease, Ed.S.Akiyama, T.Inoue and T.Nishi), CMC Press, Japan (1981).
19. W.T.Whang and S.C.Wu, J.Polym.Sci., A, 26, 2749 (1988).
20. M.-J.Brekner and C.Feger, J.Polym.Sci., A, 25, 2479 (1987).
21. "New Heat Resistant Polymers"(in Japanease, Ed. I.Mita), Sogo Gijutsu Center, Japan, (1987).
22. E.D.Wachsman and C.W.Frank, Polymer, 29, 1191 (1988).
23. M.Hasegawa, M.Kochi, I.Mita and R.Yokota, Eur.Polym.J., 25, 349 (1989).
24. K.Iida, M.Waki, S.Nakamura, M.Ieda and G.Sawa, Jpn.J.Appl.Phys., 23, 1573 (1984).
25. B.V.Kotov, T.G.Gordina, V.S.Voishchev, O.V.Kolninov and

A.V.Pravednikov, Polym.Sci.U.S.S.R., 19, 711 (1977).
26. H.Ishida, S.T.Wellinghoff, E.Baer and J.L.Koenig, Macromolecules, 13, 826 (1980).
27. M.Hasegawa, T.Yamashita, K.Horie, Q.Jin, M.Kochi, I.Mita and R.Yokota, in preparation.
28. M.Fryd, in "Polyimides" (Ed. K.L.Mittal), Vol 1, Plenum Press, N.Y. p.377 (1984).
29. N.Takahashi, D.Y.Yoon and W.Parrish, Macromolecules, 17, 2583 (1984).
30. T.P.Russel, H.Gugger and J.D.Swalen, J.Polym.Sci., Phys.Ed., 21, 1745 (1983).
31. L.G.Kazaryan, D.Ya.Tsvankin, B.M.Ginzburg, Sh.Tuichiev, L.N.Korzhavin and S.Ya.Frenkel, Polym.Sci.U.S.S.R., 14, 1344 (1972).
32. G.Conte, L.D'Illario, N.N.Pavel and E.J.Giglio, J.Polym.Sci., Phys.Ed., 14, 1553 (1976).
33. S.Isoda, H.Shimada, M.Kochi and H.Kambe, J.Polym.Sci., Phys.Ed., 22, 1979 (1984).
34. T.P.Russel, J.Polym.Sci., Phys.Ed., 22, 1105 (1984).
35. T.P.Russel and H.R.Brown, J.Polym.Sci., B, 25, 1129 (1987).
36. "Photophysical and Photochemical Tools in Polymer Science (Ed. M.A.Winnik), Reidel, Dordrecht, The Netherlands (1986).
37. H.Itagaki, K.Horie and I.Mita, Prog.Polym.Sci., 15, 361 (1990).
38. R.Hayashi, S.Tazuke and C.W.Frank, Macromolecules, 20, 983 (1987).
39. K.Y.Law and R.O.Loutfy, Polymer, 24, 439 (1983).
40. E.F.Meyer, A.M.Jamieson, R.Shimha, J.H.M.Palmen, H.C.Booij and F.H.J.Maurer, Polymer, 31, 243 (1990).
41. K.Horie, I.Mita, J.Kawabata, S.Nakahama, A.Hirao, N.Yamazaki, Polym.J., 12, 319 (1980).
42. F.Mikes, H.Morawetz and K.S.Dennis, Macromolecules, 17, 60 (1984).
43. F.W.Wang, R.E.Lowry and B.M.Fancoli, Polymer, 27, 1529 (1986).
44. H.Rutherford and I.Soutar, J.Polym.Sci., Phys.Ed., 15, 2213 (1977).
45. K.Horie, H.Ando and I.Mita, Macromolecules, 20, 54 (1987).
46. T.Naito, Doctoral thesis, The University of Tokyo (1991).
47. C.S.P.Sung, I-J.Chin, W-C.Yu, Macromolecules, 18, 1510 (1985).
48. M.Matsumoto, N.Nakamura M.Kochi and I.Mita, Polym.Prepr.Jpn., 34, 1065 (1985).
49. M.Kochi, M.Matsumoto, K.Horie and I.Mita, ibid, 34, 2353 (1985).
50. M.Kochi, K.Oguro and I.Mita, Eur.Polym.J., 24, 917 (1988).
51. M.Hennecke and J.Fuhrmann, Macromol.Chem., Macromol.Symp., 5, 181(1986).
52. H.Hasimoto, M.Hasegawa, T.Yamashita and K.Horie, LCP Conf., p.86 (1990).
53. W.C.Tao, J.W.Thomas and C.W.Frank, Polymer, 29, 1625 (1988).

CHAPTER 1

MOLECULAR AGGREGATION AND FLUORESCENCE SPECTRA OF AROMATIC POLYIMIDES.

1.1 Molecular Aggregation of Aromatic Polyimides Studied with Intermolecular Charge-Transfer Fluorescence.

INTRODUCTION

A large number of data for the thermal, mechanical and electrical properties of aromatic PIs have been accumulated by many research groups for the past 20 years.[1-3] Their excellent physical properties are correlated with not only the rigidity of the main chains but also strong intermolecular interaction caused by the stacking of aromatic rings. The PI films having excellent mechanical properties were prepared by the molecular orientation and sufficient heat treatment.[4,5]

Although the microscopic structures in PIs have been so far observed by using WAXD[6-9] and SAXS[10-12], these method are limited to elucidation of crystalline structure and middle range-ordered structure, respectively. Fluorescence spectroscopy is known to be very useful in the investigation of the microstructures and molecular aggregation in common solid polymers.[13.-16] Since strong absorption of PIs in the range from u.v. to vis makes difficult to introduce an external probe, the intrinsic emissions of PIs were examined.

The objective of this section is to assign the emissions of aromatic PIs and to examine the relation between the aggregation structures and the fluorescence spectra from the changes in the emission and excitation spectra of PIs by heat treatment and orientation.

EXPERIMENTAL

Pyromellitic dianhydride(PMDA), benzophenonetetracarboxylic dianhydride(BTDA), biphenyltetracarboxylic dianhydride (BPDA), p-phenylenediamine(PDA) and 4,4'-oxydianiline(ODA) were recrystallized from

dioxane, acetic anhydride, ethyl acetate, and methanol-tetrahydrofran mixture, respectively, and then vacuum dried. The precursors of PIs, poly(amic acid)s (PAAs), were prepared by adding a stoichiometric amount of dianhydride powder to the N,N-dimethylacetamide (DMAc) solution of diamine with continuous stirring in a nitrogen atmosphere.[17] DMAc used was first dried with molecular sieves(4A) and then distilled. A viscous yellow PAA solution (10 wt%) was obtained after several hours. PAA(BPDA/PDA) composed of biphenyltetracarboxylic dianhydride (BPDA) and PDA and PAA(BPDA/ODA) composed of BPDA and ODA were supplied by Ube Industries Ltd.

The weight-average molecular weight ($\bar{M}_w$) of PAAs was determined by light-scattering method.

PAA films were prepared by casting onto a glass plate, followed by drying at 60 ℃ in vacuum for 24 h. Imidization of PAA films was carried out thermally at determined temperatures in a vacuum oven to obtain 30-50 μ m thick films.

The emission and excitation spectra, and u.v.-vis absorption spectra of PIs were measured at room temperature using a fluorescence spectrophotometer (Hitachi, model 850) and a u.v.-vis spectrophotometer (Jasco, model UVIDEC-660), respectively. The excitation and emission spectra were recorded without the correction for incident lamp intensity and the sensitivity of detector at each wavelength, respectively. The samples were excited at various wavelengths in a front-face arrangement to minimize self-absorption. The bandpasses are 5 nm for both the excitation and emission monochromators, respectively. The progress of thermal imidization was observed using an i.r.spectrophotometer (Jasco, model IR-G). The degree of molecular packing of PI(BTDA/ODA) was estimated by differential scanning calorimetry (DSC) (Du Pont, model 990).

RESULTS AND DISCUSSION

The assignment of the emission spectra for PI films

The emission spectra of several commercial PI films and their chemical structures are shown in Figure 1.1-1. There are four characteristic features in these spectra. First, the emission peaks appear in a considerably longer wavelength region than those of common aromatic molecules. Second, they are broad and structureless. Third, the emission intensities as a whole are very weak. There is a clear tendency that the emissions are weaker for longer wavelengths as shown in Figure 1.1-2, although the intensities depend somewhat on thermal history. Fourth, it seems that with increasing

electron-withdrawing ability of imide moiety and the electron-donating ability of diamine moiety which are estimated from the chemical structures of their moieties the emission spectra become red-shifted. These characteristics suggest that a series of spectra are due to CT interaction. In order to examine the fitness of the emission behavior to CT theory,[18-20] a series of PIs were prepared as shown in Figure 1.1-3. Figure 1.1-4 (a) and (b) shows the emission spectra of the PIs imidized at 150 ℃ for 1h, 200 ℃ for 1h, and 250 ℃ for 2h stepwise (step 250 ℃) for two systems in which the diamine components were fixed to PDA and ODA.

The following relationship is anticipated in the case of a weak CTC with a fixed electron donor.

$$h \nu_{CT} = - E_a + C$$

where h, ν_{CT} and E_a is Planck's constant, the peak wavenumber of the CT absorption band and the electron affinity of electron acceptor. C is a constant for a series of the components used. Figure 1.1-5 shows the plot of E_a of dianhydrides corresponding to imide moieties vs the wavenumber of the emission peak in Figure 1.1-4 (a) and (b). The values of E_a in the literature were used.[1] It is reasonable to use the E_a values of dianhydrides instead of those of imide moieties because there is little difference between them for the ability as acceptor[21] The linearity of the plots for two system (PDA and ODA) indicates that these emission spectra generated by 350 nm excitation are attributed to weak CTC.

The fluorescence spectra and the change in molecular aggregation by annealing

If the observed emissions of aromatic PIs is due to intermolecular CTC, the emissions should be sensitive to the molecular aggregation. The effects of annealing on the emission and excitation spectra of PI(BPDA/PDA) were studied. In Figure 1.1-6, the emission and excitation spectra of PI(BPDA/PDA) imidized at step 250 ℃ (dashed lines) shows a broad band with a peak at 525 nm when excited at 350 nm. The intensity of this band increases by annealing at 330 ℃ for 2 h without large shift of peak wavelength. It is to be noted that a new band peaking at 465 nm in the excitation spectrum appears due to the same annealing. The excitation at 465 nm provides an emission spectrum peaking at about 540 nm where a mirror image is observed between the excitation and emission spectra. The new emission is slightly sharper than the band generated by 350 nm excitation. Since the same annealing makes Debye ring related to intermolecular order in WAXD pattern somewhat

sharp[20], the appearance of new excitation bands and the enhancement of the emission intensity by the annealing are due to the increase in the degree of molecular packing. From the response of the emissions by the annealing, it is clear that both emissions is due to not intra but intermolecular CTCs. The difference of the position and band width in two emissions of PI(BPDA/PDA) may reflect the presence of two kinds of intermolecular CTCs with different steric structures. The author name for convenience the emission due to 350 nm excitation and that due to 465 nm excitation as CT_1 and CT_2, respectively. The same effect of annealing was also observed for PI(BPDA/ODA) having a flexible ether linkage in the main chain.

Figure 1.1-7 shows plots similar to Figure 1.1-5 for CT_1 and CT_2 in PI(BPDA/PDA), showing that the curve for CT_2 deviates from linearity unlike the case of CT_1. The result suggests that CT_2 trends to be stronger CTC than CT_1.

The appearance of CT_2 due to the annealing is also observed in the visible absorption spectrum. Figure 1.1-8 shows the absorption and difference spectra between the annealed and not annealed samples for PI(BPDA/PDA)(35 μ m thick). A new band in the difference spectrum corresponding to the excitation spectrum shows clearly that CT_2 is a ground state complex.

The degree of molecular packing in PI solids can be changed not only by heat treatment of PIs but also by varying the initial imidization temperature T_i. The chain mobility of partially imidized PAA during heating process is related to the molecular aggregation of final PI. Table 1.1-1 shows that both the density and T_g of PI(BPDA/PDA) and PI(BPDA/ODA) increase with increasing T_i. Fig. 1.1-9 (a) and (b) illustrates the relationship between the emission intensity and density for PI(BPDA/PDA) and PI(BPDA/ODA) imidized under the conditions listed in Table 1.1-1.[22] The linearity in the plots means that the concentration of CT sites is closely related to the degree of packing. The increase in the emission intensity for PI(BPDA/PDA) is faster than for PI(BPDA/ODA), and the increase in the density of PI(BPDA/PDA) is also larger than that of PI(BPDA/ODA) for the same imidization condition. This behavior is consistent with the fact that the PIs having more rigid chain trend to have a higher packing coefficient.[23]

Another example of the effect of T_i is given for Kapton-type PI, PI(PMDA/ODA). According to the analysis with SAXS,[10] it was suggested that PI(PMDA/ODA) has a two-phase structure composed of ordered and less-ordered phases. As for PI(BPDA/PDA) and PI(BPDA/ODA), the emission intensity of PI(PMDA/ODA)(ca. 50 μ m), although it is very weak, increases markedly with increasing T_i as shown in Fig. 1.1-10, indicating that the intermolecular CTC are more easily formed at higher T_i. More recently,

Wachsman and Frank[24] showed that the emission intensity for PI(PMDA/ODA) increases with increasing cure temperature. In Fig 1.1-10, the decrease in the emission intensity for the PI imidized at 430 ℃ for 2 h may be due to the formation of some quenchers. Since the correlation between the volume fraction of the ordered phase (ϕ_o) determined by SAXS and the emission intensity could be found, it appears that the CT structure exists mainly in the ordered phase although there is no clear evidence. A small red shift in the emission peaks is observed in this PI with increasing T_i. This behavior is interpreted as the formation of the more stabilized structure of the CTC due to high temperature curing although the possibility of multilayered structure[25] between CTCs can not be excluded.

The third example of effect of T_i is given for PI(BTDA/ODA). Figure 1.1-11(a) shows DSC curves of the PI prepared under several conditions. In the thermogram (a), the endotherm at 220 ℃, the exothermic peak at about 260 ℃, and the endothermic peak at about 425 ℃ are considered to be due to T_g, pre-crystallization and melting, respectively. With increasing cure temperature, the exotherm of pre-crystallization is reduced, and T_g increases gradually up to about 260 ℃. The exothermic peak disappears completely by annealing at 300 ℃ for 2 h. It is interesting that, in spite of little difference in the exothermic peak area between thermogram (a) and (b), the emission intensity for condition (b) in Figure 1.1-11(b) is larger than for (a). Moreover although the PI cured under the condition (d) is more densely packed and more extensively crystallized compared with the case of condition (c), the change in the emission spectrum is not so large. These results indicate that the increase in the intensity is not related to the crystalline fraction, but that CTC is formed in the amorphous region.

The effects of molecular orientation on the emission and excitation spectra

Kochi et al. reported that PI(BPDA/PDA) can be transformed to high-strength, high-modulus film by thermal imidization of cold drawn PAA[4]. In these drawn samples, uniaxial orientation proceeds during thermal imidization. Figure 1.1-12 demonstrates the effect of the molecular orientation (draw ratio(DR) of PAA; 53.6%) on the emission and excitation spectra. The emission intensity (350 nm excitation) for the isotropic PI increases by a factor of two due to orientation without remarkable change in the excitation spectrum. Additional annealing at 330 ℃ for 2 h causes a marked change in the excitation spectrum, and CT_2 emission appears.

In Fig. 1.1-13, the CT_1 emission intensity (350 nm excitation) increases linearly with DR, for PI(BPDA/PDA) both without and with annealing at 330 ℃ for 2 h (curve 2 and 4, respectively). This phenomenon corresponds to the

fact that PI(BPDA/PDA) is easy to pack densely. The CT_2 emission intensity normalized with respect to film thickness decreases with DR on the contrary. The result suggests that the formation of CT_2 which is more compact than CT_1 is sterically suppressed due to uniaxial orientation of main chains. The presence of two different CTCs in PI(BPDA/PDA) is supported from the result in which the emission intensities of CT_1 and CT_2 show quite different behavior with respect to DR. For the case of flexible PI(BPDA/ODA), the emission intensity (350 nm excitation) is independent of DR. This corresponds to the fact that the molecular packing of PI(BPDA/ODA) is loose compared with that of PI(BPDA/PDA).

CONCLUSION

The emission spectra of PIs with different chemical structures were first measured in detail. The emission spectrum of PI is due to intermolecular CT interaction. Remarkable changes in the CT emission and excitation spectra for PI(BPDA/PDA) and PI(BPDA/ODA) are caused by annealing. This is attributed to the change in the degree of molecular aggregation. For PI(BPDA/PDA), with increasing DR of PAA before imidization, the emission intensity of CT_1 increases but that of CT_2 decreases. It was suggested that two kinds of CT structures exist in PI(BPDA/PDA) solid and that CT_2 is well-packed complex compared with CT_1.

The intermolecular CT emission is useful to examine the short-range structures and the molecular packing of aromatic PIs.

REFERENCES

1. "Polyimides" Vol.1,2, (Edited by K.L.Mittal), Plenum Press, N.Y.(1984).
2. "Polyimides"(Edited by M.I.Bessonov, M.M.Koton, V.V.Kudryavtsev and L.A.Laius), Plenum Press, N.Y.(1987).
3. "Polyimides"(Edited by C.Feger, M.M.Khojasteh and J.E.McGrath) Elsevier, (1989).
4. M.Kochi, T.Uruji, T.Iizuka, I.Mita and R.Yokota, J.Polym.Sci.:Part C, 25, 441 (1987).
5. R.Yokota, R.Horiuch, M.Kochi, H.Soma and I.Mita, J.Polym.Sci.:Part C, 26, 215 (1988).
6. T.Takahashi, D.Y.Yoon and W.Parrish, Macromolecules, 17, 2583 (1984).
7. T.P.Russel, H.Gugger and J.D.Swalen J.Polym.Sci.:Phys.Ed., 21,1745 (1983).
8. L.G.Kazaryan, D.Ya.Tsvankin, B.M.Ginzburg, Sh.Tuichiev, L.N.Korzhavin and S.Ya.Frenkel, Polym.Sci.U.S.S.R., 14, 1344 (1972).
9. G.Conte, L.D'Illario, N.N.Pavel and E.J.Gigrio, J.Polym.Sci.:Phys.Ed., 14, 1553 (1976).
10. M.Kochi, H.Shimada and H.Kambe, J.Polym.Sci.:Phys.Edn., 22, 1979 (1984).
11. T.P.Ressel, J.Polym.Sci.:Phys.Edn., 22, 1105 (1984).
12. T.P.Ressel and H.R.Brown, J.Polym.Sci.:Part B, 25, 1129 (1987).
13. "Photophysical and Photochemical Tools in Polymer Science"(Edited by M.A.Winnik), Reidel, Dordecht, The Netherlands (1986).
14. K.Horie and I.Mita, Adv.Polym.Sci., 88, 77 (1989).
15. H.Itagaki and K.Horie, Prog.Polym.Sci., 15, 361 (1990).
16. H.Ushiki and K.Horie, "Handbook of Polymer Science and Technology", Vol 4, (Edited by N.P.Cheremisinoff), Marcel Dekker, Inc., (1989).
17. R.A.Dine-Hart and W.W.Wright, J.Appl.Polym.Sci., 11, 609 (1967).
18. R.S.Mulliken and W.B.Person, 'Molecular Complexes', Wiley-Interscience, N.Y.(1969).
19. R.S.Mulliken, J.Am.Chem.Soc., 74, 811 (1952).
20. R.S.Mulliken, J.Phys.Chem., 56, 801 (1952).
21. M.Chowdhury, J.Phys.Chem., 66, 353 (1962).
22. M.Kochi, T.Horigome, I.Mita and R.Yokota, Proc.2nd Int'l.Conf. on Polyimides, Ellenville (1985), Proceedings, p454.
23. S.Mumata, F.Fujisaki and N.Kinjo, Polymer, 28, 2282 (1987).
24. E.D.Wachsman and C.W.Frank, Polymer, 29, 1191 (1988).
25. T.Otsubo, S.Mizogami, I.Otsubo, Z.Tozuka, A.Sakagami, Y.Sakata and S.Misumi, Bull.Chem.Soc.Jpn., 46, 3519 (1973).

Table 1.1-1 The densities and T_gs of PI(BPDA/PDA) and PI(BPDA/ODA) imidized under various conditions.

*measured by dynamic mechanical loss.

Initial imidization	PI (BPDA/PDA)		PI (BPDA/ODA)	
	Density (g/cm^3)	T_g* (°)	Density (g/cm^3)	T_g* (°)
150°, 2 hr; 200° 5 hr	1.4194	282	1.3619	—
270°, 2 hr	1.4465	328	1.3828	294
300°, 2 hr	1.4608	349	1.3869	303
329°, 2 hr	1.4655	350	1.3884	306

*Measured by dynamic mechanical loss.

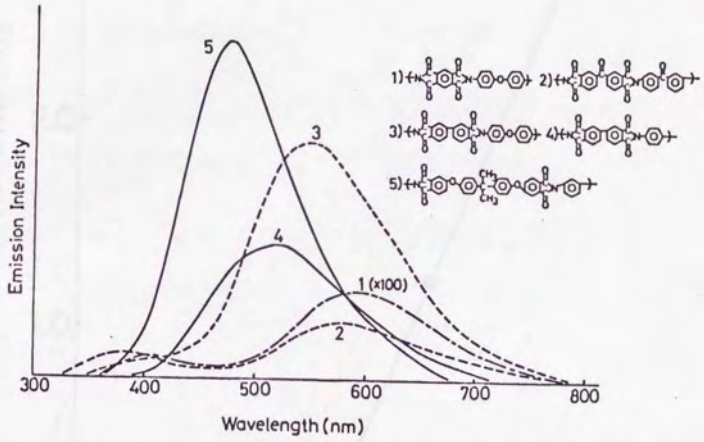

Figure 1.1-1 The fluorescence spectra (300 nm excitation) for several commercial polyimide films and the chemical structures.

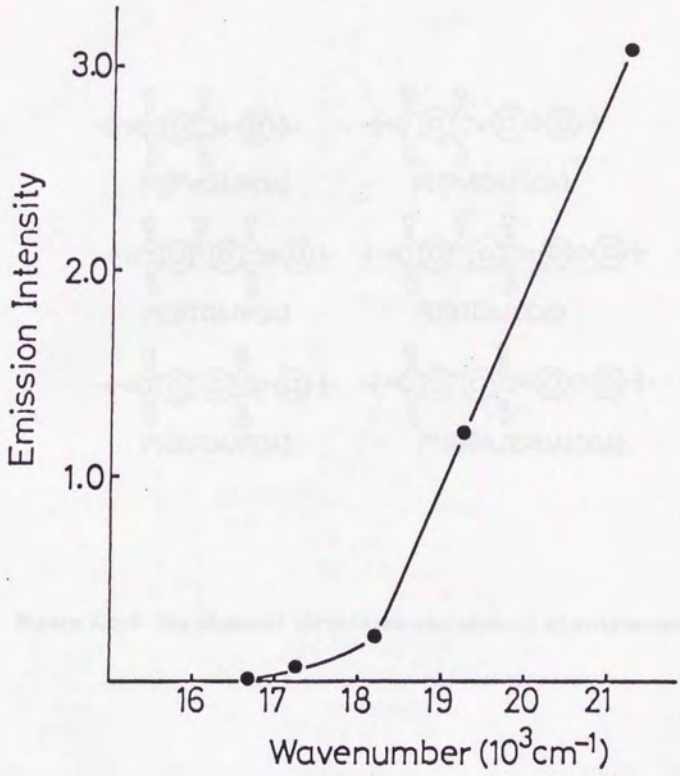

Figure 1.1-2 The relationship between the wavenumber at emission peak and the emission intensity.

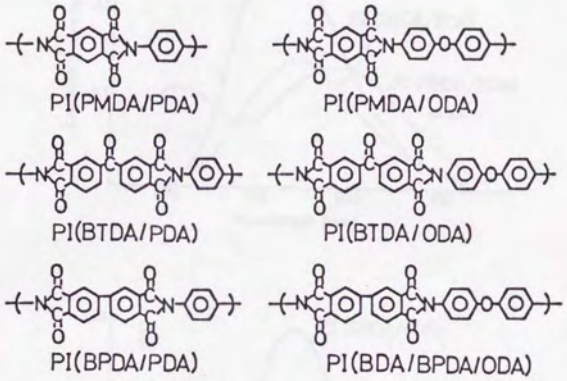

Figure 1.1-3 The chemical structures and symbols of polyimides.

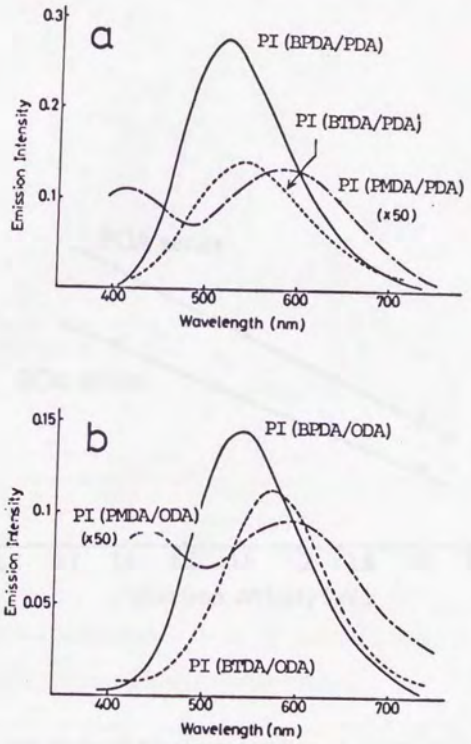

Figure 1.1-4 The fluorescence spectra (350 nm excitation) for PI films containing p-phenylenediamine (a) and oxydianiline (b).

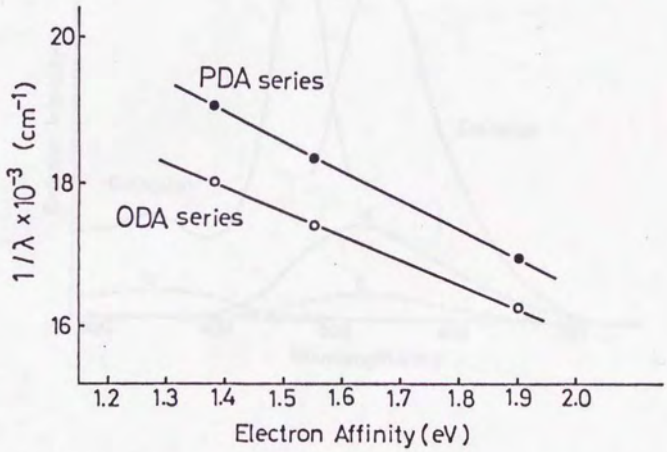

Figure 1.1-5 The plots of electron affinity of dianhydride component vs wavenumber at emission peak.

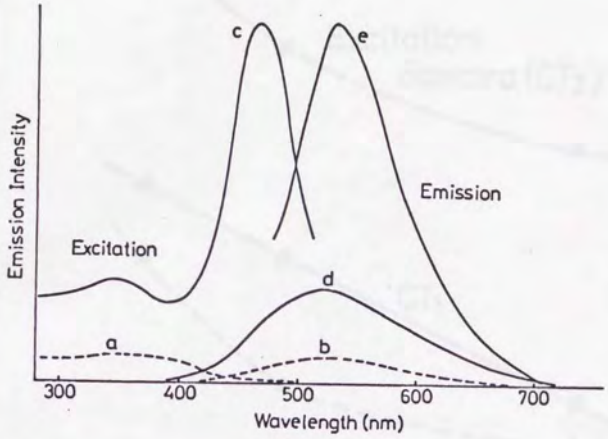

Figure 1.1-6 Effects of annealing at 330 ℃ for 2 h on the fluorescence and excitation spectra of PI(BPDA/PDA).

The excitation(a) and emission spectra(350 nm excitation(b) of the PI without annealing.

The excitation(c) and emission spectra(350 nm excitation)(c) and (465 nm excitation)(e) of the annealed PI.

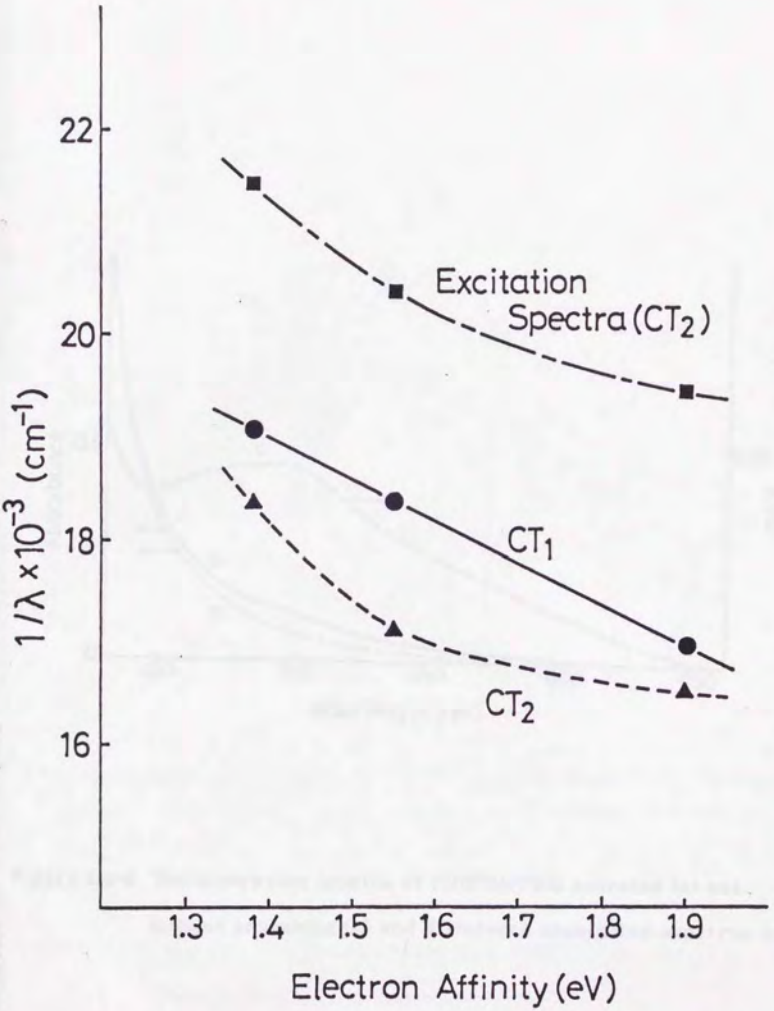

Figure 1.1-7 The plots of electron affinity of dianhydride component vs wavenumber at excitation peak of CT_2 and emission peak of CT_1 and CT_2 for PI containing PDA.

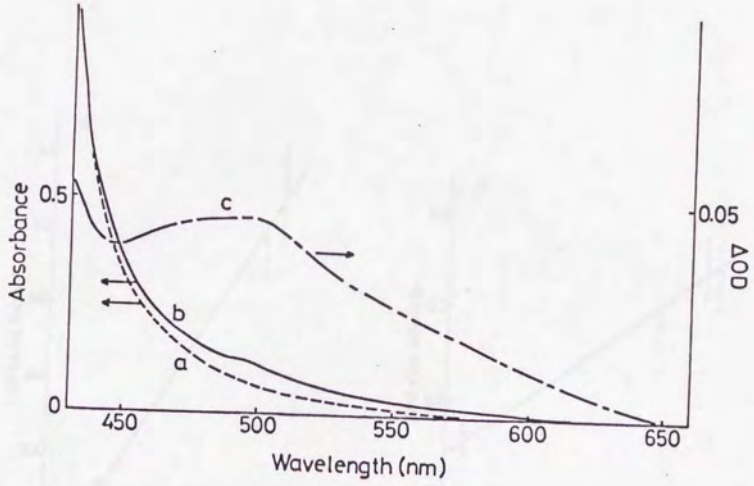

Figure 1.1-8 The absorption spectra of PI(BPDA/PDA) annealed (a) and without anneaking (b) and difference absorption spectrum (c).

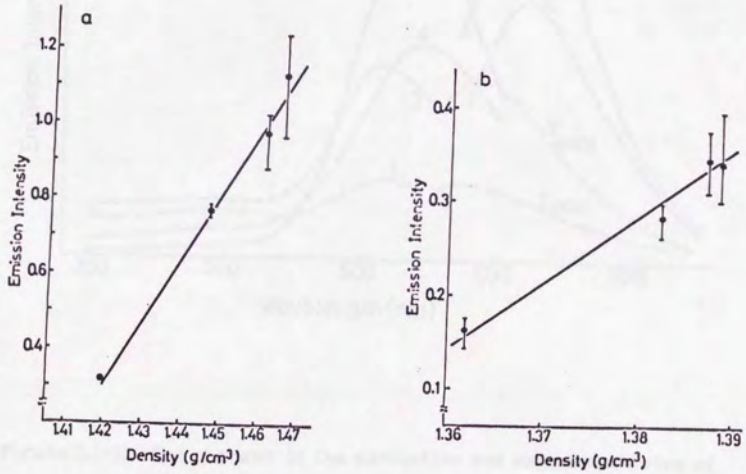

Figure 1.1-9 The emission intensity (350 nm excitation) vs density of PI(BPDA/PDA)(a) and PI(BPDA/ODA)(b).

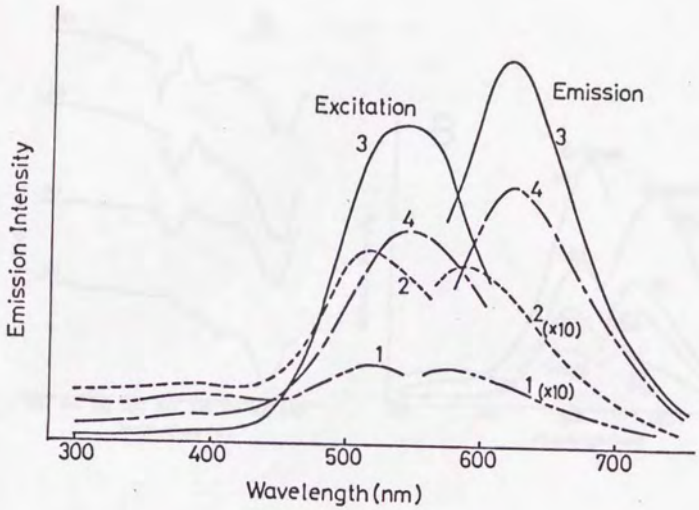

Figure 1.1-10 The changes in the excitation and emission spectra of PI(PMDA/ODA) with the increase in imidization temperature. (1) 90 ℃ 3.5 h, 150 ℃ 8 h, 190 ℃ 4 h, 240 ℃ 5 h stepwise. (2) 250 ℃ 12 h (3) 350 ℃ 12 h (4) 430 ℃ 2 h

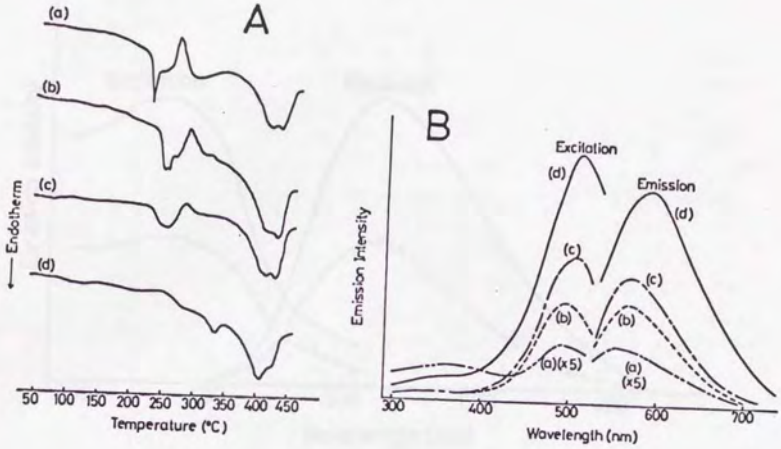

Figure 1.1-11(A) DSC thermograms of PI(BTDA/ODA) with different cure temperature.

(B) The changes in the excitation and emission spectra of PI(BTDA/ODA) with the increase in cure temperature.

(a) 110 ℃ 1 h, 140 ℃ 1 h, 170 ℃ 24 h stepwise.

(b) (a)+210 ℃ 7 h (c) (a)+225 ℃ 2 h (d) (a)+300 ℃ 2 h

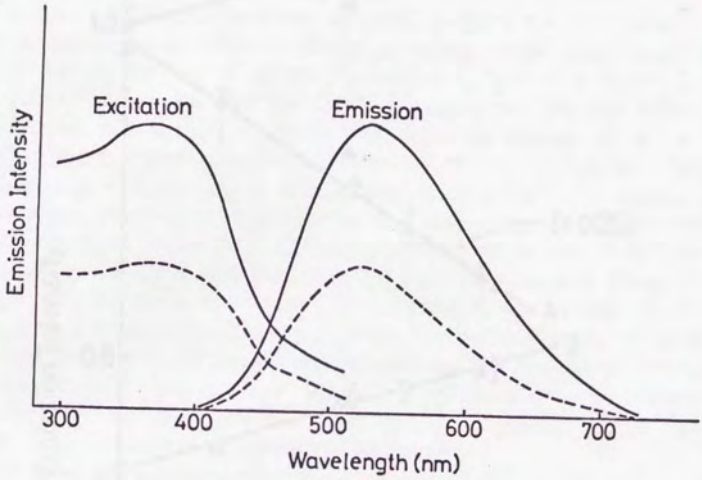

Figure 1.1-12 The effects of molecular orientation on the excitation and fluorescence spectra of PI(BPDA/PDA). solid line; DR=54%, broken line; DR=0%.

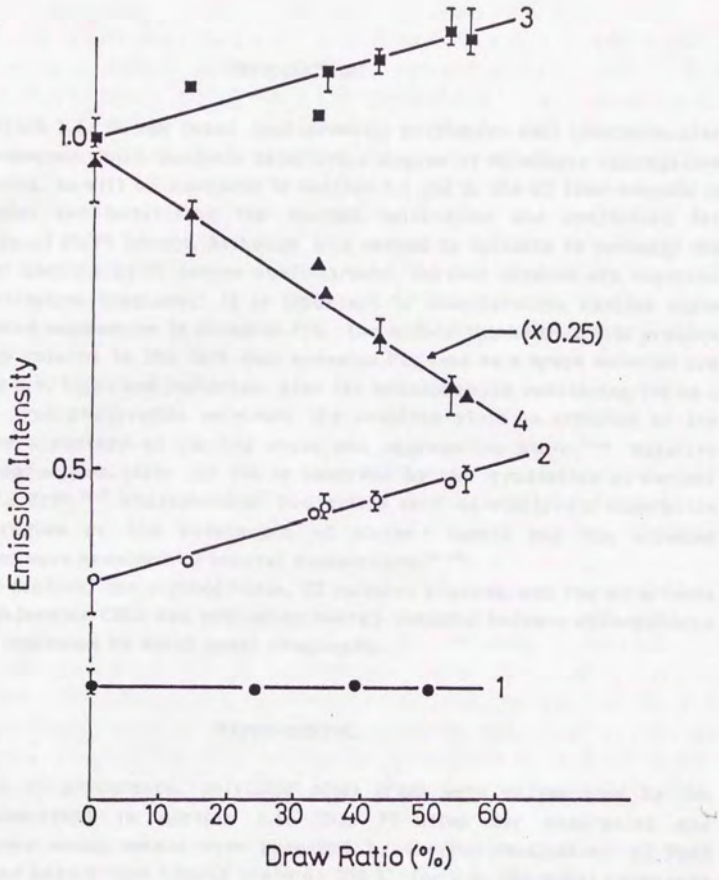

Figure 1.1-13 Relationships between the emission intensity and DR for PAAs.

(1) PI(BPDA/ODA) without annealing (350 nm excitation)

(2) PI(BPDA/PDA) without annealing (350 nm excitation)

(3) PI(BPDA/PDA) with annealing (350 nm excitation)

(4) PI(BPDA/PDA) with annealing (465 nm excitation)

1.2 Electronic Spectra of the model compounds of Polyimide and Excitation Energy Transfer in Solid Polyimide.

INTRODUCTION

In section 1.1, It was found that aromatic polyimides emit intermolecular CT fluorescence which reflects sensitively degree of molecular aggregation of PI chains. As will be discussed in section 2.1 and 3, the CT fluorescence is also useful for monitoring the thermal imidization and evaluation for miscibility of PI/PI blends. Although this method is suitable to estimate the molecular packing of PI chains qualitatively, further studies are required for quantitative treatment. It is important to elucidate the excited state and emission mechanisms in aromatic PIs. The author thinks that this problem is closely related to the fact that aromatic PIs used as a space material are stable to u.v. light and radiation. Also for benzophenone containing PIs as a negative type photoresist material, the reaction yield is affected by the electronic structure at excited state and aggregation state.[1-4] Ablative Photodecomposition (APD) for PIs is observed by the irradiation of excimer laser(e.g., KrF).[5-7] Photophysical properties such as electronic absorption in the region of the wavelength of excimer lasers and the emission mechanisms were examined by several researchers.[8-10]

In this section, the excited state, CT emission process, and the structures of intermolecular CTCs and excitation energy transfer between chromophores in PI are discussed by using model compounds.

EXPERIMENTAL

Several PI precursors, poly(amic acid) (PAA) were polymerized by the method described in section 1.1. Thin PI films for absorption and fluorescence measurements were prepared by thermal imidization of PAAs spin-coated onto a thin quartz plate at 250 ℃ for 2 h. The model compounds of PI(BPDA/PDA)(PI consisting of biphenyltetracarboxylic dianhydride (BPDA) and p-phenylenediamine (PDA)) were synthesized by thermal imidization of the corresponding amic acids formed by condensation between amine and anhydride in DMAc solution, followed by recrystallization and vacuum drying.

The following abbreviations are used; aniline (AN), p-phenylenediamine

(PDA), cyclohexylamine (CHA), methylenedicyclohexylamine (MDCA), methylenedianiline (MDA), 2,6-diethylaniline (DEAN), biphenyltetracarboxylic dianhydride (BPDA), phthalic anhydride (PA), succinic anhydride (SA). The symbols of polyimides and model compounds are represented by PI(X/Y) and M(X/Y), respectively where PI and M are polyimide and model compound, and X and Y are di or monoanhydride and di or monoamine of components. The chemical structures of samples used and symbols are summarized in Figure 1.2-1.

The fluorescence and u.v.-vis absorption spectra were measured at room temperature in air using a fluorescence spectrophotometer (Hitachi, model 850) and a u.v.-vis spectrophotometer (Jasco, model UVIDEC-660). Spectroscopic grade-solvents were used for measurements of electronic spectra. The phosphorescence of model compound was measured in degassed and rigid solution at 77 K in a cryostat (oxford). The molar extinction coefficients (ε) at each wavelength for PI(BPDA/PDA) thin film on a quartz plate were determined on the basis of ε at 350 nm obtained by separate experiment where film thickness and density and absorbance were measured.

The excitation and fluorescence spectra were corrected for wavelength-dependent intensity of lamp and for wavelength-dependent sensitivity in detectors respectively, using Rhodamine B standard solution (Wako Pure Chemical) for 200-600 nm and ethylene glycol solution of methylene blue for 600-720 nm. Absorbances of the samples used are about 0.1.

The fluorescence quantum yield (ϕ_f) of PI(BPDA/PDA) film is estimated by using the degassed benzene solution of perylene as a standard (ϕ_f=0.89).[11] Perylene used was recrystallized three times from toluene (m.p.=270 ℃). The ϕ_f of perylene dispersed in poly(methyl methacrylate) (PMMA) matrix polymerized with AIBN in air at 50-70 ℃ in a square quartz cell was determined to be 0.81 in a side-face arrangement by using toluene solution of perylene. Finally the ϕ_f of PI film is determined in a front-face arrangement with the perylene doped PMMA film prepared by solution cast, assuming that the ϕ_f of perylene in as-cast PMMA is 0.81.

The fluorescence decay (350 nm excitation) was measured using a hand-made apparatus in Tazuke laboratory of Tokyo Institute of Technology.

RESULTS AND DISCUSSION

Electronic Spectra of PI(BPDA/PDA) and Model Compounds

In this section, PI(BPDA/PDA) which has rigid main chain and is emissive is

focused. Figure 1.2-2 (a)-(d) shows the absorption spectra of PI(BPDA/PDA) thin film on a quartz plate and model compounds in hexafluoro-2-propanol (HFP). M(BPDA/AN) is insoluble to common organic solvents except for dichloroacetic acid and HFP. In (a), PI(BPDA/PDA) has broad and structureless band from 400 to 250 nm and a shoulder at 350 nm. In (b), both M(SA/AN) and M(SA/PDA) have no absorption longer than 280 nm. Therefore, PDA moieties are not excited by 350 nm light used for the characterization of the molecular packing. In (c) the comparison of M(BPDA/CHA) and M(PA/CHA) shows that biphenyl bond in M(BPDA/CHA) contributes to conjugation because the intensity of absorption for M(BPDA/CHA) is stronger than two times intensity for M(PA/CHA) and has a long wavelength tail. The presence of the conjugation indicates that the torsional angle around biphenyl bond is smaller than 90 degree.[12] As shown in (d), both M(PA/PDA) and M((PA/AN) have little absorption at 350 nm and the intensity of absorption for M(PA/PDA) is equivalent to two times intensity for M(PA/AN). Furthermore, there is little difference between the absorption spectrum of M(PA/CHA) in (c) and that of M(PA/AN) in (d) for both the shape and intensity. These results show that the conjugation between phthalimide ring and benzene ring in amine moiety is very small. From the data obtained by other investigator in which n, π^* transition in N,N-dimethylaniline (DAN) is disturbed by the torsion of the bond around dimethylamino and phenyl groups,[13,14] it is suggested that the phenyl groups on nitrogen freely rotate. In (d), M(BPDA/AN) has a spectrum similar to M(BPDA/CHA), indicating that in M(BPDA/AN) N-substitute benzene contributes only slightly to conjugation or intramolecular CT at ground state between the benzene and biphenyl diimide moieties as well as in the case of M(PA/AN) and M(PA/PDA). Accordingly these results led to the conclusion that 350 nm light is mainly absorbed biphenyl diimide moieties. Ishida et al.[15] examined the absorption spectra of M(PMDA/CHA), M(PMDA/AN) and M(PMDA/ADE)(ADE :4-aminodiphenylether) and assigned 310-330 nm band for M(PMDA/CHA) to π, π^* due to benzimide and n, π^* transitions due to imide carbonyl group at about 340 nm. The bands at 300-320 nm for samples, M(BPDA/AN) and M(BPDA/CHA), may be due to π, π^* transition, judging from the magnitude of ε (for n, π^* transition the value of ε is generally less than several hundreds). The difference for spectral shape between PI(BPDA/PDA) and M(BPDA/AN) is considered to be due to the difference of molecular aggregation or medium.

Figure 1.2-3 shows excitation and fluorescence spectra for M(BPDA/CHA) and M(PA/CHA) in HFP solution. Other model compounds used are non-fluorescent. Comparatively strong fluorescence peaking at 430 nm for M(BPDA/CHA) is observed in HFA solution but is neither observed for

PI(BPDA/PDA) nor for M(BPDA/AN). Non-fluorescent nature in M(BPDA/AN) is considered to be due to effective deactivation via intramolecular charge-transfer (D^+A^- state) at excited state between N-substituted benzene and biphenyl diimide, even if there is only slight intramolecular CT interaction between them at ground state. The author infers that D^+A^- state is formed via coplanar conformation between benzimide and phenyl group on nitrogen because coplanar state is desirable conformation to the intramolecular CT interaction. Then fluorescence measurement for M(BPDA/DEAN) for which it is impossible to make the coplanar conformation owing to steric hindrance due to ortho-alkyl groups was carried out in three solvents (benzene, dichloromethane and HFP). It is expected for M(BPDA/DEAN) that intramolecular fluorescence due to some conjugation between benzimide and phenyl group, or fluorescence similar to that of M(BPDA/CHA)(when the angle of nitrogen-phenyl bond is equal to 90 degree) is observed. In Figure 1.2-4 the fluorescence intensity decreases with the increase in solvent polarity with gradual red shift. These fluorescences are clearly different with that of M(BPDA/AN). The absorption peaks (320 nm) are practically independent of solvent polarity. The result strongly supports the above-described consideration about the emission and deactivation mechanisms in M(BPDA/AN). Such intramolecular fluorescence is not observed for PI(BPDA/PDA) film. This suggests that the conformation around nitrogen-phenyl bonds in solid PI(BPDA/PDA) has the coplanar state so that the fluorescence of both biphenyldiimide units and phenyl-substituted biphenyldiimide units are quenched via intramolecular charge-transfer.

The phosphorescence measurement is also carried out for M(BPDA/CHA). The M(BPDA/CHA) in degassed toluene at 77 K shows phosphorescence around 550 nm and structured fluorescence at 380 nm (the fluorescence red-shifts up to 430 nm in HFP owing to the solvent effects) as shown in Figure 1.2-5. The phosphorescence of another imide compound, N,N-dimethylpyromellitimide, in dioxane was reported in the literature (phosphorescence lifetime τ_p=0.45 s).[16] The excitation and fluorescence spectra at 77 K show clear vibrational structures compared to those in fluid solution at room temperature. The τ_p is 2-3 s. On the basis of a general criterion for aromatic carbonyl compounds,[17] from such long lifetime the lowest triplet excited state (T_1) is assigned as π, π^*.

Figure 1.2-6 (a) shows energy diagram for photophysical process occurring in the isolated PI(BPDA/PDA) chains. Biphenyldiimide units in PI(BPDA/PDA) chains are first excited by 350 nm light. From the local three processes excited state localized on biphenyldiimide units, three processes, i.e., intersystem crossing to T_1, fluorescence emission and intramolecular

charge-transfer (D^+A^-) compete. The phosphorescence is quenched in PI film. The fluorescence of Biphenyldiimide units is not observed due to the presence of relatively rapid process from S_1 to D^+A^- state. Finally effective deactivation occurs from D^+A^- to ground state.

Although the author have not yet detected D^+A^- state directly, photoconductive behavior in aromatic PIs supports the presence of D^+A^- state.

Steric Structures of CTC in aromatic PIs

The CTCs in aromatic PIs have loose steric structures unlike low molecular-weight CT crystals.[18,19] As electron donor (amine moiety) and acceptor (benzimide moiety) coexists in PI chains, it is expected that a CTC is intermolecularly formed between them. The studies on CTC composed of PMDA or phthalimide with aromatic compounds[20-26] in solution support strongly that CTCs in PIs are formed by intermolecular spatial overlap between imide and amine moieties. However WAXD studies[27] on highly oriented PI(PMDA/PDA) fiber presented a crystalline structure where face-to-face structure of pyromellitimide rings each other is shown without overlap between imide and amine moieties as shown in Figure 1.2-7. In order to examine if there is attractive interaction of pyromellitimide rings each other in isotropic amorphous state, the electronic spectra of PI(PMDA/MDCA) were measured. If ground state dimer between pyromellitimide rings exists in isotropic solid state, fluorescence or absorption bands due to it should be observed as reported in PET[28,29] and LC polyester.[30] Figure 1.2-8 shows the absorption, excitation, and fluorescence spectra of PI(PMDA/MDCA) thin film (a), and of M(PMDA/CHA) in dichloromethane (b) and in PMMA (c). The consistency of (a) with (b) in their spectra shows that the fluorescence of PI(PMDA/MDCA) is due to pyromellitimide moiety and not due to ground state dimer. In (b), the consistency of the absorption and excitation spectra remains the possibility in which the observed fluorescence is due to excimer. In order to exclude the possibility, the spectra of M(PMDA/CHA) in PMMA in which the excimer is not formed were recorded. The spectra similar to those in solution were also obtained in PMMA, showing that the fluorescence of PI(PMDA/MDCA) and M(PMDA/CHA) in solution are not due to excimer. Therefore, the author considers that there is little attractive interaction between imide moieties in isotropic PIs.

Figure 1.2-9 illustrates that CTC is intermolecularly formed because the mixing of dichloromethane solution of M(PMDA/CHA) and N,N,-dimethylaniline (DMAN) induces the appearance of a new band in longer wavelength region. Thus it was supported that CTC in PIs is intermolecular overlap between

imide and amine moieties.

Excitation energy transfer in solid PI(BPDA/PDA)

In order to examine if excitation energy transfer participates in the CT fluorescence of PI(BPDA/PDA), the fluorescence anisotropy r was measured. r is given by

$$r = (I_{vv} - GI_{vh}) / (I_{vv} + 2GI_{vh})$$

where I is fluorescence intensity, and the subscripts v and h denote vertically and horizontally polarized lights, respectively. The first and suffixes mean excitation and emission side, respectively. The G ($=I_{hv}/I_{hh}$) factors were determined as a function of emission wavelength using a quinine sulphate standard solution. Figure 1.2-10 shows that r value (350 nm excitation) decreases with the increase in cure temperature. Since r values are independent of emission wavelength, the CT fluorescence consists of one component. The depolarization is due to energy transfer between chromophores, the other factors, the rotational diffusion of chromophores and reabsorption of the emission, are removed. In Figure 1.2-11, polarization P which is connected with r by a formula r=2P/(3-P) decreases with the increase in the fluorescence quantum yield for PI films, indicating that the increase in CTC concentration (the decrease in average distance between CTCs) gave the increase in the energy migration efficiency between intermolecular CT sites.

The fluorescence decay (350 nm excitation) for PI(BPDA/PDA) film was measured to examine the energy transfer from the excited state of biphenyldiimide units to emissive CTC state in more detail. As shown in Figure 1.2-12, the decay is not single-exponential and a double-exponential analysis gave a pre-exponential factors A_1=0.045, A_2=9.0, and lifetimes τ_1=0.31 ns, τ_2=1.4 ns (χ^2=1.18). It should be noted that no rising component immediately after the excitation is observed. This is due to a very rapid energy transfer from the local excited state of biphenyldiimide units via intramolecular D^+A^- to emissive CTC state. The emission mechanism at CTC forming site is shown in Figure 1.2-6 (b). The process of direct energy transfer from excited state of biphenyldiimide to the emissive CTCs is expected to be negligible because overlap integral between the fluorescence of biphenyldiimide unit (380 nm) in Figure 1.2-5 and CT absorption band (400-600) in Figure 1.2-9 is very small.

CONCLUSIONS

In this section, the photophysical processes for solid PI(BPDA/PDA) were examined. It was shown from the studies on model compounds that biphenyldiimide units in PI(BPDA/PDA) are first excited by 350 nm and then the fluorescence from the local excited state is deactivated intramolecularly. The fact that no fluorescence due to biphenyldiimide is observed for solid PI(BPDA/PDA) and M(BPDA/AN) in solution suggests that intramolecular charge-transfer mechanism participates to the deactivation process.

No attractive interaction between pyromellitdiimide units in isotropic polypyromellitimide was detected in the absorption and fluorescence spectra of PI(PMDA/MDCA). A predominant interaction is due to CT between imide moiety as a electron acceptor and amine moiety as a donor.

The polarization decreases with the increase in fluorescence quantum yield, indicating that the increase in energy migration efficiency between CTCs is caused by the increase in CTC concentration.

REFERENCES

1. A.A.Lin, V.R.Sastri, G.Tesoro, A.Reiser and R.Eachus, Macromolecules, 21, 1165 (1988).
2. H.Higuchi, T.Yamashita, K.Horie and I.Mita, Chem.Materials, in press.
3. J.S.Scaiano, J.C.Netto-Ferreira, A.F.Becknell and R.D.Small, Prep.8th Int.Conf., Photopolymers, p393.
4 Y.Shindo, T.Sugimura, K.Horie and I.Mita, Eur.Polym.J., 26, 683 (1990).
5. R.Srinivasan and V.Mayne-Banton, Appl.Phys.Lett., 41, 576 (1982).
6. J.H.Brannon, J.R.Lankard, A.I.Baise, F.Burns and J.Kaufman, J.Appl.Phys., 58, 2036 (1985).
7. A.Yabe, H.Niino, Kino Zairyo, 9, No.10, 5 (1989) (in Japanese).
8. H.R.Philipp, H.S.Cole, Y.S.Liu and T.A.Sitnik, Appl.Phys.Lett., 48, 192 (1986).
9. J.P.LaFemina, G.Arjavalingam and G.Hougham, J.Chem.Phys., 90, 5154 (1989).
10. G.Arjavalingam, G.Hougham and J.P.LaFemina, Polymer, 31, 840 (1990).
11. W.H.Melhuish, J.Phys.Chem., 65, 229 (1961).
12. W.R.Remington, J.Am.Chem.Soc., 67, 1838 (1945).
13. W.G.Brown and H.Reagan, J.Am.Chem.Soc., 69, 1032 (1947).
14. G.H.Beaven, "Streric Effects in Conjugated Systems" (Edited by .W.Gray), Chapter 3, Butterworths, London (1958).
15. H.Ishida, S.T.Wellinghoff, E.Baer and J.L.Koenig, Macromolecules, 13, 826 (1980).
16. N.N.Barashkov, L.I.Semenova and R.N.Nurmukhametov, Polym.Sci.U.S.S.R., 25, 1264 (1983).
17. G.Porter and P.Suppan, Pure Appl.Chem., 9, 499 (1964).
18. J.C.A.Boeyens and F.H.Herbstein, J.Phys.Chem., 69, 2160 (1965).
19. Z.V.Zvonkova, I.V.Bulgarovskaya and O.V.Kolninov, Dokl.Phys.Chem., 229, 715 (1976).
20. M.Chowdhury, J.Phys.Chem., 66, 353 (1962).
21. L.L.Ferstandig, W.G.Toland and C.D.Heaton, J.Am.Chem.Soc., 83, 1151 (1961).
22. T.Matsuo, Bull.Chem.Soc.Jpn., 38, 2110 (1965).
23. H.M.Rosenberg and E.C.Eimutis, J.Phys.Chem., 70, 3494 (1966).
24. G.D.Short, C.A.Parker, Spectrochim.Acta, 23, 2487 (1967).
25. R.Potashnik, C.R.Goldschmidt and M.Ottolenghi, J.Phys.Chem., 73, 3170 (1969).
26. J.Prochorow and R.Siegoczynski, Chem.Phys.Lett., 3, 635 (1969).
27. "Polyimides"(Edited by M.I.Bessonov, M.M.Koton, V.V.Kudryavtsev

and L.A.Laius), Plenum Press, N.Y.(1987).
28. M.Hennecke and J.Fuhrmann, Macromol.Chem., Macromol.Symp., 5, 181 1986).
29. D.J.Hemker, C.W.Frank and J.W.Thomas, Polymer, 29, 437 (1988).
30. H.Hasimoto, M.Hasegawa, T.Yamashita and K.Horie, LCP Conf., p.86 (1990).

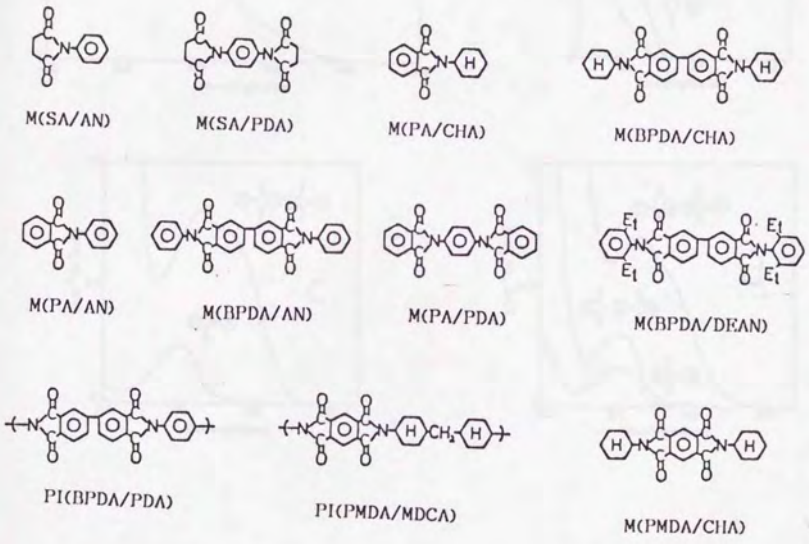

Figure 1.2-1 The chemical structures of samples used and symbols.

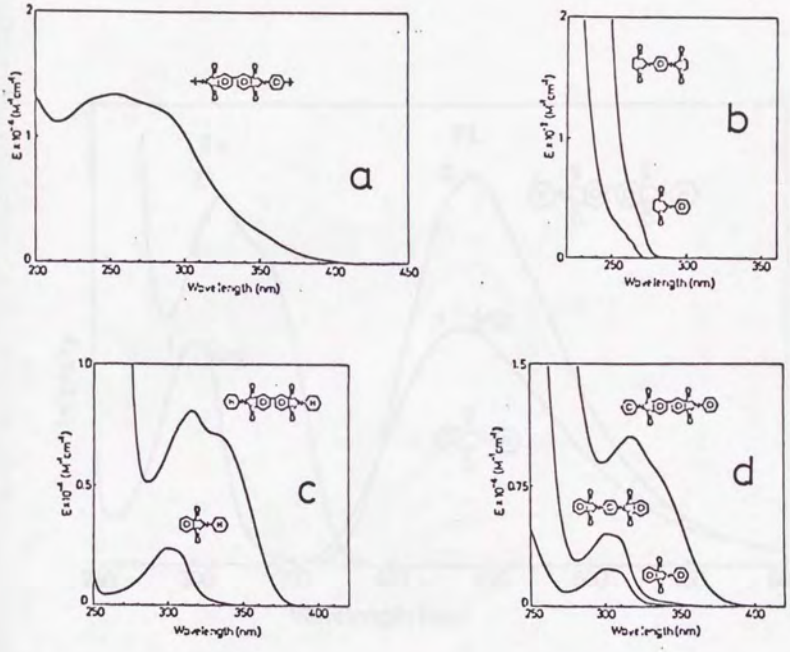

Figure 1.2-2 The absorption spectra of PI(BPDA/PDA) film and model compounds in HFP solution.

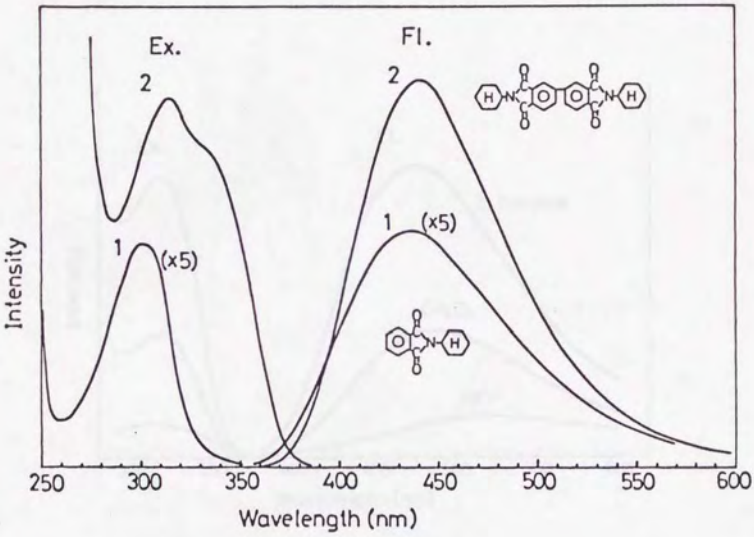

Figure 1.2-3 The excitation and fluorescence spectra of model compounds in HFP solution.

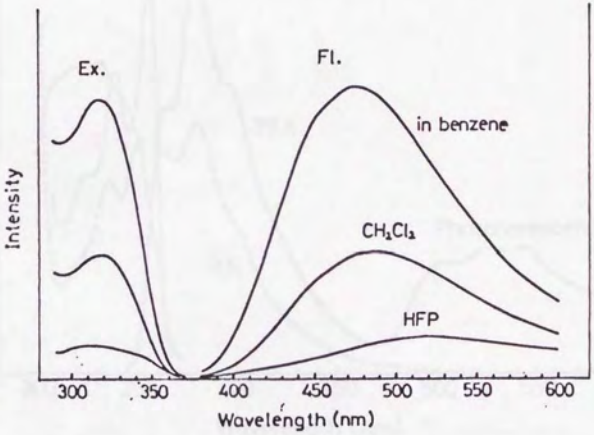

Figure 1.2-4 The fluorescence spectra of M(BPDA/DEAN) in solution.

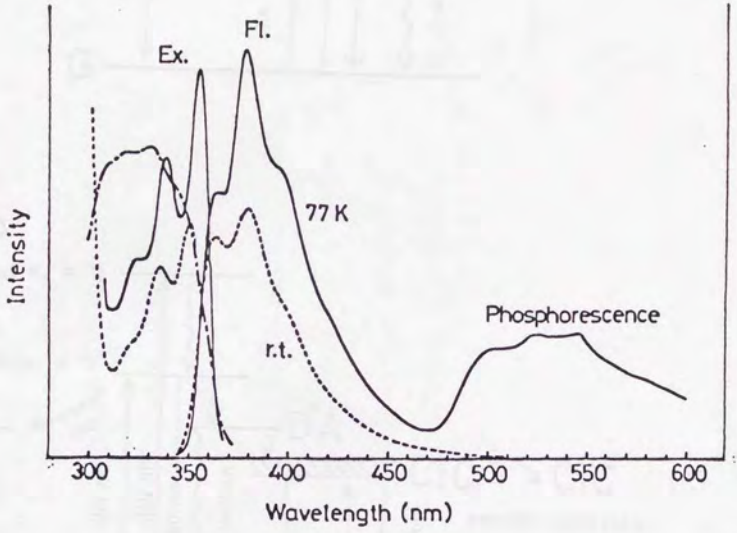

Figure 1.2-5 The fluorescence, phosphorescence and excitation spectra of M(BPDA/CHA) in degassed rigid solution at 77 K(———) and room temperature(- - -). (— • — •); the excitation spectrum for phosphorescence.

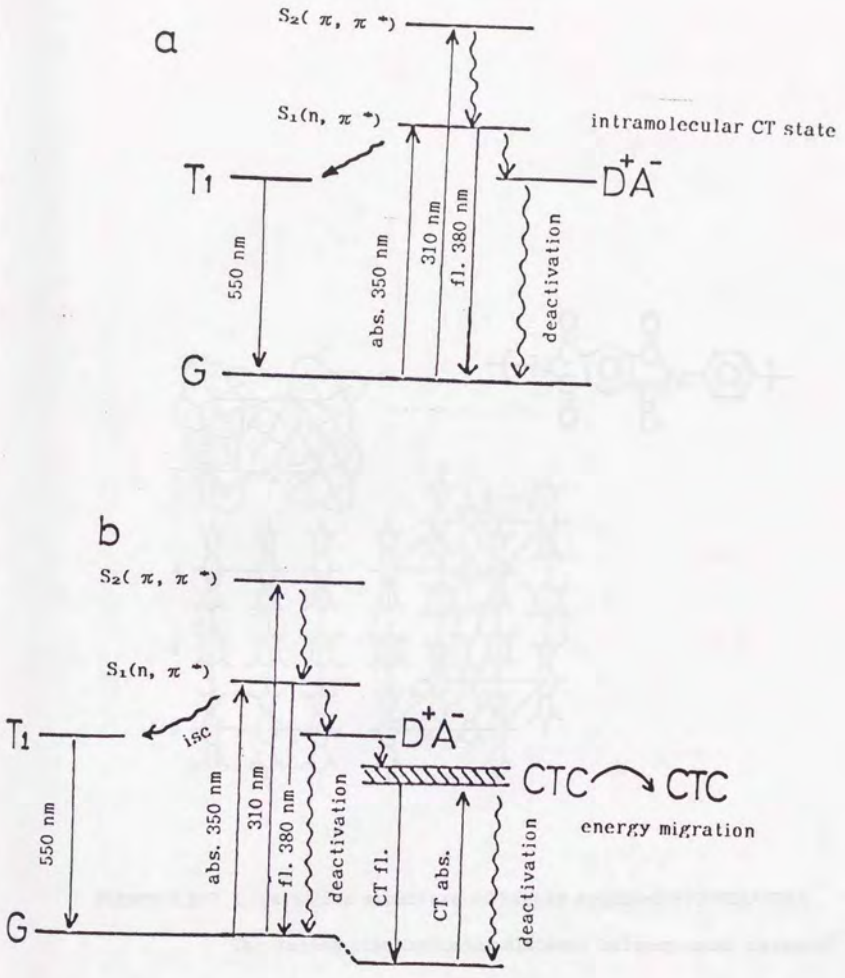

Figure 1.2-6 Energy diagram for photophysical process in isolated PI(BPDA/PDA)(a) and the aggregated state(b).

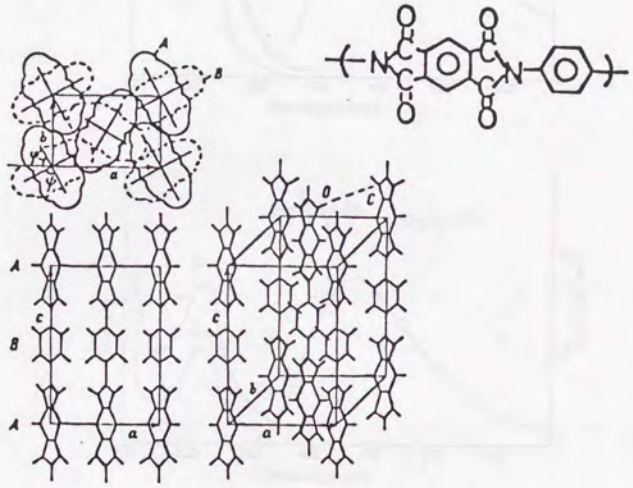

Figure 1.2-7 Crystalline structure of highly oriented PI(PMDA/PDA). The dotted line incicates distance between imide carbonyl groups.

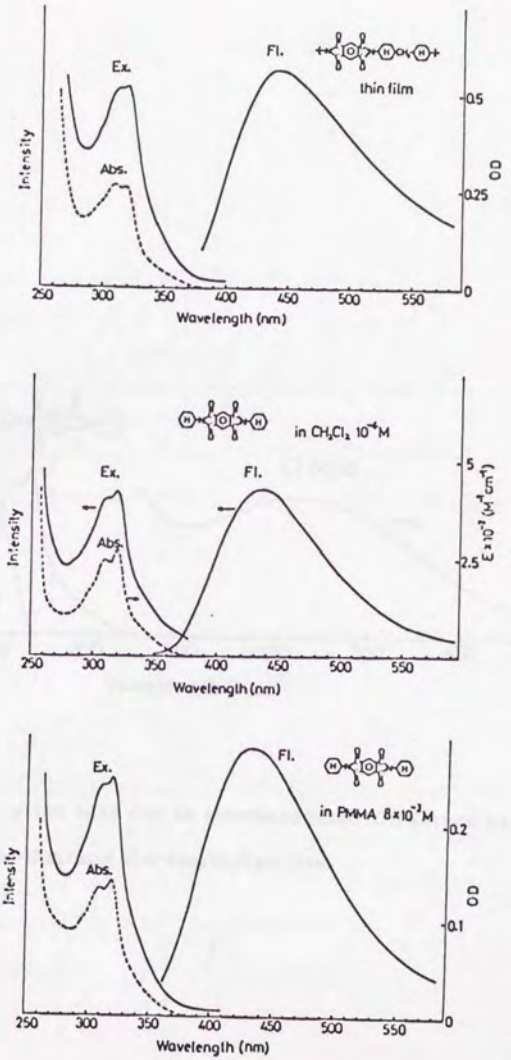

Figure 1.2-8 The absorption, excitation and fluorescence spectra of PI(PMDA/MDCA) film(a), its model compound in solution(b) and the model compound in PMMA(c).

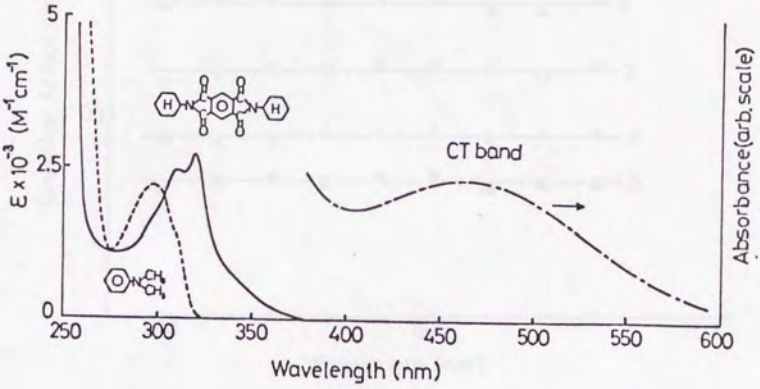

Figure 1.2-9 Absorption band due to intermolecular CTC formed between M(PMDA/CHA) and N,N-dimethylaniline.

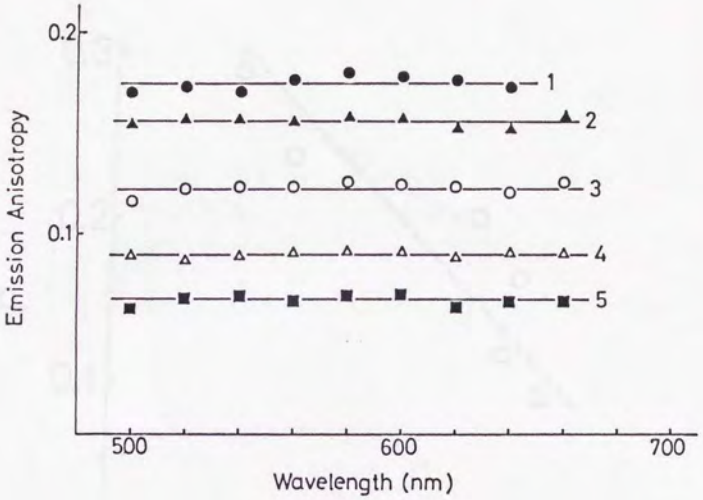

Figure 1.2-10 The change in emission anisotropy (350 nm excitation) for PI(BPDA/PDA) with the increase in cure temperature.

(1) imidized at 150 ℃ 1 h, 200 ℃ 1 h, 250 ℃ 2 h

(2) (1)+330 ℃ 2 h (3) (2)+350 ℃ 1 h

(4) (3)+380 ℃ 1 h (5) (4)+400 ℃ 1 h

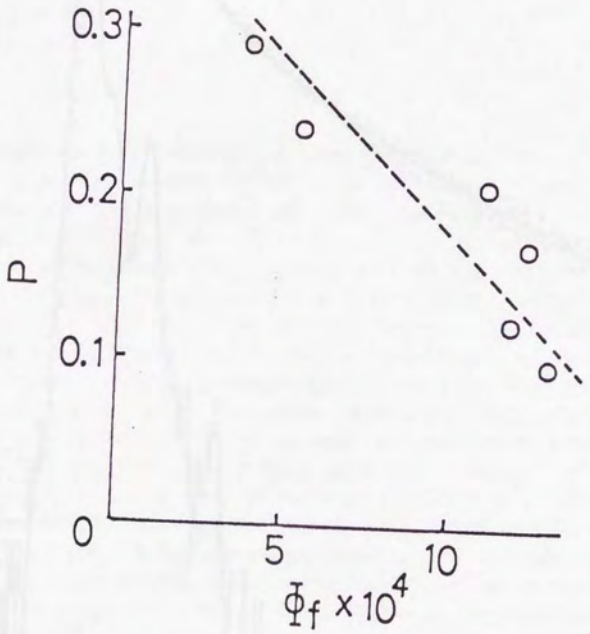

Figure 1.2-11 The relationship between ϕ_f and P for PI(BPDA/PDA).

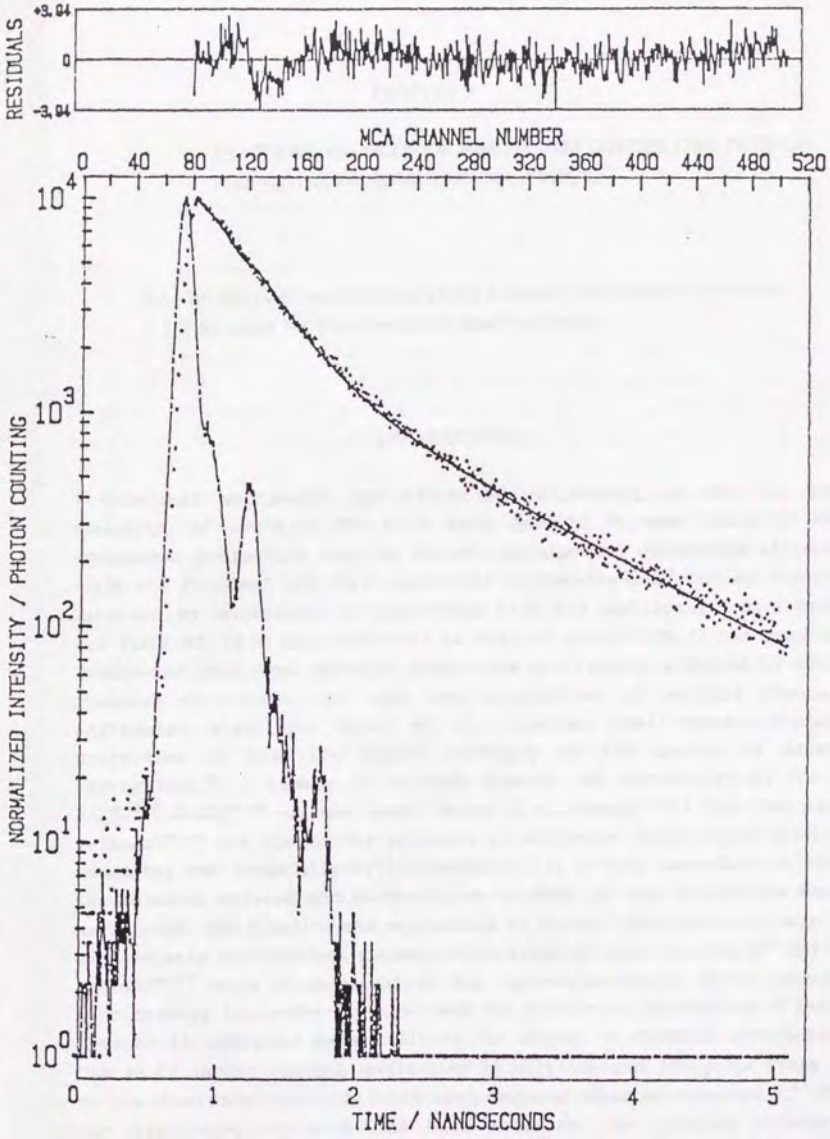

Figure 1.2-12 Fluorescence decay curve for PI(BPDA/PDA)(350 nm excitation).

CHAPTER 2

REACTIONS IN POLYIMIDE PRECURSORS CONTROLLING PHYSICAL PROPERTIES OF RESULTING POLYIMIDES.

2.1 Isothermal Imidization of an Aromatic Polyimide Precursor Studied by Fluorescence Spectroscopy

INTRODUCTION

Excellent mechanical and electrical properties, as well as thermal stability, of aromatic PIs have been applied in many kinds of fields. Mechanical properties such as Young's modulus and elongation strength of rigid rod PI films[1] and PI/PI molecular composites (MC)[2] can be remarkably improved by imidization of cold-drawn PAAs and additional heat treatment. For PI/PI MC, it is also important to control miscibility. It has been widely recognized that some physical properties are largely affected by not only chemical structures but also the orientation of polymer chains and aggregated structure. Kochi et al. reported that dynamic mechanical properties of some PIs depend strongly on the degree of molecular aggregation.[3] A number of workers studied the morphology of PIs using WAXD,[4-7] SAXS,[8-10] UV and laser Raman spectroscopy[11,12] and fluorescence method,[13,14] and showed the presence of molecular order which grew up by annealing and especially by increasing T_i. It is very important to examine the relation between the morphologies of final PIs and imidization reaction mechanisms. The kinetics and mechanisms of thermal imidization of many kinds of PAAs were systematically examined by Bessonov and coworkers[15] and other groups[16,17] using IR spectroscopy and thermogravimetry. UV-vis absorption spectroscopy has scarcely been used for studies on imidization.[18] Recently Pyun et al. analyzed quantitatively the change in chemical structure from PAA to PI during thermal imidization in solution and the solid state using uv-vis absorption spectrum of an azo-compound (diamine component).[19] But to our knowledge, no work has been done on the relation between the imidization mechanisms and molecular aggregation of final PIs. In this paper, we show how molecular order is formed with the progress of the reaction using the intermolecular CT of the PI which reflects sensitively aggregated

structures and the miscibility of PI/PI blends.[20]

EXPERIMENTAL

BPDA was recrystallized from dried acetic anhydride and then vacuum dried at 180 ℃ for 24 h. DMAc used for the preparation of PAA was dried with molecular sieves(4A) and then vacuum distilled. Zone refining PDA supplied by Honda Giken Co.,Ltd. was used after vacuum drying at room temperature without further purification. PAA(BPDA/PDA) was prepared by adding a stoichiometric amount of BPDA powder to the DMAc solution of PDA with continuous stirring in a nitrogen atmosphere. A viscous yellow PAA solution (10wt%) was obtained after several hours. PAA films were prepared by casting onto a glass plate at 50 ℃ for 2 h in air oven, followed by vacuum drying at 50 ℃ for 24 h.

Two kinds of heating furnaces were used for the thermal imidization of PAA films, a common furnace with slow heating rate (the time required up to T_i is 15-20 min), and a special furnace with a rapid heating rate (about 5 s). The rapid-heating furnace, which is mainly used for isothermal imidization, is equipped with a heating block surrounded with a heat insulator, nitrogen conduction tube and thermocontroller. Rapid heating of the samples becomes possible by quickly inserting the samples wrapped in aluminum foil into slit in the temperature-controlled heating block and by maintaining the intimate contact between the samples and inside wall in the slit. Sample temperature was detected by a thin thermocouple in contact with the samples.

Thick films (30-50 μ m) and thin films (2-5 μ m) were used for fluorescence and IR measurements, respectively. Although there is a report that imidization rate is affected by the amount of residual solvent which depends on the film thickness,[21] since the chromophores in the PI in the region from the surface to the depth at a few μ m are mainly excited by incident light of 350 nm for the fluorescence measurement because the optical density at 350 nm of 3 μ m thick films of the PAA and the PI is more than 2, it is reasonable to substitute the degree of imidization of the thick films used for the fluorescence measurement for that of the thin films used for IR measurement. In order to prevent foaming of the PAA films due to residual solvent when imidized at more than 230 ℃, preheating at 150 ℃ for 1 min prior to the isothermal reaction, which is harmless except for only slight imidization (less than 8%), was carried out.

The fluorescence spectra of the PI were measured at room temperature using a fluorescence spectrophotometer (Hitachi, model 850). The PI films

were excited at 350 nm in a front-face arrangement using 5 nm bandpasses for both the excitation and emission monochromators, respectively. The degree of imidization (i) was estimated by the absorbance ratio of 1774 cm^{-1} band (C=O stretching in imide rings) to that for the PI annealed at 300 ℃ for 20 min (i=100%) using 1517 cm^{-1} band (C=C stretching in benzene rings in PDA) as an internal standard, using an IR spectrophotometer (Jasco, model IR-700). The densities of the PI films produced under some thermal conditions were measured using a density gradient column (xylene-carbon tetrachloride system). The extinction coefficients ε at 350 nm of the PI and PAA films were determined from the film thickness, density and absorbance using a uv-vis spectrophotometer (Jasco, model UVIDEC-660).

The reduced viscosity η_{red} and ε at 350 nm of the PAA and PI are shown in Table 2.1-1.

RESULTS AND DISCUSSION

Thermal imidization of PAA occurs through nucleophilic attack on the carbonyl carbon in carboxyl group by the lone pair of amide nitrogen. Two kinds of side reactions, the formation of polyisoimide and reversible chain scission as shown in Scheme 1 are known. polyisoimide is hardly formed by thermal imidization but is observed by IR spectroscopy (isoimide: 1800 cm^{-1}) when chemically imidized.[22] Typical IR spectra of PIs cured thermally and chemically, and PAA are shown in Figure 2.1-1. Polyisoimide can be thermally rearranged to PI.[23] The chain scission of PAA into amines and anhydrides during thermal imidization is observed by IR spectroscopy (anhydride: 1850 cm^{-1}). But the amount of anhydride decreases due to resynthesis as imidization proceeds[24] and the anhydrides disappear completely when cured at above 300 ℃.

Since PI(BPDA/PDA) has very rigid main chain and high and unclear T_g, with the progress of imidization, molecular mobility decreases. It is expected that the PI formed on thermal imidization is in a non-equilibrium state so that the molecular packing of the PI depends strongly on imidization conditions such as initial imidization temperature, T_i, and heating rates up to T_i. This will be illustrated by the following preliminary experiment. The PI films possessing different molecular packing were prepared under several cure conditions in Table 2.1-2 in a furnace at a slow heating rate (time required up to T_i: 15-20 min) in vacuum. It was observed by IR measurement that the imidization is almost completed by curing at 200 ℃ for 5 h, naturally at 300 ℃ for 1 h and at 400 ℃ for 1 h, too. Also annealing time at

various conditions is long enough to complete the cure. Figure 2.1-2 shows that the intermolecular CT fluorescence intensity for the PIs prepared on the conditions in Table 2.1-2 is linearly related with the density. This indicates that it is possible to evaluate the molecular packing of the PI by using the CT fluorescence. The relation of the intensity to final cure temperature is shown in Figure 2.1-3. With increasing T_i, the fluorescence intensity increases (sample No.1, 5, 7). Comparing the PI cured at 400 ℃ for 1 h (No.7) with the PI cured at 200 ℃ for 5 h plus 400 ℃ for 1 h (No.3), in spite of the same final cure temperature (400 ℃), the fluorescence intensity of No.3 is far smaller than that of No.7. A similar result is shown in the case of 300 ℃ cure. In No.3, since the imidization at 200 ℃ for 5 h before final annealing at 400 ℃ produces a PI with loose packing[25] but with rigid polymer chains, the effect of the final annealing is reduced due to the rigid chains. The molecular packing of sample No.3 remains loose. In other words, sample No.3 is in a non-equilibrium state. On the other hand, the cure at 400 ℃ of the PAA with flexible chains (T_g=ca.140 ℃)(No.7) yields a very dense PI. This means that the degree of the molecular packing of rigid PI is not always determined by only the final cure temperatures. In fact, since the rigidity of the polymer chains increases rapidly with the progress of imidization, the relation between reaction kinetics and formation of aggregated structures is very complex. Also since the heating rates of the furnace used are slow(it takes 15-20 min), in the cure at 400 ℃ for 1 h, the samples are subjected not only to imidization reaction which completes at around 200 ℃ on the way to the temperature rising, but also to the annealing of the PI imidized at around 200 ℃. In order to consider both effects separately, imidization was carried out in the rapid-heating furnace under the conditions without the annealing effect.

Kinetics of Isothermal Imidization and Changes of CT Fluorescence

Time-conversion curves of thermal imidization at 110 ℃ in DMAc solution (polymer concentration: 10 wt%) and in solid state are shown in Figure 2.1-4. The imidization in solution proceeds rapidly compared with that in solid state although above 30% in conversion insoluble portion is obtained. But the reaction in the solid phase is very slow at 110 ℃. Possibly, the conformation changes required with the reaction are free in solution but is suppressed in the glassy state. It is known that the reaction rates in solid PAAs suddenly increases above ca. 150 ℃. Figure 2.1-5 shows time-conversion curves for isothermal imidization at 150-200 ℃ in the solid PAA. The rates increase with increasing T_i. The apparent activation energy E_a determined from Arrhenius plot of the initial rate constants was about 21 kcal/mol. The

value is consistent with the data of Bessonov et al. in which the E_a is 19 kcal/mol regardless of the chemical structure of PAAs.[15]

Isothermal imidization of the solid PAA was also examined using the intermolecular CT fluorescence of the PI. Figure 2.1-6 shows the change in fluorescence spectra during imidization. The fluorescence of the PAA peaking near 490 nm reduces rapidly with progress of imidization, and then becomes very weak around 20-30% in conversion. When the reaction proceeds further, the fluorescence of the PI peaking at 530-540 nm increases gradually. Similarly, the rapid reduction of the PAA fluorescence was also observed for imidization at 110 ℃ in solution and in the solid phase. However, the rapid reduction of the PAA fluorescence in the region of very low conversion can not be easily explained. The following possibilities are proposed. First, even if the concentration of imide moiety is low at low conversion, the ε of imide unit formed by imidization is quite large compared to the amic acid unit and thus incident light is selectively absorbed by imide units distributed randomly. Second, after effective energy transfer from amic acid units to imide units occurs, unless the intermolecular CT sites exist at low conversion, the CT fluorescence is not observed. As shown in Table 2.1-1, since the ε of the PAA and the corresponding PI are 1400 and 2300 $M^{-1}cm^{-1}$ respectively, the first possibility is excluded. Although it is not yet clear whether the rapid reduction of the PAA fluorescence at the initial stage of the reaction is attributed to the energy transfer, since our main concern is to know the relation between the aggregated structures of the final PI and thermal imidization reaction, we wish to focus on changes of the CT fluorescence of the PI in the region from the middle to the final reaction stage.

Figure 2.1-7 shows the change in the fluorescence intensity with the progress of imidization at various T_i. The reaction rates are also so large at higher T_i that it was experimentally difficult to follow the reaction in the low conversion range. As shown in Figure 2.1-7, the intensity begins to increase gradually from around 50% in conversion, showing that the formation of the CT structure occurs simultaneously with the progress of the reaction. It is evidently shown that when imidized at 150 ℃ the intensity increases only slightly as the reaction proceeds while at higher T_i such as 270 ℃ the increase in the intensity become remarkable. The fact that the molecular packing of the final PI is strongly affected by T_i suggests that the molecular mobility of the polymer chains which changes during imidization is closely related to the molecular packing of the final PI. Also it is noted that from about 60% in conversion the intensity-conversion curves begin to branch and the intensity at a certain

conversion depends strongly on T_i. If the CT fluorescence does not provide information for intermolecular aggregation but intramolecular information, only one intensity-conversion curve must be depicted regardless of T_i (do not branch). Figure 2.1-8 shows a schematic diagram based on intensity-conversion curves for changes of T_g of the polymer during isothermal imidization. More than 20 years ago Mita et al. proposed [26,27] the concept, which has been widely accepted, of stopping of polymerization of vinyl monomers and in crosslinking system at conversion of vitrification. This concept can be also applied to thermal imidization reaction in solid phase. As the reaction proceeds, the T_g of the polymer increases successively, and exceeds the T_i at certain conversion (i_g) where the polymer is in glassy state. The more T_i increases, the more i_g will increase, too. In Figure 2.1-8, it is difficult to determine experimentally the T_g of the partial imidized PAAs by thermal analysis such as TMA, DSC or dynamic mechanical analysis because imidization occurs due to heating. Laius et al. showed that the value of i_g determined from the plot of conversion vs rate constant k agrees with the data obtained by a stepwise pulse heating method.[28] The values of i_g were estimated from the plot of i vs k as shown in Figure 2.1-9. The arrows marked in Figure 2.1-7 denote i_g determined from Figure 8 at 150 and 200 ℃, respectively. In the case of 150 ℃ the vitrification occurs at only initial stage while for 200 ℃ it takes place at about 60% in conversion. It seems that the molecular packing of the final PI is already determined before the vitrification (below i_g), because above i_g molecular motion enough to rearrange the polymer chains is inadequate. In other words, the degree of increase in the fluorescence intensity (molecular packing) after the vitrification depends strongly on the amount of i_g. Accordingly, to gain more packed PI, it is necessary to have higher i_g, i.e., to increase T_i.

CONCLUSION

Isothermal imidization of a solid PAA was examined using the intermolecular CT fluorescence reflecting sensitively molecular packing of PI chains. The relationship between the fluorescence intensity and conversion clearly shows that the intensity at a certain conversion depends strongly on T_i, and the intensity increases remarkably during imidization at higher T_i, e.g., at 270 ℃. The increase in CT complex population occurs simultaneously with the progress of the reaction. The gradient in the intensity-conversion curves after the vitrification increases with increasing i_g.

REFERENCES

1. M.Kochi, T.Uruji, T.Iizuka, I.mita and R.Yokota, J.Polym.Sci., C, 25, 441 (1987).
2. R.Yokota, R.Horiuchi, M.Kochi, H.Soma and I.Mita, J.Poly.Sci., C, 26, 215 (1988).
3. M.Kochi and H.Kambe, Polym.Eng.Rev., 3, 335 (1983).
4. N.Takahashi, D.Y.Yoon and W.Parrish, Macromolecules, 17, 2583 (1984).
5. T.P.Russel, H.Gugger and J.D.Swalen, J.Polym.Sci., Polym.Phys.Ed., 21, 1745 (1983).
6. L.G.Kazaryan, D.Ya.Tsvankin, B.M.Ginzburg, Sh.Tuichiev, L.N.Korzhavin, and S.Ya.Frenkel, Poly.Sci.U.S.S.R., 14, 1344 (1972).
7. G.Conte, L.D'Illario, N.N.Pavel and E.J.Giglio, J.Polym.Sci., Polym.Phys.Ed., 14, 1553 (1976).
8. S.Isoda, H.Shimada, M.Kochi and H.Kambe, J.Polym.Sci., Polym.Phys.Ed., 22, 1979 (1984).
9. T.P.Russel, J.Polym.Sci., Polym.Phys.Ed., 22, 1105 (1984).
10. T.P.Russel and H.R.Brown, J.Polym.Sci., B, 25, 1129 (1987).
11. H.Ishida, S.T.Wellinghoff, E.Baer and J.L.Koenig, Macromolecules, 13, 826 (1980).
12. S.T.Wellinghoff H.Ishida, J.L.Koenig and E.Baer, Macromolecules, 13, 834 (1980).
13. E.D.Wachsman and C.W.Frank, Polymer, 29, 1191 (1988).
14. M.Hasegawa, M.Kochi, I.Mita and R.Yokota, Eur.Polym.J., 25, 349 (1989).
15. M.I.Bessonov, M.M.Koton, V.V.Kudryavtsev and L.A.Laius, Ed., "Polyimides", Plenum Press, N.Y., 1987.
16. S.Mumata, K.Fujisaki and N.Kinjo, in "Polyimides" Vol.1, (Edted by K.L.Mittal), Plenum Press, N.Y., 1984, p 259.
17. I.Mita, M.Akiba, A.Sato and M.Kochi, Proceedings of Eur.Tech.Conf. on Polyimides, Vol.1, Monpellier, 1989, A7.
18. N.N.Barashkov, L.I.Semenova and R.N.Nurmukhametov, Polym.Sci. U.S.S.R., 25, 1264 (1983).
19. E.Pyun, R.J.Mathisen and C.S.P.Sung, Macromolecules, 22, 1174 (1989).
20. M.Hasegawa, M.Kochi, I.Mita and R.Yokota, Polymer, in press.
21. R.Ginsburg and J.R.Susko, in "Polyimides" Vol.1, (Edited by K.L.Mittal), Plenum Press, N.Y., 1984, p 237.
22. R.A.Dine-Hart and W.W.Wright, J.Appl.Polym.Sci., 11, 609 (1967).
23. V.V.Kudryavtsev, M.M.Koton, T.K.Meleshko and V.P.Sklizkova, Polym.Sci.U.S.S.R., 17, 2029 (1975).

24. M.I.Tsapovetskii, L.A.Laius, T.I.Zhukova, L.A.Shibayev, N.G.Stepanov, M.I.Bessonov and M.M.Koton, Polym.Sci.U.S.S.R., 30, 295 (1988).
25. R.Yokota, Doctoral thesis, The University of Tokyo (1990).
26. K.Horie and I.Mita, J.Poly.Sci., Polym.Chem.Ed., 6, 2663 (1968).
27. I.Mita and K.Horie, J.Macromol.Sci.Rev., Macromol.Chem., C27, 91 (1987).
28. L.A.Laius, M.I.Bessonov and E.S.Florinskii, Polym.Sci.U.S.S.R., 13, 2257 (1971).

Table 2.1-1 η_{red} and ε of PAA and PI used.

Symbol	[a] η_{sp}/C(dl/g)	ε_{350} ($M^{-1}cm^{-1}$)
PAA(BPDA/PDA)	1.5	1400
PI(BPDA/PDA)	---	2300

a: measured at 0.5 wt% polymer concentration

Table 2.1-2 Cure history of samples.

	Cure history		
Sample No.	200 °C 5h	300 °C 1h	400 °C 1h
1	○		
2	○	○	
3	○		○
4	○	○	○
5		○	
6		○	○
7			○

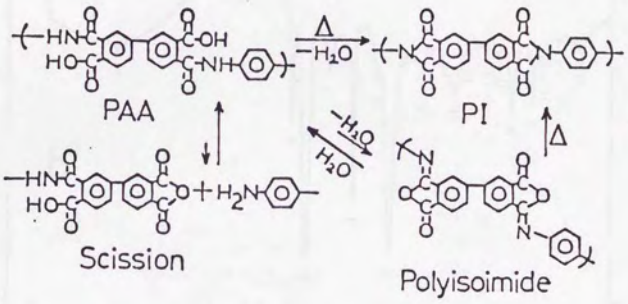

Scheme I. Reaction scheme of thermal imidization.

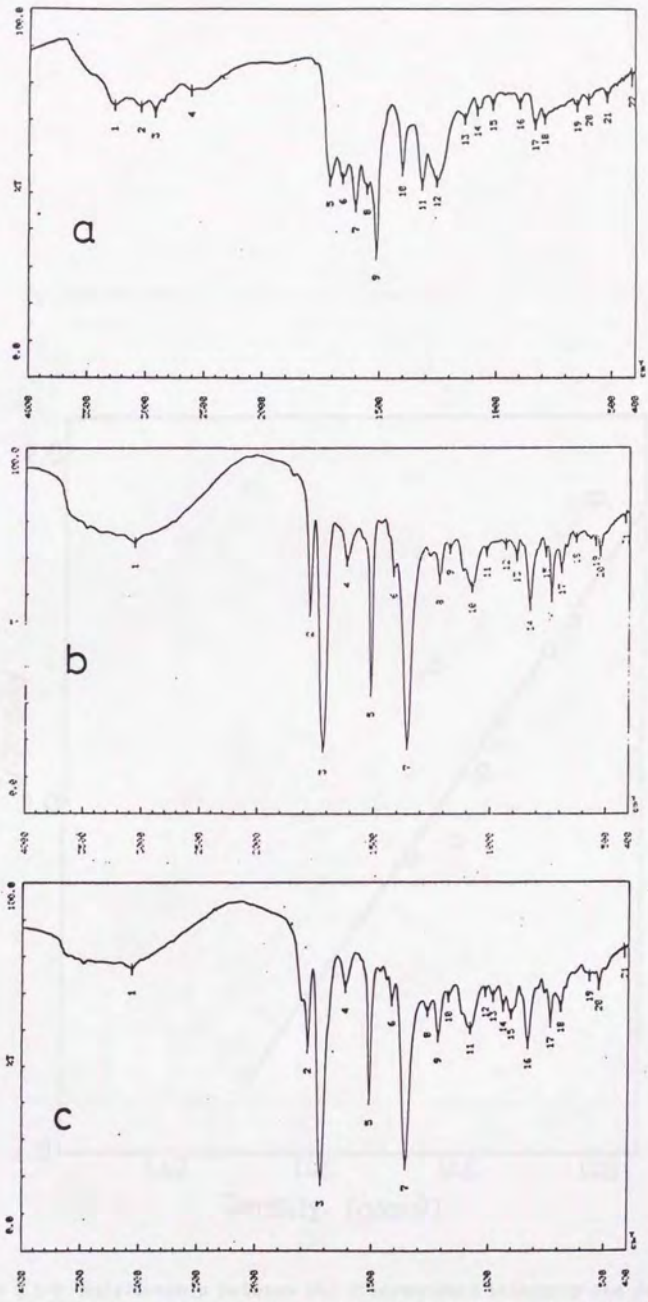

Figure 2.1-1 IR absorption spectra of PAA(BPDA/PDA)(a) and PI(BPDA/PDA) imidized thermally(b) and chemically(c)(with mixture of acetic anhydride and pyridine).

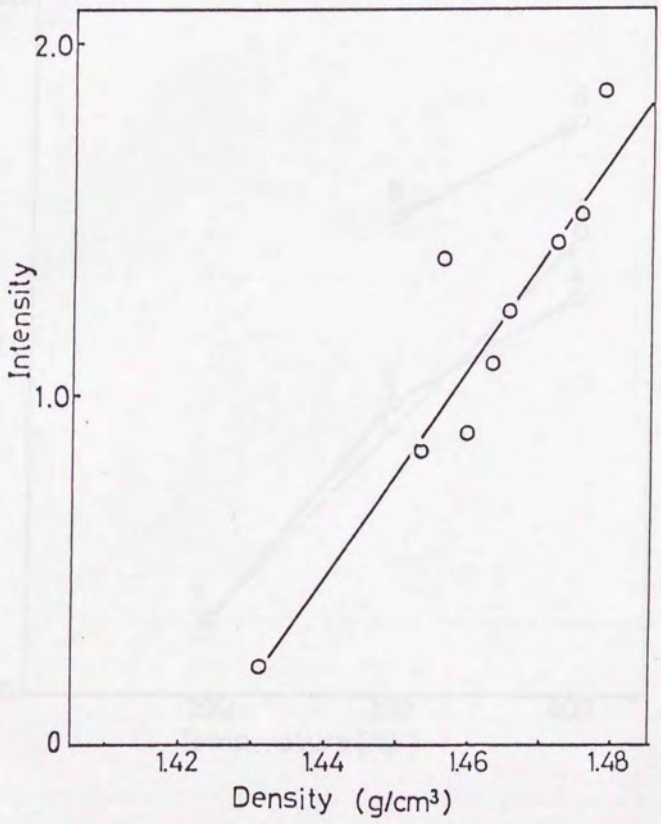

Figure 2.1-2 Relationship between the fluorescence intensity and density of PI cured under the conditions in Table 2.1-2.

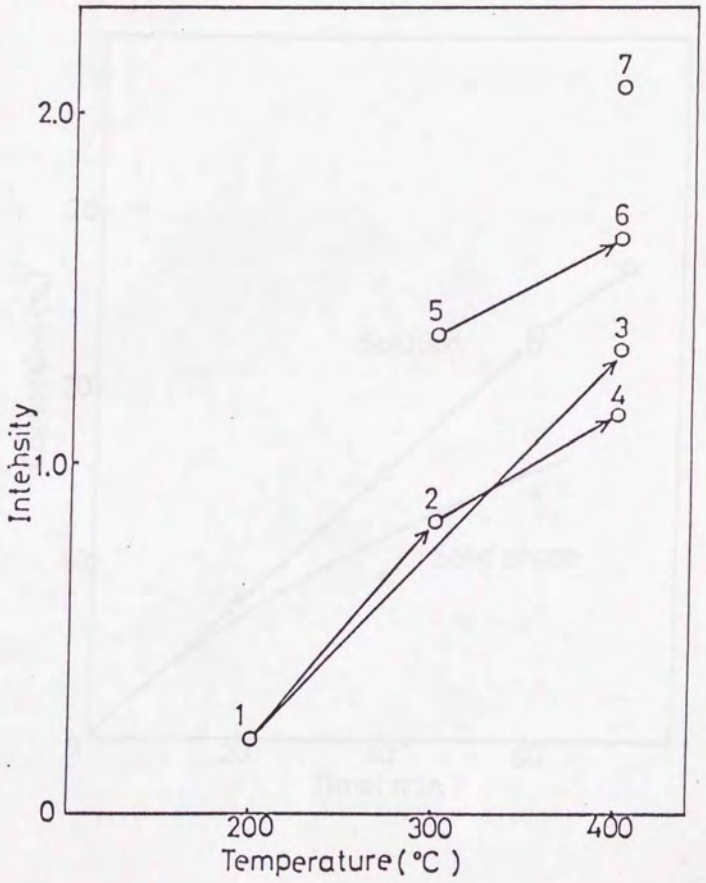

Figure 2.1-3 The changes in the fluorescence intensity against final cure temperature.

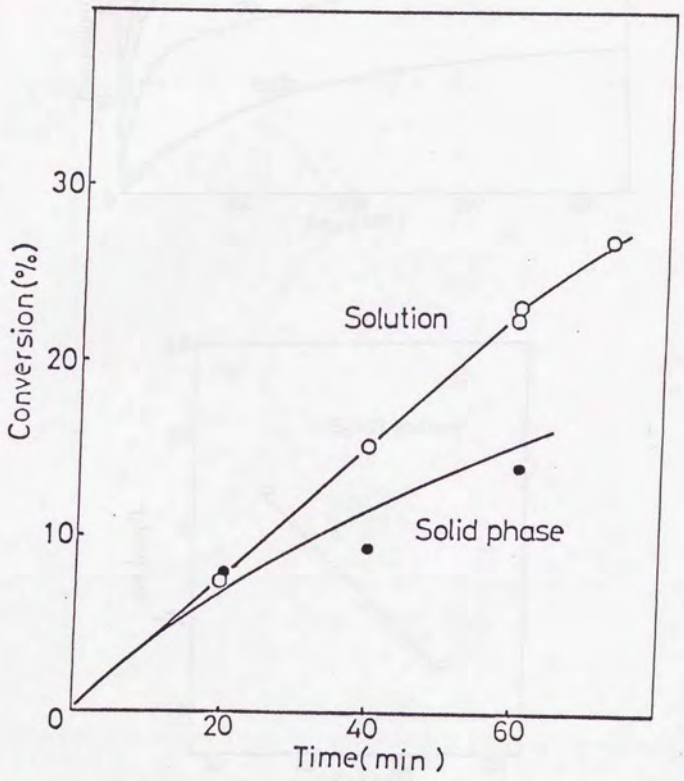

Figure 2.1-4 Time-conversion curves for isothermal imidization at 110 ℃ in DMAc solution and in solid phase.

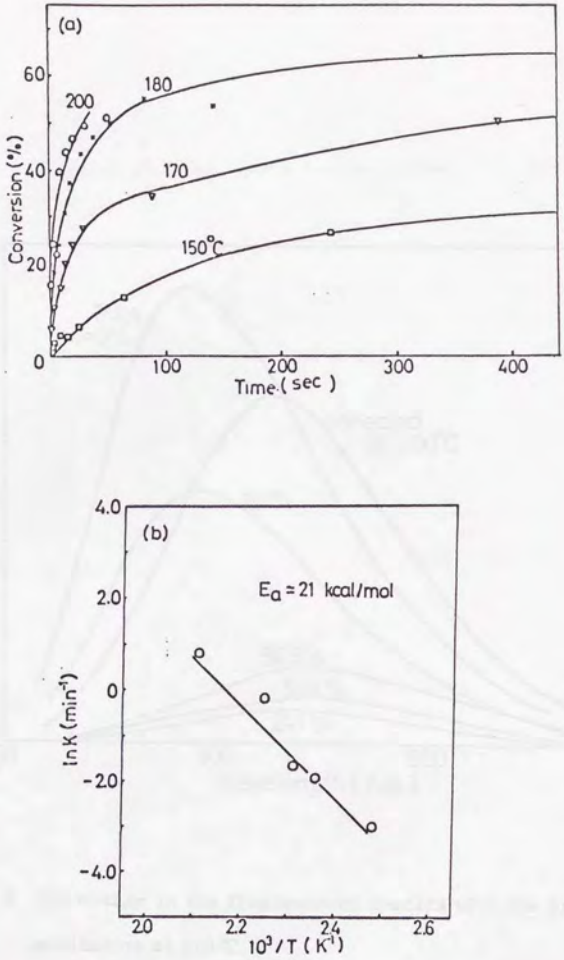

Figure 2.1-5 Time-conversion curves for isothermal imidization at 150-200 ℃ in solid phase(a) and Arrhenius plot(b).

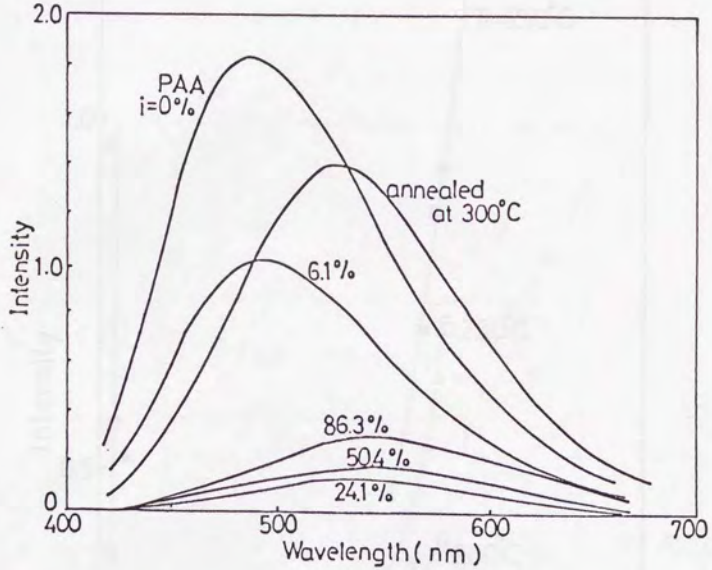

Figure 2.1-6 The change in the fluorescence spectra with the progress of imidization at 170 ℃.

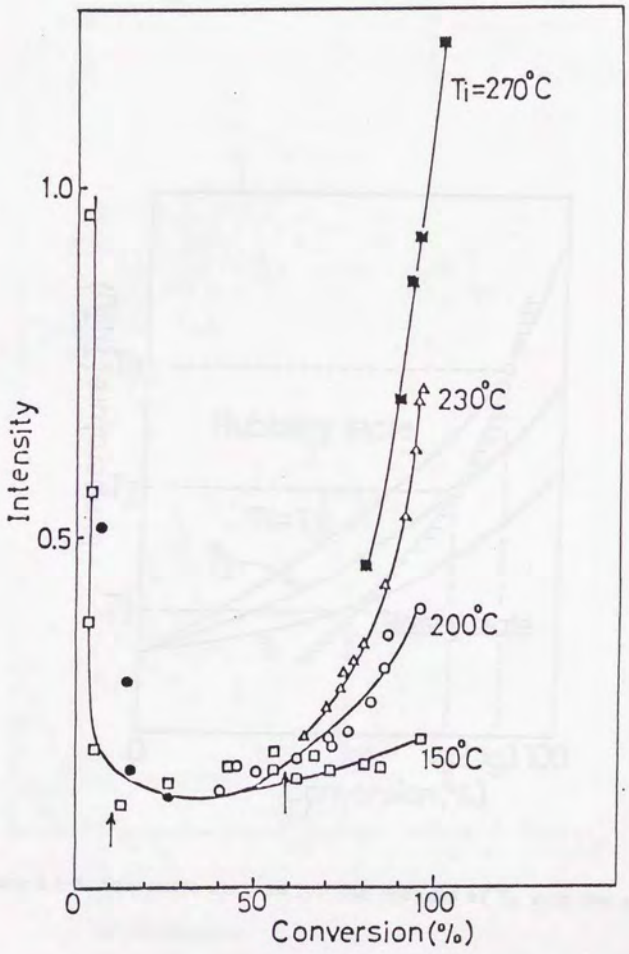

Figure 2.1-7 Fluorescence intensity as a function of conversion.

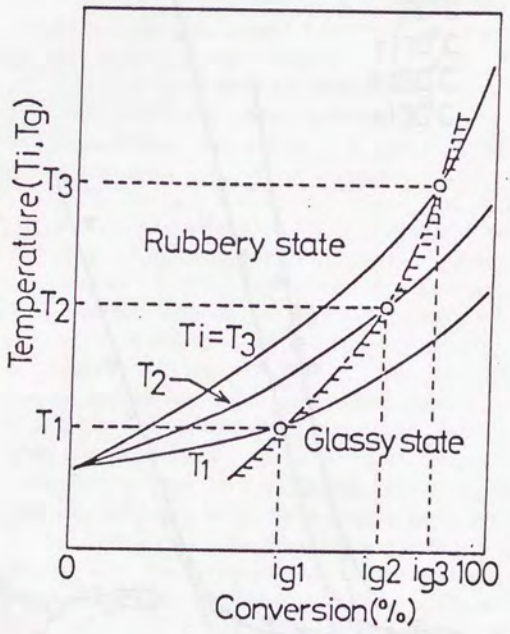

Figure 2.1-8 Schematic diagram for the changes of T_{∞} with the progress of imidization.

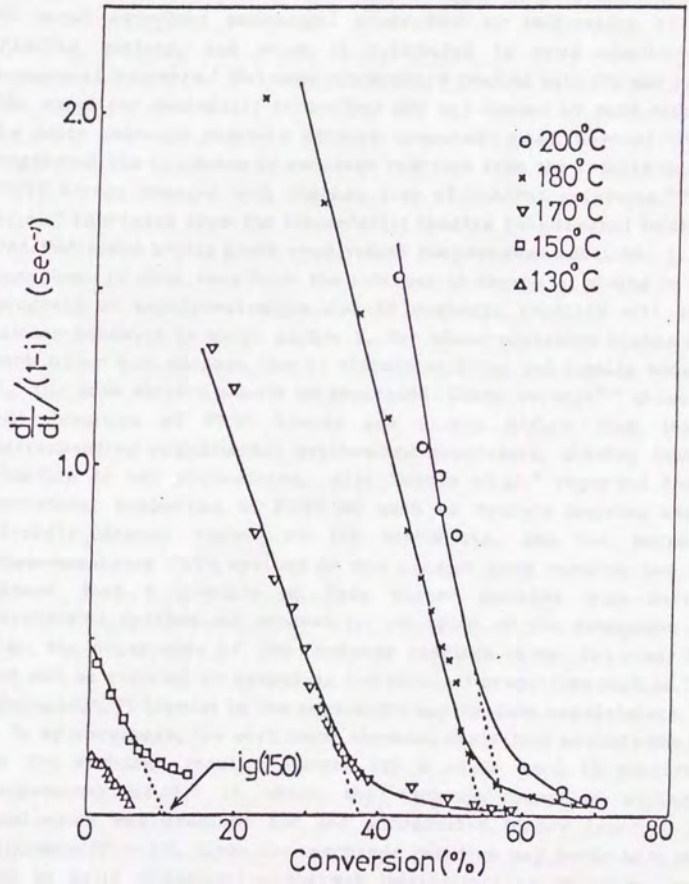

Figure 2.1-9 Apparent rate constant vs conversion.

2.2 Amide Exchange Reaction of Polyimide Precursor.

INTRODUCTION

Molecular composite (MC) consisting of rigid rod polyimide(PI) and flexible PI shows excellent mechanical properties by imidization of cold-drawn PAA/PAA mixture, and which is attributed to good miscibility between component polymers.[1] But some researchers dealing with PIs may suppose that the excellent mechanical properties are not caused by good miscibility but by amide exchange reaction between component PAAs. Several investigators suggested the existence of exchange reaction from the results in which T_g of PI/PI blends changes with storage time of PAA/PAA solutions.[2,3] Smirnova et.al.[4] concluded from the viscoelastic spectra that thermal imidization of a PAA/PAA blend yields block copolyimide via exchange reaction. It is however important to note that both the increase in degree of mixing in blends and progress of copolymerization due to exchange reaction will bring about similar behavior in which double T_g for phase-separated blends approaches each other with storage time of viscous solution and finally becomes single T_g. The both factors should be separated. Other workers[5,6] showed that T_gs and densities of PI/PI blends are always higher than that of the corresponding copolyimides synthesized separately, showing that exchange reaction is not predominant. Also Yokota et.al.[7] reported that several mechanical properties of PI/PI MC such as Young's modulus and strength strongly depend rather on the miscibility, and the macroscopically phase-separated PI/PI systems do not provide good results, and they[8] also showed that a miscible MC have higher modulus than corresponding copolyimide synthesized separately. In spite of the discussion over long time, the occurrence of the exchange reaction is not yet clear because it can not be verified by comparing the physical properties such as T_g of final products(PI/PI blends) to the separately synthesized copolyimides.

To my knowledge, few work using chemical analytical methods has been done on the exchange reaction except for a study used IR spectroscopy by Tsapovetsky et.al.[9] in which the exchange reaction during thermal imidization was examined for the accumulated binary layer of amic acid oligomers(DP $\sim$ 10). Since the exchange reaction may occur both in solution and in solid phase(during thermal imidization) or in either case, it is necessary to argue the reaction conditions separately.

In this section, the mechanisms of the reaction are discussed, and the

reaction rates in solution is estimated from $\bar{M}_w$ changes.

EXPERIMENTAL

PMDA and ODA were recrystallized from dried dioxane and methanol-THF mixture, respectively, and then vacuum dried. DMAc used for preparation of PAA was first dried with molecular sieves(4A) and then vacuum distilled. PAA derived from PMDA and ODA, PAA(PMDA/ODA), was prepared by adding a stoichiometric amount of PMDA powder into DMAc solution of ODA with continuous stirring at room temperature in a nitrogen atmosphere. A viscous PAA solution (10 wt.%) was obtained after several hours($\bar{M}_w$=9.7 × 10^4). The vacuum-dried 1-aminopyrene (APy) was used without further purification. Chemical structures of samples used are shown in Figure 2.2-1. APy of 0-20 wt.% to polymer was added into 10 wt.% PAA solution, and the solution was then stored in degassed sealed tube in the temperature range of 0-60 ℃. Reduced viscosities, η_{red}, were measured at 1 g/dl at 25 ℃ using a Ubbelohde viscometer. For the viscosity measurement in PAA/APy/DMAc, APy/DMAc solution was used as a reference(t_o). $\bar{M}_w$ was determined at 25 ℃ as a function of the storage time in the angle range of 40-130 degree by a LS measurement(Union Giken LS-601).

RESULTS AND DISCUSSION

The author tried to analyze amide exchange reaction by using fluorescence of pyrenyl group. An initial intention was to estimate the degree of exchange reaction from the fluorescence intensity of pyrenyl group covalently introduced into PAA chains due to exchange reaction of PAA with APy. As a model compound of pyrene-labelled PAA, N-pyrenylphthalamic acid derived from phthalic anhydride and APy was synthesized, but unfortunately it was not fluorescent. Then APy fluorescence (peaking at 432 nm) itself could be used because the decrease in free APy can be assumed as the progress of exchange reaction. But as APy was chemically unstable during storage, the solution became colored intensively with time. Hence both the absorbance and fluorescence intensity for the dilute solutions had weak reproducibility. Accordingly, it is impossible to analyze exchange reaction using fluorescence of APy. After all, the exchange reaction was monitored with $\bar{M}_w$ changes.

It is well-known that molecular weight of PAA decreases in solution with

storage time. Effects of polymer concentration, water, and temperature on molecular weight drop have been studied.[10-21] One may consider that amide exchange reaction is closely related to the molecular weight drop.[11,20] Possible type of reactions causing the $\bar{M}_w$ drop and the exchange between PAA and APy in solution are shown in Figure 2.2-2. Connection of reactions (a) and (b) is considered to be the most probable mechanism of $\bar{M}_w$ drop in solution, i.e., cleavage of amide linkage due to catalytic effect of a carboxyl group in the ortho-position,[22,23] with subsequent hydrolysis of the terminal anhydride group due to water present in the system.[24]

It is suggested from several experimental evidences that direct hydrolysis of amide bond as shown in Figure 2.2-2(d) does not proceed practically. The fact that the molecular-weight of an esterified PAA does not practically change in solution during storage suggests that hydrolysis occurs not through direct hydrolysis of amide linkage but through the formation of anhydride end groups with subsequent hydrolysis of anhydrides.[17,25,26] Nisizaki et al.[27] found that little hydrolysis for aromatic polyamide occurs in 1 % NaOH aqueous solution during storage of three months. Bender et.al.[22] measured rate constants of the hydrolysis of phthalamic acid and benzamide in 0.001 M HCl and found that the rate for phthalamic acid is faster than for benzamide by a factor of about 10^5, indicating that mechanism of the anhydride formation is predominant. Also they[22] confirmed the formation of anhydride intermediate during hydrolysis by using a tracer experiment in NMR. Since the difference between rate constant for nucleophilic attack of water to PMDA and that of ODA is not so large,[13] it is reasonable to consider that amide exchange reaction proceeds through mechanism of anhydride formation rather than direct aminolysis.

Figure 2.2-3(a),(b) and (c) shows the effects of the storage temperature on η_{red}, $\bar{M}_w$ and, number of scission per polymer chain, Z, respectively, in PAA/DMAc system. The values of Z were calculated on the basis of an assumption in which molecular weight distribution, $\bar{M}_w/\bar{M}_n$, is constant during storage (if $\bar{M}_w(0)/\bar{M}_n(0) \fallingdotseq \bar{M}_w/\bar{M}_n \fallingdotseq 2$, $Z=\bar{M}_n(0)/\bar{M}_n-1 \fallingdotseq \bar{M}_w(0)/\bar{M}_w-1$, where $\bar{M}_w(0)$ and $\bar{M}_n(0)$ denote initial weight- and number-average molecular weights). It is clearly shown from the decrease in both the η_{red} and $\bar{M}_w$ with storage time that chain scission occurs rather than the occurrence of conformation changes of polymer chains due to slight imidization (Figure 2.2-2(f)) or deterioration of solvent quality due to water released by imidization,[19,21] because the degree of imidization was very small in the range of 0-60 ℃. The increase in temperature accelerates the decrease in η_{red} and $\bar{M}_w$ and the increase in Z. In the later stage of storage the value of $\bar{M}_w$ becomes nearly constant with their absolute values depending on the temperature. This

behavior is also shown in the literature concerning $\bar{M}_w$ drop of PAA in solution.[10-21] With increasing water content, viscosity drop at the initial stage becomes remarkable. However Miwa et.al.[21] showed that in DMAc solution of PAA(BPDA/PDA) the $\bar{M}_w$ is little affected by further addition of water in the later stage. If the equilibrium constant for dissociation in Figure 2.2-2(a), which is less than 10^{-5} in a reference,[14,15] is constant in the whole stage, $\bar{M}_w$ should continue to decrease gradually as long as water remains. This is contrary to the explanation that stop of $\bar{M}_w$ drop is due to the consumption of water in the system by anhydride end groups. Moreover as will be discussed later, stop of $\bar{M}_w$ drop is also observed despite the case where enough APy to react with PAA remains. According to David et.al.,[20] both $Z(=\bar{M}_n(0)/\bar{M}_n-1)$ and $\bar{M}_w(0)/\bar{M}_w-1$ should increase linearly with time with different gradients when only random chain scission occurs. Although it is not yet clear, The stop of $\bar{M}_w$ drop in the later stage may be due to the change in the reactivity of terminal anhydride with water which is related to the shape of polymer coils.

An amide exchange reaction can be caused by chain scission into amine and anhydride, with subsequent reconnection between different terminal amines and anhydrides (Figure 2.2-2(a) and (c)). In order to accelerate the reaction, large amounts of Apy(20 wt.% to PAA, i.e., 0.092 mol/l) was added into 10 % PAA solution. In this system, the ratio of APy to repeating unit concentration is 0.37. The changes in η_{red}, $\bar{M}_w$, and Z in PAA/Apy/DMAc system are shown in Figure 2.2-4(a), (b), and (c), respectively. Comparing to the results in PAA/DMAc system without APy, the rates of $\bar{M}_w$ drop in the initial stage increases really by the addition of APy. For example, in PAA/DMAc, Z is about 2 after a week at 60 ℃ while is about 5 in PAA/APy/DMAc. The stop of the reaction was also observed as well as in the case of PAA/DMAc, in spite of the fact that enough APy to react with PAAs remains in the system.

Figure 2.2-5 shows Arrhenius plots for apparent rate constants, k, for the initial $\bar{M}_w$ drop (the gradient for the linear portion of Z value against time). Although the absolute value of k for PAA/APy/DMAc system is lager than for PAA/DMAc in the experimental temperature range, similar E_a values, 13 kcal/mol were obtained for PAA/DMAc and PAA/APy/DMAc. E_a value obtained from the rate constant in Δ Z-time curve where Δ Z denotes difference between Z for PAA/APy/DMAc and for PAA/DMAc equals to 13 kcal/mol. The result is consistent with the activation energy(10 kcal/mol) for decomposition of PAA(PMDA/ODA) in DMF by Bel'nikevich et.al.[19] Let us now turn to reaction scheme in Figure 2.2-2. The scheme of exchange reaction is rewritten as follows.

$$AB \underset{k_2}{\overset{k_1}{\rightleftarrows}} A+B \xrightarrow{k_3[C]} AC+B \qquad (1)$$

where AB, A and B denote amide, anhydride and amino groups, respectively, and C and AC are water or APy and APy end-capped amide group.

$$\frac{d[AC]}{dt} = k_3[C][A] \qquad (2)$$

From the steady-state approximation,

$$\frac{d[A]}{dt} = k_1[AB]-k_2[A]^2-k_3[C][A] = 0 \qquad (3)$$

eq.(2) and (3) gives

$$\frac{d[AC]}{dt} = \frac{k_1k_3[C][AB]}{k_2[A]+k_3[C]} \qquad (4)$$

Provided that a condition $k_2[A] \gg k_3[C]$ is realized, eq.(4) reduces to

$$\frac{d[AC]}{dt} = \frac{k_1k_3[C][AB]}{k_2[A]} \qquad (5)$$

Assuming $k_2[A] \ll k_3[C]$ under an excess of APy, eq.(5) becomes a simple form.

$$\frac{d[AC]}{dt} = k_1[AB] \qquad (6)$$

In fact, it is difficult to get k_2 and k_3 experimentally. The last equation means that dissociation of amide bonds is rate-determining step in the exchange reaction, and that the rate of chain scission is independent of [C]. If the reaction obeys eq.(6), only one E_a and k should be determined regardless of addition of APy, respectively. As shown in Figure 2.2-5, k for PAA/APy/DMAc is always larger than for PAA/DMAc, indicating that the decomposition of amide linkage is not rate-determining step for $\bar{M}_w$ drop.

Furthermore, the effect of APy concentration on $\bar{M}_w$ drop is examined. As shown in Figure 2.2-6(a),(b) and (c), the changes in η_{red}, $\bar{M}_w$, and Z at 60 ℃ become marked with increasing APy concentration. Figure 2.2-7 shows the

plot of Z per unit time(gradient at initial linear portion) against APy concentration at 60 ℃. It should be noted that the initial gradient, dZ/dt(∝ [AC]/dt), is proportional to [C]. The value of Z at [C]=0 corresponds to the rate of hydrolysis of anhydride end groups due to water in the system. According to eq.(2), from the gradient of dZ/dt(∝ d[AC]/dt) vs [C] curve in Figure 2.2-7, the terminal anhydride concentration, [A](=[B]), can be estimated although it depends on k_3 used. Although it is difficult to determined the value of k_3 exactly, it was roughly estimated from a reaction of phthalic anhydride(PAn) with APy and was 10^{-3} $M^{-1}s^{-1}$ at 25 ℃ in DMAc, and an extrapolated value at 60 ℃, 3×10^{-3} $M^{-1}s^{-1}$, was obtained using an activation energy, 6 kcal/mol[17]. Several kinetic parameters determined experimentally and calculated are summarized in Table 2.2-1.

For real terminal anhydrides in PAA(PMDA/ODA) chains, amide and carboxyl groups on the benzene ring in PAn play a role as electron withdrawing groups, resulting in the increase in acylation rate for APy, comparing to PAn without substituents. Svetlichnyi et.al.[29] studied the reaction between 4-aminodiphenyl ether(ADE) and various anhydrides. By using the value of 1.52 eV for the electron affinity of monoaminated PMDA(MAPMDA)[30] which is a model of terminal anhydride, the rate constant for the reaction of terminal anhydride with ADE was estimated to be 2.0 $M^{-1}s^{-1}$ at 25 ℃. This value is

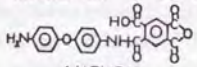

MAPMDA

larger 20 times than 0.1 $M^{-1}s^{-1}$ obtained from the reaction between ADE and PAn without substituents. It is thus expected that rate of the reaction of real terminal anhydride with APy is faster about 20 times than for the reaction of PAn with APy because of the effects of the electron withdrawing substituents(-CONHAr and -COOH), and is 2×10^{-2} $M^{-1}s^{-1}$ at 25 ℃ and 6×10^{-2} $M^{-1}s^{-1}$ at 60 ℃ (extrapolated). After all the terminal anhydride concentration, [A](=[B]), was roughly estimated as about 2×10^{-5} mol/l at 60 ℃.

Let us consider the exchange reaction between different PAAs in solution. When PAA(PMDA/ODA) was mixed with other PAA in solution, if the equilibrium constant is similar, [A](equals to terminal amine concentration,[B]) is almost 2×10^{-5} mol/l at 60 ℃ for PAA/PAA system in solution. As shown in Figure 2.2-7, the exchange reaction is not affected at all by the very small amount of APy (2×10^{-5} mol/l). Accordingly, it is expected that the exchange reaction between different PAAs at 60 ℃ may be little, provided that the reactivity of the terminal anhydrides with the terminal amines formed by cleavage of amide bonds in PAA(PMDA/ODA) is similar to that of the terminal

anhydrides with APy.

By comparing rate constants for two systems, i.e., MAPMDA/APy and MAPMDA/ADE, where ADE is a model of terminal amine, the rate constant for the latter system is larger than for the former by a factor of 100 as shown in Table 2.2-1. By simply assuming that the gradient in dZ/dt vs [C] plots for real PAA/PAA system is larger 100 times than for PAA/APy, Z per one hour at 60 ℃ was obtained to be 4×10^{-3}. It is concluded from the result that the exchange reaction in PAA/PAA system in solution at 60 ℃ is negligible unless storage time is not so long. Also this indicates that it is negligible when PAA/PAA blend films are prepared by solution casting at 50-60 ℃.

At lower temperatures the equilibrium shifts toward amic acid. The [A] calculated from activation energies[17] of amide bond cleavage(22 kcal/mol) and acylation(6 kcal/mol) is 5×10^{-6} mol/l at 25 ℃ and 10^{-6} mol/l at 1 ℃. The calculated value at 1 ℃ is almost consistent with the value estimated from the fact that rate of the exchange reaction at 1 ℃ in the initial stage is slower about 36 times than at 60 ℃ as shown in Figure 2.2-4(c). Accordingly it is concluded that the exchange reaction between different PAAs proceeds scarcely during the storage of PAA/PAA solution under a condition(1 ℃, during one month at least). Moreover it should be noted that this estimation is applicable to the phenomenon only for the initial stage of the reaction. By taking into account the decrease in the reaction rate in the later stage during storage (behavior for stop of $\bar{M}_w$ drop), the exchange reaction will become unfavorable compared with above estimation. Furthermore, according to Bel'nikevich et.al.,[19] imidization proceeds predominantly compared with decomposition of amide bonds above 25 ℃ in solution, indicating that imidization occurs prior to exchange reaction during storage of PAA/PAA solution at higher temperature so that random copolymer can not be formed due to exchange reaction even if the solution was stored during infinite time.

CONCLUSION

Amide exchange reaction proceeds through decomposition of amide linkage into anhydride and amine end groups. Apparent activation energies for $\bar{M}_w$ drop, 13 kcal/mol were obtained in PAA/DMAc and PAA/APy/DMAc, respectively. Dependence of $\bar{M}_w$ drop on APy concentration shows that the exchange reaction between different PAAs in solution at lower temperatures is little during storage about one month at least.

REFERENCES

1. R.Yokota, R.Horiuchi, M.Kochi, H.Soma and I.Mita J.Polym.Sci.:Part C, 26, 215(1988).
2. M.Ree, D.Y.Yoon and W.Volksen, Polym.Mat.and Sci.Eng.ACS., 60, 179(1989).
3. C.Feger, ACS Polym.Div., San Diego Conf., January 22, 1990.
4. V.Ye.Smirnova, M.I.Bessonov, T.I.Zhukova, M.M.Koton, V.V.Kudryavtsev, V.P.Sklizkova and G.A.Lebedev, Polym.Sci. U.S.S.R., 24, 1375(1982).
5. P.M.Tanunina, Z.I.Gomoreva, E.G.Lur'e, V.D.Vorob'ev, M.L.Dobrokhotova, E.I.Efimova and T.I.Safronova, Plast.Massy., No.9, 45(1975).
6. T.L.St.Clair, M.K.Gerber and C.R.Gautreaux, Polym.Mat.and Sci.Eng.ACS, 60, 183(1988).
7. R.Yokota, Doctoral thesis, The University of Tokyo(1990).
8. R.Yokota, H.Soma, V.Sinigersky, M.Kochi and I.Mita, Polym.Prepr.Jpn., 37, No.4, 1058(1988).
9. M.I.Tsapovetsky and L.A.Laius, in "Polyimides: Materials, Chemistry and Characterization", C.Feger, M.M.Khojasteh and J.E.McGrath(Eds.), Elsevier, p379, 1989.
10. G.M.Bower and L.W.Frost, J.Polym.Sci.:Part A, 1, 3135(1963).
11. L.W.Frost and I.Kesse, J.Appl.Polym.Sci., 8, 1039(1964).
12. C.E.Sroog, A.L.Endrey, S.V.Abramo, C.E.Berr, W.M.Edwards and K.L.Orivier, J.Polym.Sci.:Part A, 3, 1373(1965).
13. R.A.Dine-Hart and W.W.Wright, J.Appl.Polym.Sci., 11, 609(1967).
14. A.Ya.Ardashnikov, I.Ye.Kardash and A.N.Pravednikov, Polym.Sci. U.S.S.R.,13, 2092(1971).
15. A.N.Pravednikov, I.Ye.Kardash, E.N.Teleshov and B.V.Kotov, Polym.Sci. U.S.S.R., 13, 483(1971).
16. V.Ye.Eskin, I.A.Baranovskaya, M.M.Koton, V.V.Kudryavtsev, and V.P.Sklizkova, Polym.Sci.USSR., 18, 2699(1976).
17. P.P.Nechayev, Ya.S.Vygodskii, G.Ye.Zaikov and S.V.Vinogradova, Polym.Sci.USSR., 18, 1903(1976).
18. N.G.Bel'nikevich, N.A.Adrova, L.N.Korzhavin, M.M.Koton, Yu.N.Ponov and S.Ya.Frenkel', Polym.Sci. U.S.S.R., 15, 2057(1973).
19. N.G.Bel'nikevich, V.M.Denisov, L.M.Korzhavin and S.Ya.Frenkel', Polym.Sci. U.S.S.R., 23, 1406(1981).
20. M.-J.Brekner and C.Feger, J.Polym.Sci.:Part A, 25, 2479(1987).
21. T.Miwa and S.Numata, Polymer, 30, 893(1989).
22. M.L.Bender, Y.L.Chow and F.Chloupek, J.Am.Chem.Soc., 80, 5380(1958).
23. H.Morawetz and J.Shafer, J.Am.Chem.Soc., 84, 3783(1962).

24. E.V.Kamzolkina, P.P.Nechayev, Ya.S.Vygodskii and G.E.Zaikov, Dokl.Phys.Chem., 233, 156(1977).
25. S.Nishizaki and T.Moriwaki, Ind.Chem.Mag., 71, 1559(1968).
26. S.N.Khar'kov, Ye.P.Krasnov, Z.N.Lavrova, S.A.Baranova, V.P.Aksenova, and A.S.Chegolya, Polym.Sci. U.S.S.R., 13, 940(1971).
27. S.Nishizaki, A.Fukami, Ind.Chem.Mag., 71, 1565(1968).
28. C.David and D.B.Volant, Eur.Polym.J., 14, 29(1978).
29. V.M.Svetlichnyi, K.K.Kalnin'sh, V.V.Kudryavtsev and M.M.Koton, in "Polyimides", M.I.Bessonov, M.M.Koton, V.V.Kudryavtsev and L.A.Laius(Eds.), Plenum, p18, 1987.
30. V.M.Denisov, V.M.Svetlichnyi, V.A.Gindin, V.A.Zubkov, A.I.Kol'tsov, M.M.Koton and V.V.Kudryavtsev, in "Polyimides", M.I.Bessonov, M.M.Koton, V.V.Kudryavtsev and L.A.Laius(Eds.), Plenum, p25, 1987.

Table 2.2-1 Rate constants for several reactions of anhydride with amine and terminal amine concentration [A] determined by IR spectroscopy and calculated one.

	rate constant($M^{-1}s^{-1}$)				
T (℃)	PAn/APy	MAPMDA/APy[a]	PAn/ADE	MAPMDA/ADE[a]	[A](mol/l)
25	10^{-3}	2×10^{-2}	0.1	2	5×10^{-6}
60[b]	3×10^{-3}	6×10^{-2}	0.3	6	2×10^{-5}

[a] estimated using an electron affinity(1.52 eV) of MAPMDA(ref. 29 and 30).

[b] calculated using an activation energy(6 kcal/mol)(ref.17).

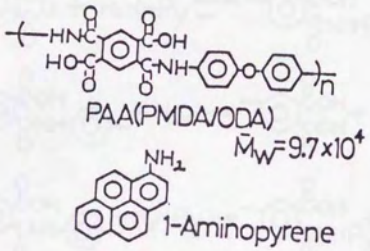

Figure 2.2-1 The chemical structures of samples used.

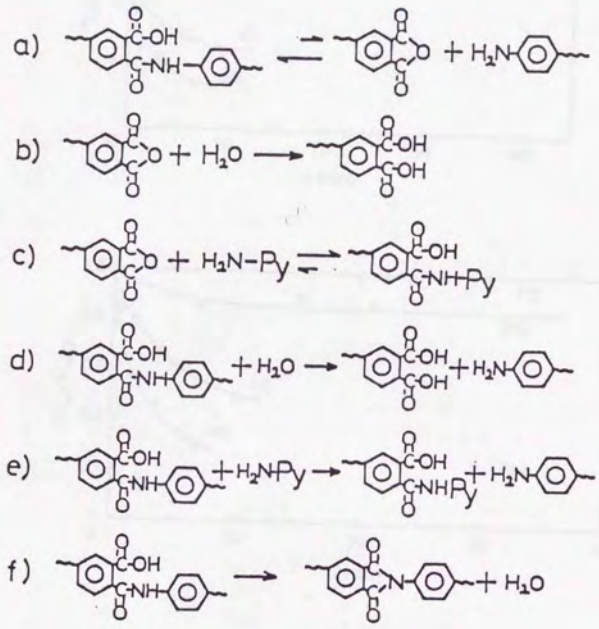

Figure 2.2-2 Reaction scheme of PAA in solution containing APy.

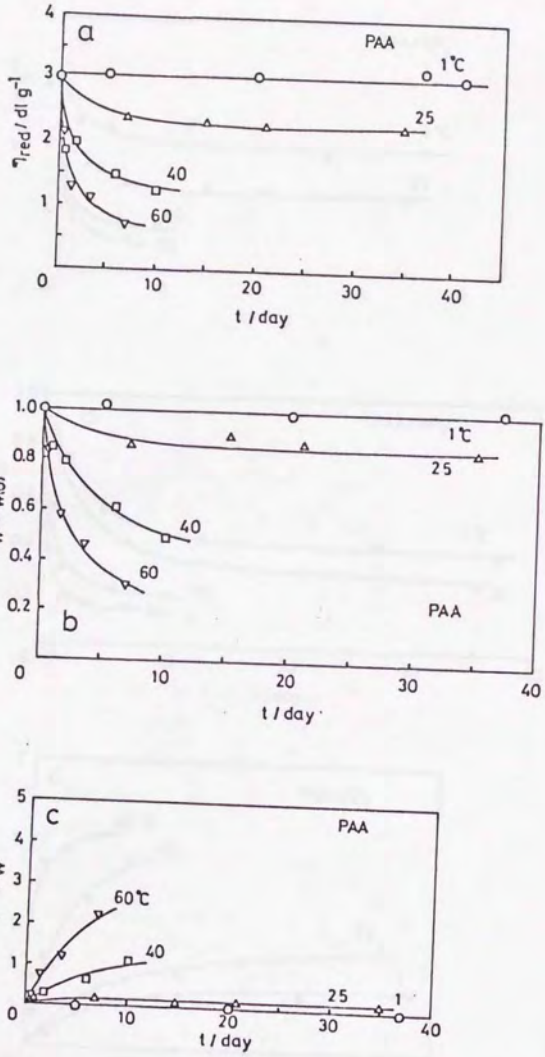

Figure 2.2-3 The changes in η_{red}(a), $\bar{M}_w$(b) and Z(c) for PAA/DMAc during storage at 0-60 ℃.

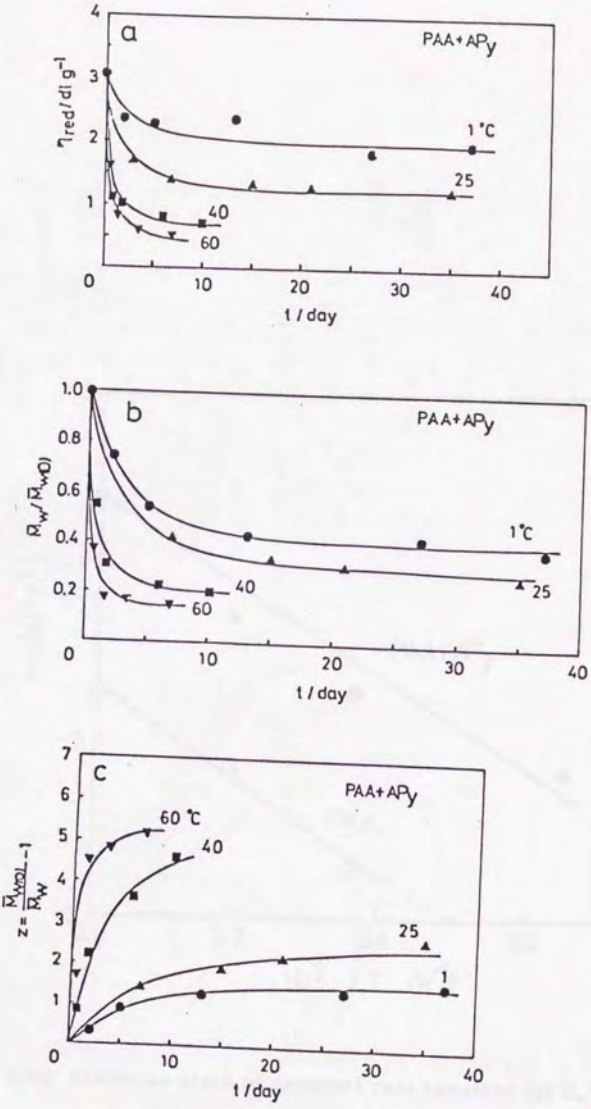

Figure 2.2-4 The changes in η_{red}(a), $\bar{M}_w$(b) and Z(c) for PAA/APy/DMAc during storage at 0-60 ℃.

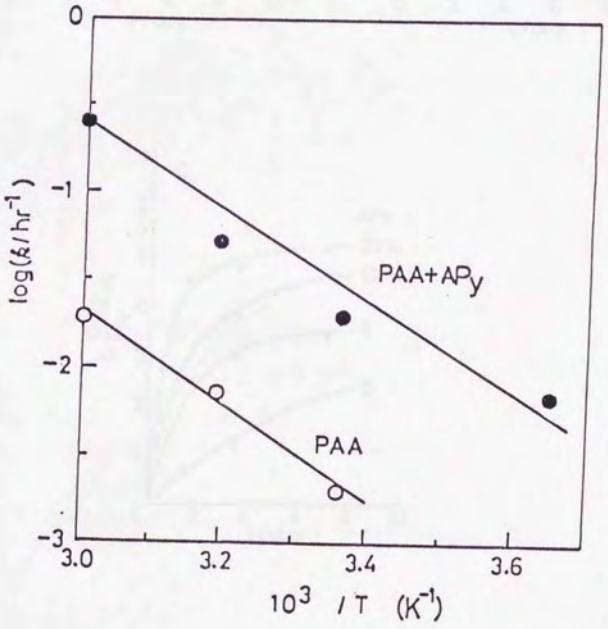

Figure 2.2-5 Arrhenius plots of apparent rate constant for $\bar{M}_w$ drop in PAA/DMAc and PAA/APy/DMAc.

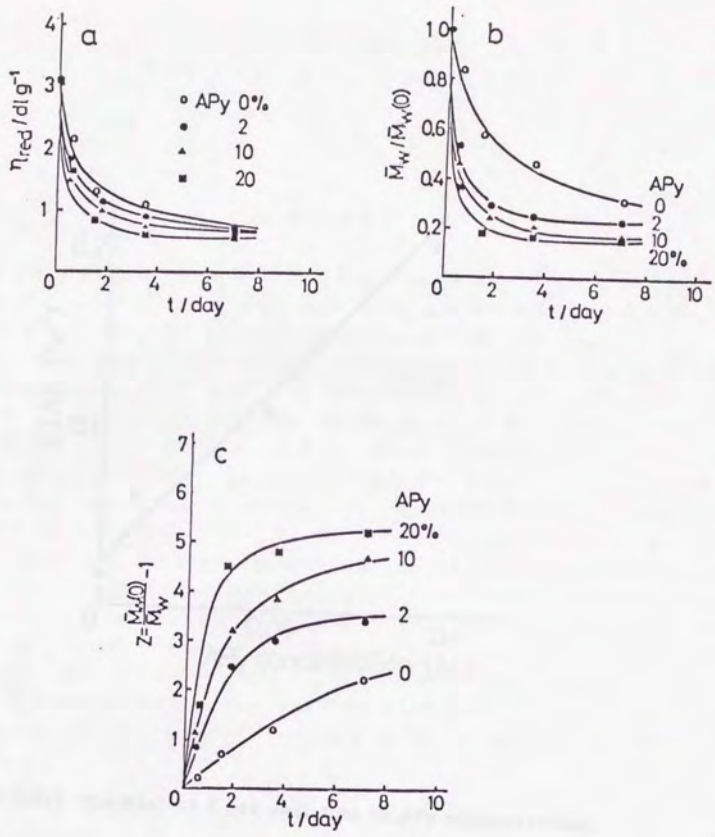

Figure 2.2-6 The effect of APy concentration on the changes in η_{red}(a), $\bar{M}_w$(b) and Z(c) during storage at 60 ℃.

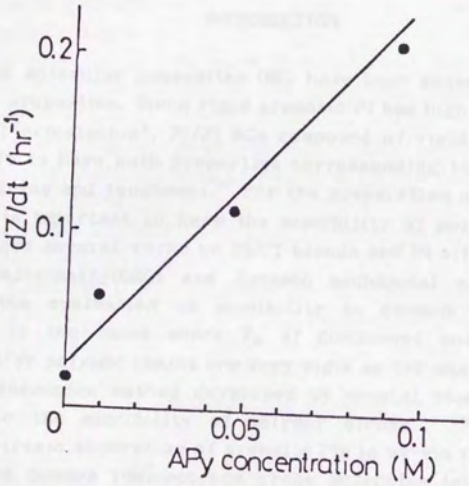

Figure 2.2-7 The plot of Z per unit time vs APy concentration.

CHAPTER 3

MISCIBILITY OF POLYIMIDE/POLYIMIDE BLENDS AND CHARGE-TRANSFER FLUORESCENCE SPECTRA

INTRODUCTION

Rigid rod molecular composites (MC) have been shown to have outstanding mechanical properties. Since rigid aromatic PI has high modulus and strength by uniaxial orientation[1], PI/PI MCs composed of rigid rod and flexible PIs are possible to have both properties corresponding to each component such as high modulus and toughness.[2] For the preparation of PI/PI MC or other PI alloys, it is important to know the miscibility of polymer mixtures.[3,4] So far, there are several works on PI/PI blends and PI alloys.[5-12] Differential scanning calorimetry(DSC) and dynamic mechanical analysis(DMA), usually used for the evaluation of miscibility in common polymer blends, are unsuitable to the cases where T_g of component polymers is close each other[13] and/or polymer chains are very rigid as for wholly aromatic PIs.

Photoluminescence method developed by several research groups is very sensitive to the miscibility of polymer blends.[14-19] Unfortunately, the strong electronic absorption of aromatic PIs in uv-vis region makes difficult to introduce common luminescence probe molecules into PI system. In this section, it is shown that the intrinsic fluorescence in solid PI which is due to intermolecular CT interaction[20] is very useful to study the miscibility of PI/PI blends.

EXPERIMENTAL

PAA was synthesized as described in section 1.1. The chemical structures and symbols of PIs used are shown in Figure 3-1. The weight-average molecular-weight $\bar{M}_w$ of PAAs determined by a light-scattering method (Union Giken, model LS-601), extinction coefficient ε and density are summarized in Table 3-1. Homo PAA films were prepared by casting 10 wt% PAA solution in N,N-dimethylacetamide (DMAc) onto a glass plate at 50 ℃, followed by vacuum drying at 50 ℃ for 24 h. Imidization does not practically occur at around 50

℃. PAA/PAA binary blends were prepared by dissolving the given ratio of solid PAAs into dry DMAc at 7-8 wt% in polymer concentration at 0-5 ℃ away from moisture in air, and followed by vacuum drying at 50 ℃ for 24 h. Then PAA/PAA blend films were thermally imidized stepwise at 150 ℃ for 1 h, 200 ℃ for 1 h, and 250 ℃ for 2 h (step 250 ℃) in a vacuum oven to obtain PI/PI blend films (30-40 μ m thick).

Fluorescence measurements were carried out using a fluorescence spectrophotometer (Hitachi, model 850). The spectra were obtained at room temperature in a front-face arrangement using 5 nm bandpasses for both the excitation and emission side. The reabsorption of the fluorescence is negligible in all cases.

Refractive indices n_D of homo PI films were measured using a Abbe's refractometer. The morphology of the phase-separated blends was observed using a phase-contrast microscope.

Dynamic mechanical measurements were carried out using a viscoelastometer (Toyo Baldwin, Rheovibron model Rheo-200) at 110 Hz at a heating rate of 3 ℃ /min.

Densities of the blend films were measured using a density gradient column (xylene-carbon tetrachloride).

Extinction coefficient ε was determined from the absorbance, density, and film thickness using a a uv-vis spectrophotometer (Jasco, model UVIDEC-660).

RESULTS AND DISCUSSION

Miscibility of PAA/PAA and PI/PI blends

Since PI/PI blends are generally obtained by thermal cyclization reaction of PAA/PAA blends, the morphology of PI/PI blends formed depends upon three factors, the miscibility of initial PAA/PAA blends, the rigidity of component PI chains which increases as the reaction proceeds, and translational diffusion of the PI chains. The following factors should be noted on the basis of rigidity of PI chains.

(1) The miscibility of PI/PI blends in thermodynamical equilibrium state.

When PI chains are flexible, phase-equilibrium can be realized by sufficient thermal treatment above the T_g of PI/PI blends. Accordingly, even if the PAA/PAA blend is immiscible, it is possible to change the blend morphology of the PI/PI blend from inhomogeneous to homogeneous by sufficient heat treatment if the PI/PI blend is miscible in thermodynamical equilibrium state.

(2) The miscibility of PI/PI blends formed under non-equilibrium conditions.

When PI chains are very rigid, the PI/PI blend formed is in non-equilibrium state because molecular mobility of the PI chains decreases rapidly as imidization proceeds. This means that miscibility of the PI/PI blend depends strongly on that of initial PAA/PAA and imidization conditions.

Since thermal imidization of PAAs is intramolecular cyclization reaction, so large molecular motion is not required for the reaction. This can be understood from the fact that the reaction proceeds gradually even if the T_g going up with imidization exceeds imidization temperature T_i. On the other hand, very large motion of PI chains (translational diffusion) is required for the change in blend morphology. Therefore it is empirically expected that when imidized at step 250 ℃ T_i will be always lower than T_g which increases as imidization proceeds, because both the deformation of the films and adhesion between the films and aluminum wrapping foil are not observed during imidization at step 250 ℃.

As example of case (2), PI(BPDA/PDA)/PI(PMDA/ODA) blend is cloudy owing to phase separation, and both component polymer chains are very rigid.[1,21] Actually, when imidized at step 250 ℃, there was little difference between the PAA/PAA and PI/PI blends in the phase-separated structures, showing that the morphology of PAA/PAA is fixed. This means that the miscibility of the PI/PI blend depends on the miscibility of initial PAA/PAA blend. Imidization at step 250 ℃ is kinetically controlled process, and the PI/PI blend formed is in non-equilibrium state.

The experimental result that additional heat treatment at above T_g of both component PIs for the PI/PI imidized at step 250 ℃ does not change the blend morphology indicates that the PI/PI imidized at 250 ℃ is perfectly frozen. Although the PI/PI is not in thermodynamical equilibrium state, it is important to argue the degree of mixing for the frozen PI/PI.

As mentioned above, since the miscibility of rigid PI/PI blends depends strongly on that initial PAA/PAA blends, it is very important to control the miscibility of PAA/PAA blends. Effect of T_{cast} on the miscibility of PAA/PAA blends is remarkable. This point is discussed later.

One may point out possibility of amide exchange reaction in PAA/PAA system in solution[22] or in solid state.[11] But the results in section 2.2 show that the exchange reaction is not predominant under our experimental conditions.

Fluorescence Spectra of PI/PI blends

In section 1.1 it was shown that PI(BPDA/PDA) emits comparatively strong

fluorescence among PIs used, and PI(PMDA/PDA) and PI(PMDA/ODA) are almost non-fluorescent. Consequently the fluorescence of PI(BPDA/PDA) mixed with the non-fluorescent PI will present information for the degree of self-aggregation of PI(BPDA/PDA) chains (in other words, degree of mixing). Two blend systems, transparent PI(BPDA/PDA)/PI(PMDA/PDA) and cloudy PI(BPDA/PDA)/PI(PMDA/ODA) blends were selected for fluorescence measurements.

Figure 3-2 shows the blend ratio dependence of the fluorescence spectrum for transparent PI(BPDA/PDA)/PI(PMDA/PDA). With the addition of non-fluorescent PI(PMDA/PDA) into fluorescent PI(BPDA/PDA), the fluorescence intensity decreases for the blend. As shown in Figure 3-3, the experimental data (open circles) deviate to the lower direction from simple additive law corresponding to the perfectly phase-separated blends. The additive law curves are calculated on the basis of the following equation.

$$I_{bl} = \frac{\varepsilon_1 C_1}{\varepsilon_1 C_1 + \varepsilon_2 C_2} I_1 + \frac{\varepsilon_2 C_2}{\varepsilon_1 C_1 + \varepsilon_2 C_2} I_2$$

where I, ε, and C represent fluorescence intensity, extinction coefficient in $M^{-1}cm^{-1}$, and concentration in mol/l, respectively. Suffixes bl, 1, and 2 denote blend, PI(BPDA/PDA), and non-fluorescent PIs (PI(PMDA/PDA) or PI(PMDA/ODA) or PI(PMDA/PDA;ODA)), respectively. I_2 is negligible. For the phase-separated blend, eq.(1) should be corrected to the loss of incident light due to light-scattering. But since the light absorption at 350 nm in PI/PI blends is very strong (absorbance is more than 3), and the scattering light intensity is small at the whole blend ratios (within 5%), the correlation to the loss of the fluorescence and incident light is practically negligible. Also the author confirmed using a thermotropic liquid crystalline polymer(LCP) in amorphous state (transparent) and in LC state (turbid) that the position of the LCP's fluorescence is independent of the turbidity of film. Accordingly, the changes in the fluorescence intensity and position are essential phenomenon for the cloudy PI/PI blends. The fluorescence behavior for PI(BPDA/PDA)/PI(PMDA/PDA) in Figure 3-3 means that PI(PMDA/PDA) chains enter into PI(BPDA/PDA) phase and the formation of the intermolecular CTC in PI(BPDA/PDA) is hindered as the result. If no interaction between the component polymers exists, the experimental data should approach to the additive law curves (broken line), and the spectral shape for blends and for homo PI(BPDA/PDA) should be identical. But in Figure 3-4 the spectral shapes for PI(BPDA/PDA)/PI(PMDA/PDA) are not consistent with that for homo PI(BPDA/PDA), showing the presence of some

interchain interactions in this blend.

For immiscible PI(BPDA/PDA)/PI(PMDA/ODA), the blend ratio dependence of the fluorescence spectra is shown in Figure 3-5. With the addition of PI(PMDA/ODA) into PI(BPDA/PDA), the fluorescence increases first, then decreases as shown in Figure 3-3. It is interesting to note that the fluorescence intensity at blend ratio of 8/2 is stronger than that for pure PI(BPDA/PDA) although the reason is not yet clear. The intensity as a function of blend ratio indicates that the miscibility of PI(BPDA/PDA)/PI(PMDA/PDA) is better than that of PI(BPDA/PDA)/PI(PMDA/ODA) because the intensity for the former is smaller than that for the latter at the whole blend ratios.

It is reasonable to assume that for PI(BPDA/PDA)/PI(PMDA/ODA) some electronic interaction between component PIs is little except for contact at the interface because phase separation occurs. Although it is not clear, the unusual behavior in PI(BPDA/PDA)/PI(PMDA/ODA) such as fluorescence enhancement and spectral shift may be due to internal stress generated during thermal imidization of the phase-separated PAA/PAA blend.

Dynamic Mechanical Spectra

As refractive indices of homo PI(BPDA/PDA) and homo PI(PMDA/PDA), which depends on cure condition, are 1.544 and 1.553 respectively, if in PI(BPDA/PDA)/PI(PMDA/PDA) the phase separation occurs, the films should become cloudy owing to the difference of n_D.[23] Practically, the blend films prepared from T_{cast} of 50 ℃ are clear at the whole blend ratios, the domains due to phase separation are not observed by optical microscope. This indicates that the domains are smaller than the wavelength of visible light.

In order to obtain further information on the degree of mixing, dynamic mechanical spectrum was measured for the blends and component PIs. Fortunately, DMA is applicable to the component PIs imidized at step 250 ℃ although when the PIs are post-cured at more than 330 ℃ the PIs do not show clear α loss peak. Figure 3-6 (a)-(1) and (b) shows storage modulus E' and loss modulus E'' curves for homo PI(BPDA/PDA) and PI(BPDA/PDA)/PI(PMDA/PDA) (5/5, T_{cast}=50 ℃), respectively. Unfortunately, it was impossible to measure the modulus of thermally imidized PI(PMDA/PDA) because the PI film is very brittle in spite of the fact that initial PAA has high molecular-weight. Homo PI(BPDA/PDA) shows a α loss peak at about 310 ℃ and a broad β loss peak at around 230 ℃. The blend has also a α loss peak at the temperature corresponding to pure PI(BPDA/PDA), showing PI(BPDA/PDA) phase exists partially in the blend. The broad loss peak at

around 370 ℃ for the blend is very likely different from α loss peak due to PI(PMDA/PDA) because it has been reported that the calculated T_g is about 700 ℃ [24] (it is difficult to determine the T_g experimentally because of thermal degradation) and different from β loss peak due to PI(PMDA/PDA) as described below. Accordingly, it appears that the peak at 370 ℃ is due to the partial mixing phase. Although the author do not have the data for pure PI(PMDA/PDA) imidized at step 250 ℃, from the following experimental results it is reasonable to assume that β loss peak of PI(PMDA/PDA) around 80 ℃. Dynamic mechanical spectra of PI(PMDA/PDA;ODA) copolymers (PDA=0-80 mol%) imidized at step 250 ℃ show that β loss peak always appear at around 80 ℃ regardless of PDA content in the copolyimide. According to Kochi et al., the position of β loss peak for PI(PMDA/ODA) is independent to cure condition unlike the T_g depends on cure condition.[21] Furthermore, the dynamic mechanical spectra of chemically imidized PI(PMDA/PDA) can be measured. The E" curve for the PI shows a β loss peak around 80 ℃.[25] On the basis of T_g criterion for miscibility of polymer blends, in the E" curve of the blend where β loss peak appears at intermediate position between PI(BPDA/PDA)(230 ℃) and PI(PMDA/PDA)(80 ℃), the effect of mixing is observed. This becomes clear in comparison with the phase-separated PI(BPDA/PDA)/PI(PMDA/ODA) in Figure 3-6 (c) where each β loss peak of PI(BPDA/PDA) and PI(PMDA/ODA) appears independently.

On the other hand, as shown in Figure 3-6 (c) the E" curve for cloudy PI(BPDA/PDA)/PI(PMDA/ODA)(5/5, T_{cast}=50 ℃) shows a α loss peak corresponding to PI(BPDA/PDA) without peak due to partial mixing phase. The E' curve decreases rapidly above 310 ℃ as well as in the case of homo PI(BPDA/PDA). No effect of mixing is observed for PI(BPDA/PDA)/PI(PMDA/ODA) when T_{cast} is 50 ℃. The conclusion obtained by DMA in which the degree of mixing for PI(BPDA/PDA)/PI(PMDA/PDA) is better than for PI(BPDA/PDA)/PI(PMDA/ODA) coincides qualitatively with the fluorescence data.

PI(BPDA/PDA)/PI(PMDA/PDA:ODA) blend

Since PI(BPDA/PDA)/PI(PMDA/PDA) and PI(BPDA/PDA)/PI(PMDA/ODA) are transparent and cloudy, respectively, when random copolymer PI(PMDA/PDA;ODA) (PDA=20-90 mol%) is used as a component of the blends it is expected that with increasing PDA content in the copolyimide the morphology in the blend of PI(BPDA/PDA) with the copolyimide changes from heterogeneous to homogeneous and that the fluorescence in the blend reduces successively. The copolyimides imidized at step 250 ℃ were non-fluorescent. The observation of the blend morphology by a

phase-contrast microscope (Figure 3-7) shows really successive reduction in domain size with increasing PDA content in the copolyimide. In Figure 3-8, the fluorescence of the blends reduces with slight spectral shift as the blend becomes homogeneous. The changes in the intensity and the peak position are plotted in Figure 3-9. It is interesting to note that the additive law curve (broken line) is nearly independent of PDA content, while the experimental data rapidly decreases with the increase in PDA content. Further experimental evidence is necessary to explain such spectral shift. But in any way, the reduction in intermolecular CT fluorescence can be strongly correlated to the increase in miscibility for the PI/PI blend.

Casting Temperature dependence of miscibility in PI/PI blends

Dependence of miscibility in PI/PI blends on T_{cast} at the stage of PAA was also examined. It is clearly shown that the miscibility depends strongly on T_{cast}. As shown in Figure 3-10, the domain size reduces as T_{cast} increases and finally the blend films become transparent above 120 ℃. On the other hand, the fluorescence reduces drastically as shown in Figure 3-11. The decrease in the intensity with the increase in T_{cast} for PI(BPDA/PDA)/PI(PMDA/PDA) and PI(BPDA/PDA)/PI(PMDA/ODA) is plotted in Figure 3-12.

The dynamic mechanical spectra for PI(BPDA/PDA)/PI(PMDA/ODA) (5/5, T_{cast}=130 ℃) and PI(BPDA/PDA)/PI(PMDA/PDA) (5/5, T_{cast}=120 ℃) are shown in Figure 3-13 (a) and (b), respectively. Figure 3-13 (a) shows a broad β loss peak at 150 ℃ ranging between 80 ℃ (β relaxation of PI(PMDA/ODA)) and 230 ℃ (β relaxation of PI(BPDA/PDA)), and single α loss peak at 330 ℃ ranging between 310 ℃ (α relaxation of PI(BPDA/PDA)) and 360 ℃ (α relaxation of PI(PMDA/ODA)), showing that the blend is miscible. Similarly, Figure 3-13 (b) shows a very broad β relaxation and disappearance of α loss peak due to PI(BPDA/PDA), showing that the degree of mixing in the blend becomes good compared with Figure 3-6(b). The disappearance of α loss peak due to PI(BPDA/PDA) is considered to be due to some reinforced effect due to very rigid PI(PMDA/PDA). Similar reinforced effect was observed in another system, PI(BPDA/ODA)/PI(PMDA/PDA). No α loss peak due to PI(BPDA/ODA) is observed in the blend, contrary to the fact that homo PI(BPDA/ODA) shows a clear α loss peak at 290 ℃.[25] Since PI(PMDA/PDA) does not show clear T_g as described above, if phase separation occurs, only α loss peak due to PI(BPDA/ODA) should be observed. This indicates that the blend is miscible so that segmental motions of PI(BPDA/ODA) was suppressed by very rigid PI(PMDA/PDA). Accordingly, the author considers that in PI(BPDA/PDA)/PI(PMDA/PDA) the disappearance of α loss peak due to

PI(BPDA/PDA) is attributed to the increase in the degree of mixing. The connection of the viscoelastic spectra and the fluorescence data shows that the reduction in the CT fluorescence intensity reflects the increase in the miscibility of the PI/PI blends.

The effect of T_{cast} on density of PI/PI blends is shown in Figure 3-14. Although the amount of the density change is small, the shapes of the curves are similar to those of intensity-T_{cast} curves in Figure 3-12 except for the increase in density at 120 or 130 ℃. The decrease in density with the increase in T_{cast} is considered to be the decrease in the intermolecular CTC population due to interpenetration between the component PIs.[25] Thus the intermolecular CT fluorescence reflects sensitively the miscibility of PI/PI blends.

By the way, why the miscibility becomes improved with increasing T_{cast}? The author proposes the following possibility.

(1) The PAA/PAA blends possess UCST (upper critical solution temperature) phase diagram.

(2) Homogeneous state in the PAA/PAA solution is fixed due to rapid evaporation of solvent.

(3) The PAA forming lyotropic liquid crystal melts at higher T_{cast} and becomes isotropic.

It is known that the blends in which both component polymers have sufficiently large $\bar{M}_w$ do not generally show an UCST phase diagram because the entropy change in mixing ΔS_{mix} is little.[13] Since the sudden changes at certain temperature as shown in Figure 3-12 are considered to be transition phenomenon, the third factor may predominantly contribute to the behavior rather than the second. Recently, Whang et al.[26] reported that an aromatic PAA in N-methyl-2-pyrrolidone (NMP) forms lyotropic liquid crystal at room temperature and becomes isotropic more than 80 ℃. Their data supports my consideration mentioned above. However if melting of LC at a higher temperature may bring about the increase in ΔS_{mix} when PAA/PAA solution was cast at higher temperature, the possibility of case (1) remains.

Nature of intermolecular CT fluorescence

As discussed in section 1.1, several wholly aromatic PIs emit intermolecular CT fluorescence when excited at 350 nm and longer wavelength

(450-550 nm). The presence of two excitation bands is consistent with the experimental results of Iida et al. in which photocurrent spectrum of PI(PMDA/ODA) due to CT interaction possesses two bands at approximately 350 and 460 nm.[27]

Wachsman and Frank[28] argued that for PI(PMDA/ODA) the increase in the fluorescence intensity with increasing cure temperature is due to two possibilities. The first is due to an increase in the population of coplanar state between pyromellitimide and diphenyl ether groups by conformational changes (intramolecular CT). The second is due to the formation of fluorescent sandwich structure (intermolecular CT). On the other hand, Erskine et al.[29] found that the long wavelength absorption edge in transmission spectra of Kapton film shifts toward long wavelength with pressure and the observed changes are strictly reversible. They concluded that the long wavelength absorption band is attributed to intermolecular CTC between pyromellitimide and diphenyl ether moieties. Their data strongly support my opinion in which the long wavelength absorption band is due to intermolecular CTC. From the results of this section, it is obvious that the CT fluorescence emitted by short wavelength excitation (350 nm) is also due to intermolecular CT. If the CT fluorescence generates intramolecularly, the fluorescence in PI/PI blends ought to be independent of the blend morphology. Accordingly, it is concluded that both the short and long wavelength excitation bands originate from intermolecular CTC.

CONCLUSIONS

The fluorescence intensity as a function of blend ratio indicates that the miscibility of PI(BPDA/PDA)/PI(PMDA/PDA) is better than that of PI(BPDA/PDA)/PI(PMDA/ODA) because the fluorescence intensity of the former is smaller at the whole blend ratios than that of the latter. This is supported by the results of dynamic mechanical analysis.

The domains in PI(BPDA/PDA)/PI(PMDA/PDA;ODA) reduce successively with increasing PDA content in the copolyimide, and the CT fluorescence intensity of the blends decreases successively.

It was clearly shown that as T_{cure} increases the miscibility of PI(BPDA/PDA)/PI(PMDA/ODA) and PI(BPDA/PDA)/PI(PMDA/PDA) increases, and the density and the fluorescence intensity drastically decrease. The dynamic mechanical spectra, blend morphologies and the change in density indicate that the reduction in the intermolecular CT fluorescence intensity correlates strongly to the increase in the degree of mixing in the binary

blends composed of fluorescent PI and non-fluorescent PI. This method is useful for the qualitative evaluation of the miscibility for PI/PI blends having very rigid polymer chains.

REFERENCES

1. M.Kochi, T.Uruji, T.Iizuka, I.Mita and R.Yokota, J.Polym.Sci., C, 25, 441 (1987).
2. R.Yokota, R.Horiuchi, M.Kochi, H.Soma and I.Mita, J.Polym.Sci., C, 26, 215 (1988).
3. M.Takayanagi, T.Ogata, M.Morikawa and T.Kai, J.Macramol.Sci.Phys., B17(4), 591 (1980).
4. W.F.Hwang, D.R.Wiff, C.L.Benner and T.E.Helminiak, J.Macromol.Sci.Phys., B22(2), 231 (1983).
5. S.Numata, N.Kinjo and D.Makino, Polym.Eng.Sci., 28, 906 (1988).
6. (a) S.Stankovic, G.Guerra, D.J.Williams, F.E.Karasz and W.J.MacKnight, Polym.Comm., 29, 14 (1988).
   (b) G.Guerra, S.Choe, D.J.Williams, F.E.Karasz and W.J.MacKnight, Macromolecules, 21, 231 (1988).
   (c) G.Guerra, D.J.Williams, F.E.Karasz and W.J.MacKnight, J.Polym.Sci., B, 26, 301 (1988).
   (d) L.Leung, D.J.Williams, F.E.Karasz and W.J.MacKnight, Polym.Bull., 16, 457 (1986).
7. C.B.Bucknall and A.H.Gilbert, Polymer, 30, 213 (1989).
8. J.E.Harris and L.M.Robson, J.Appl.Polym.Sci., 35, 1877 (1988).
9. J.M.Adduchi, "Polyimides", (Ed. K.L.Mittal), Plenum Press, N.Y., 1984, Vol 2, p.1023.
10. P.M.Tanunina, Z.I.Gomoreva, E.G.Lur'e, V.D.Vorob'ev, M.L.Dobrokhotova, E.I.Efimova and T.I.Safronova, Plast.Massy., No.9, 45 (1975).
11. V.Ye.Smirnova, M.I.Bessonov, T.I.Zhukova, M.M.Koton, V.V.Kudryavtsev, V.P.Sklizkova and G.A.Lebedev, Polym.Sci.U.S.S.R., 24, 1375 (1982).
12. Y.Yamamoto, M.Kitahashi and S.Etoh, Polym.Prepr.Jpn., 37, 2396 (1988).
13. "Polymer Blends" (Ed. S.Akiyama, T.Inoue and T.Nishi), CMC Press, Japan, 1981.
14. (a) S.N.Semerak and C.W.Frank, Macromolecules, 14, 443 (1981).
   (b) J.W.Thomas and C.W.Frank, Macromolecules, 18, 1034 (1985).
15. (a) F.Amrani, J.M.Hung and H.Morawetz, Macromolecules, 13, 649 (1980).
   (b) F.Mikes, H.Morawetz and K.S.Dennis, Macromolecules, 17, 60 (1984).
16. G.H.Frendrickson and E.H.Helfand. Macromolecules, 19, 2601 (1986).
17. (a) J.L.Halarly, J.M.Ubrich, J.Nunzi, L.Monnerie and R.S.Stein, Polymer, 25, 956 (1984).
   (b) J.M.Ubrich, F.B.C.Larbi, J.L.Halarly, L.Monnerie, B.J.Baner and C.C.Han, Macromolecules, 19, 810 (1986).
18. D.A.Holden and J.Strauss, Polym.Eng.Sci., 28, 1373 (1988).

19. B.Albert, R.Jerome, P.Teyssie, G.Smyth, N.G.Boyle and V.J.McBrierty, Macromolecules, 18, 388 (1985).
20. (a) M.Hasegawa, M.Kochi, I.Mita and R.Yokota, J.Polym.Sci., C, 27, 263 (1989).
(b) M.Hasegawa, M.Kochi, I.Mita and R.Yokota, Eur.Polm.J., 25, 349 (1989).
21. M.Kochi, H.Shimada and H.Kambe, J.Poly.Sci., Poly.Phys.Ed., 22, 1979 (1984).
22. M.Ree, D.Y.Yoon and W.Volksen, ACS Spring Conf., Polym.Mat.and Sci. Eng., 60, 179 (1989).
23. L.Bohn, "Polymer Handbook" (Ed. J.Brandrup and E.H.Immergut), 2nd Ed., Willey Press, N.Y., 1975, p. III -211.
24. "Polyimides" (Ed. M.I.Bessonov, M.M.Koton, V.V.Kudryavtsev, and L.A.Laius), Plenumm Press, N.Y.1987, p.194.
25. R.Yokota, Doctoral thesis, The University of Tokyo, 1990, p.159.
26. W.T.Whang and S.C.Wu, J.Plym.Sci., A, 26, 2749 (1988).
27. K.Iida, M.Waki, S.Nakamura, M.Ieda and G.Sawa, Jpn.J.Appl.Phys., 23, 1573 (1984).
28. E.D.Wachsman and C.W.Frank, Polymer, 29, 1191 (1988).
29. D.Erskine, P.Y.Yu and S.C.Freilich, J.Polym.Sci., C, 26, 465 (1988).

Table 3-1 Weight-average molecular weights Mw of PAAs and extinction coefficients and densities of PI films.

Symbol	$\bar{M}w$	$^{a}\varepsilon_{350}$	Density(g/cm^3)
PI(BPDA/PDA)	75000	2600	1.4239
PI(PMDA/ODA)	110000	1200	1.3807
PI(PMDA/PDA)	89000	1600	1.5107
PI(PMDA/PDA:ODA)			
PDA:ODA=10:0	89000	1600	1.5107
9:1	43000	1600	1.4944
8:2	45000	1500	1.4677
7:3	40000	1300	1.4475
5:5	30000	1300	1.4139
3:7	67000	1200	1.3990
2:8	59000	1200	1.3934
0:10	40000	1200	1.3805

[a]The values of ε depend on the cure temperature.

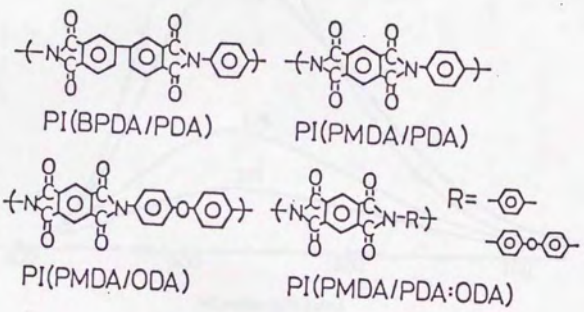

Figure 3-1 The chemical structures and symbols of PIs used.

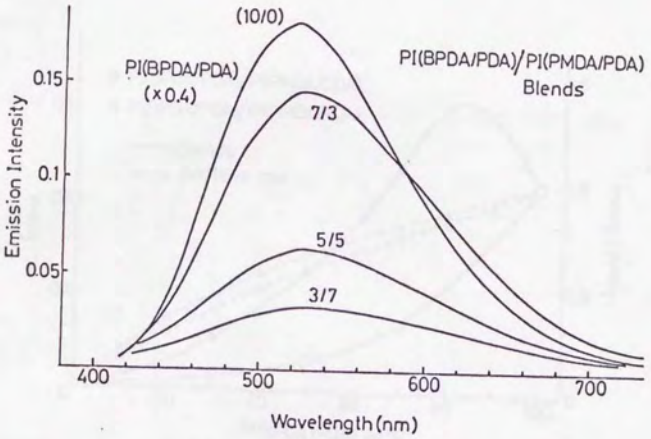

Figure 3-2 The fluorescence spectra of PI(BPDA/PDA)/PI(PMDA/PDA) blends as a function of blend ratio.

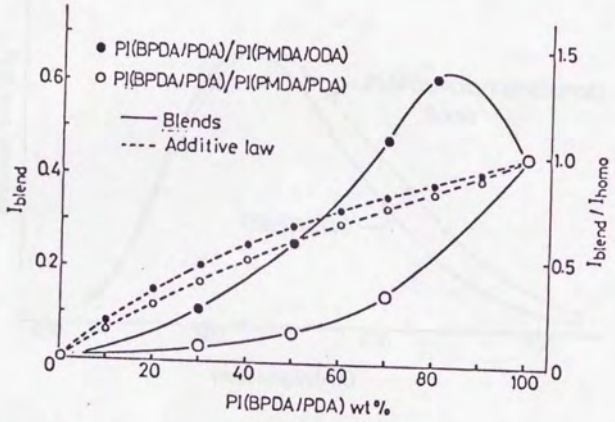

Figure 3-3 The change in fluorescence intensity for PI(BPDA/PDA)/PI(PMDA/PDA)(a) and PI(BPDA/PDA)/PI(PMDA/ODA)(b) against blend ratio.

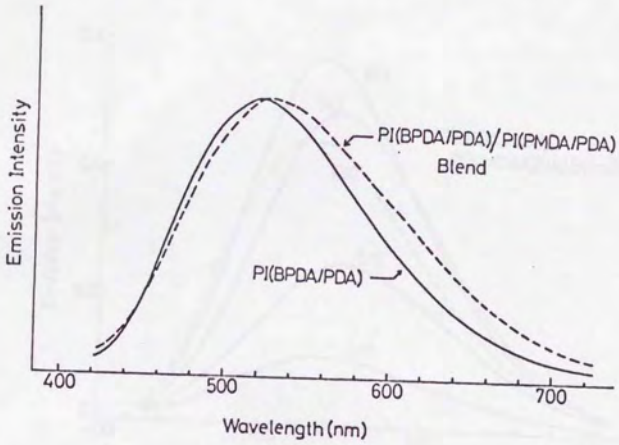

Figure 3-4 The fluorescence spectra of PI(BPDA/PDA)/PI(PMDA/PDA)(5/5) blend and homo PI(BPDA/PDA) normalized at 525 nm.

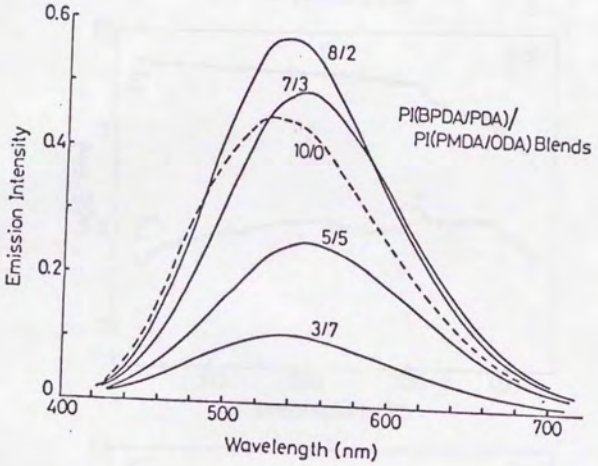

Figure 3-5 The fluorescence spectra of PI(BPDA/PDA)/PI(PMDA/ODA) blends as a function of blend ratio.

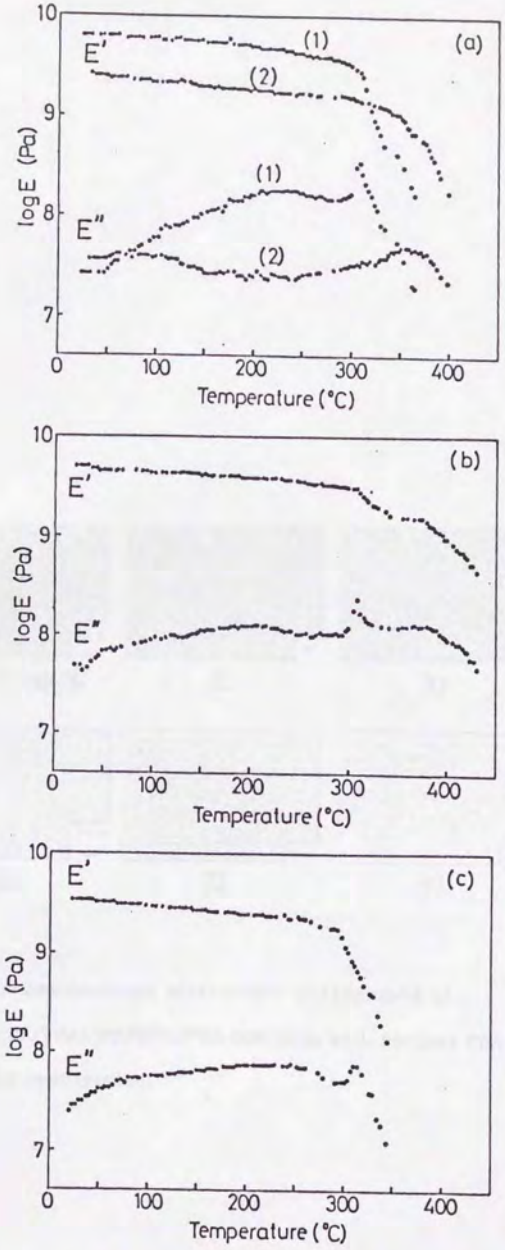

Figure 3-6 The dynamic mechanical spectra of homo (1)PI(BPDA/PDA) and (2) homo PI(PMDA/ODA)(a), PI(BPDA/PDA)/PI(PMDA/PDA)(5/5)(b) and PI(BPDA/PDA)/PI(PMDA/ODA)(5/5)(c). T_i=step250 ℃, T_{cast}=50 ℃

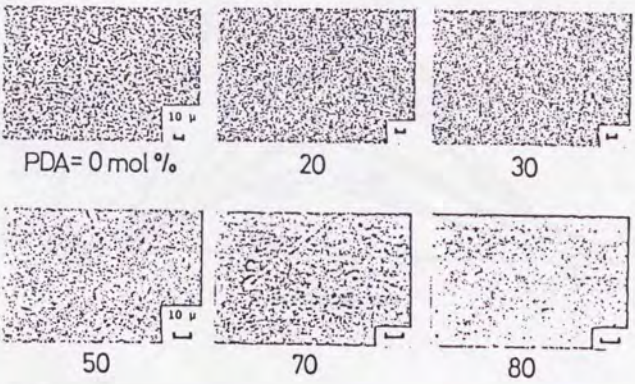

Figure 3-7 The phase-contrast microscopic photographs of PI(BPDA/PDA)/PI(PMDA/PDA:ODA)(5/5) with various PDA content in the copolyimide.

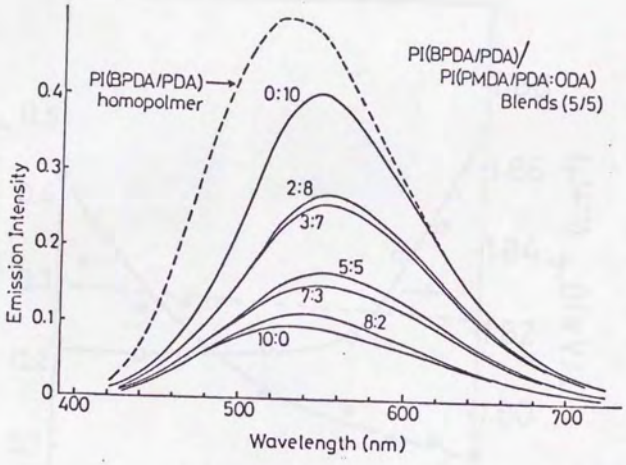

Figure 3-8 The fluorescence spectra of PI(BPDA/PDA)/PI(PMDA/PDA:ODA) (5/5) blends as a function of PDA content in the copolyimide.

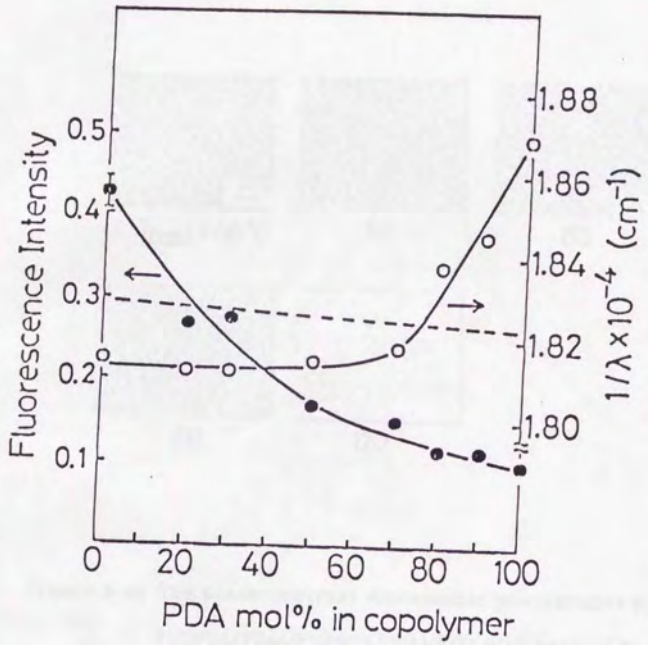

Figure 3-9 The changes in fluorescence intensity and peak position for PI(BPDA/PDA)/PI(PMDA/PDA:ODA)(5/5) against PDA content in the copolyimide.

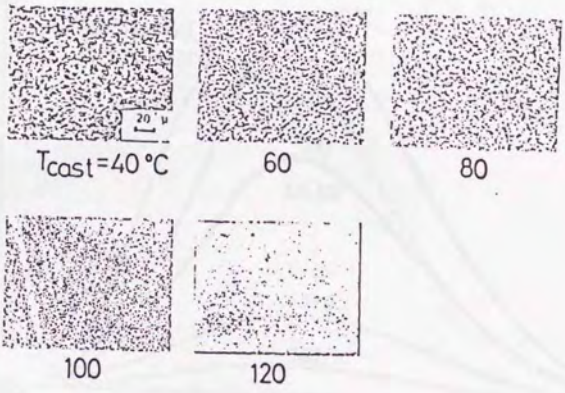

Figure 3-10 The phase-contrast microscopic photographs of PI(BPDA/PDA)/PI(PMDA/ODA)(5/5) with various T_{cast}.

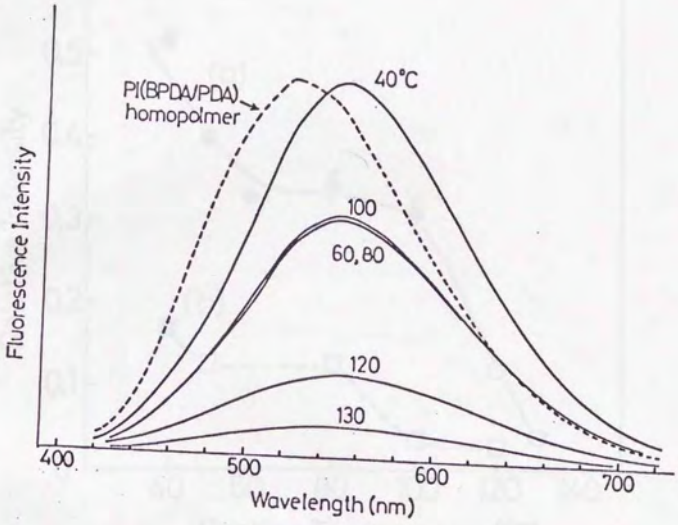

Figure 3-11 The fluorescence spectra of PI(BPDA/PDA)/PI(PMDA/ODA) (5/5) blends as a function of T_{cast}.

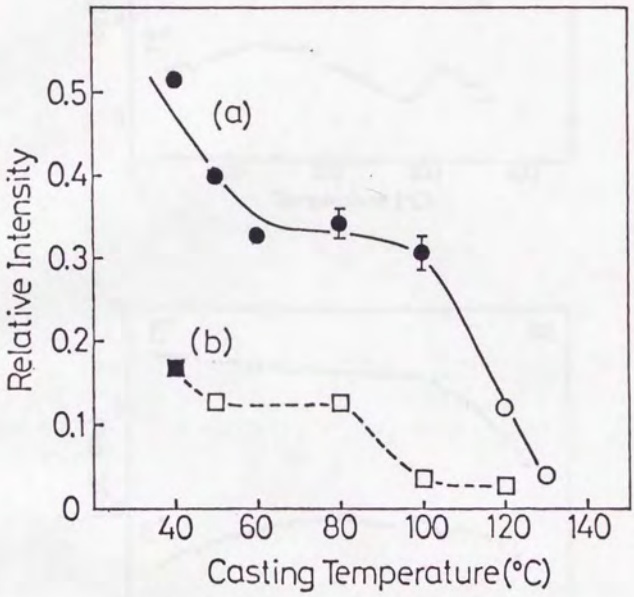

Figure 3-12 The changes in fluorescence intensity for PI(BPDA/PDA)/PI(PMDA/ODA)(5/5)(a) and PI(BPDA/PDA)/PI(PMDA/PDA)(5/5)(b) against T_{cast}. Open and filled marks denote optically clear and cloudy blend film, respectively.

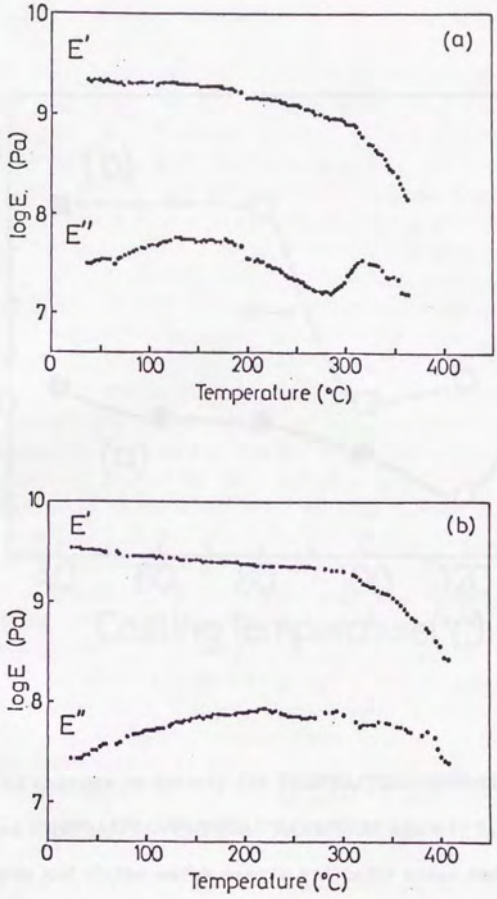

Figure 3-13 The dynamic mechanical spectra of PI(BPDA/PDA)/PI(PMDA/ODA) (5/5, T_{cast}=130 ℃)(a), and PI(BPDA/PDA)/PI(PMDA/PDA) (5/5, T_{cast}=120 ℃)(b).

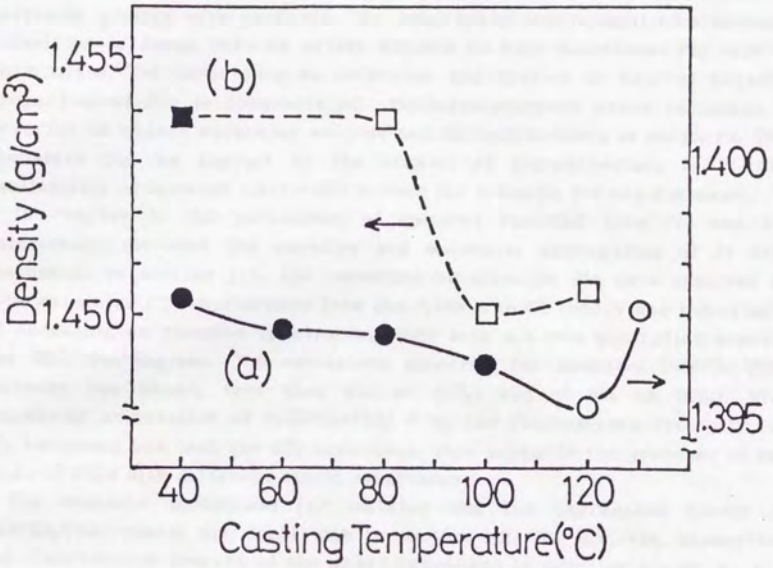

Figure 3-14 The changes in density for PI(BPDA/PDA)/PI(PMDA/ODA)(5/5)(a) and PI(BPDA/PDA)/PI(PMDA/PDA)(5/5)(b) against T_{cast}. Open and filled marks denote optically clear and cloudy blend film, respectively.

SUMMARY

In general introduction, the history and the present condition of polyimide studies were surveyed. The remarkable development of electronic industries in Japan induced active studies on high functional PIs such as phtoresists. The importance of molecular aggregation to control physical properties of PIs is demonstrated. Photoluminescence probe technique is powerful to detect molecular motions and microstructures in polymers. This technique can be applied to the studies of microstructure in PI. The availability of internal (intrinsic) probes for aromatic PIs was discussed.

In chapter 1, the mechanisms of emission radiated from PIs and the relationship between the emission and molecular aggregation of PI were discussed. In section 1.1, the emissions of aromatic PIs were assigned as intermolecular CT fluorescence from the fitness to CT theory and the effects of annealing on emission spectra together with u.v.-vis absorption spectra and DSC thermograms. The excitation spectrum for annealed PI(BPDA/PDA) includes two bands, less than 350 nm (CT_1) and at 465 nm (CT_2). With increasing orientation of PI(BPDA/PDA) film, the fluorescence intensity for CT_1 increases but that for CT_2 decreases. This supports the presence of two kinds of CTCs with different steric structures.

The emission mechanisms for isolated and the aggregated states of PI(BPDA/PDA) chains are dealt with in section 1.2. The u.v.-vis. absorption and fluorescence spectra of the model compounds in solution shows π, π^* transition due to benzimide at 310-330 nm and n, π^* transition due to imide carbonyl group at 340-380 nm. Biphenyldiimide units are mainly excited by 350 nm. The fluorescence of Biphenyldiimide units peaking at 380 nm in toluene (at 430 nm in HFP) is quenched by phenyl group on imide nitrogen, suggesting the existence of an effective deactivation process via intramolecular charge-transfer state. The intermolecular CT structures in solid PI were also discussed using a model compound. No attractive interaction between pyromellitdiimide units was suggested in amorphous PI(PMDA/MDCA) film by comparing electronic spectra of the model compound in solution and in PMMA with those of the PI. Main interaction in aromatic PIs is of CT nature. Energy transfer in PI(BPDA/PDA) solid was examined using steady-state fluorescence depolarizaton technique. With the increase in cure temperature, the quantum yield of CT fluorescence increases and fluorescence polarization decreases, indicating the increase in energy migration efficiency between CTCs.

In chapter 2, the reactions of PAA which controls physical properties of corresponding PI were treated. In section 2.1, Isothermal imidization of an

PAA(BPDA/PDA) in solution and solid state was monitored using intermolecular CT fluorescence which is sensitive to molecular packing as discussed in chapter 1. When imidized at 110 ℃ in solution (10 wt%), the fluorescence of the as-cast films reduced rapidly and became very weak at about 30% in conversion. In solid state, as imidization proceeded, the fluorescence of the PAA reduced rapidly as well as in solution, and then the CT fluorescence of the PI increased. The relationship between the intensity and the degree of imidization clearly shows that the fluorescence intensity at a same conversion depends strongly on imidization temperature (T_i). For example, when imidized at 150 ℃ the intensity increases only slightly as the reaction proceeds, while at higher T_i such as 230 or 270 ℃ the intensity increases rapidly. This indicates that the degree of molecular order in the PI formed on isothermal imidization depends strongly on T_i.

In section 2.2, amide exchange reaction of PAA(PMDA/ODA) in solution at 0-60 ℃ was discussed. The molecular-weight changes for the PAA including 1-aminopyrene APy) were monitored using viscometry and light-scattering(LS) measurements. The addition of APy into PAA solution and the increase in storage temperature accelerates $\bar{M}_w$ drop. Apparent activation energies(E_a) for scission of PAA chains were about 13 kcal/mol both in PAA/DMAc and PAA/APy/DMAc. When stored at 60 ℃ for a week, number of scission per polymer chain in PAA/DMAc is about 2, but is about 5 in PAA/DMAc with a large amount of APy. It was concluded from the dependence of $\bar{M}_w$ drop on APy concentration that the exchange reaction between different PAA molecules during storage of PAA/PAA solution may scarcely occur under the condition(storage time and temperature) used for preparation of PAA/PAA blends.

In chapter 3, the miscibility of PI/PI blends was examined with intermolecular CT fluorescence discussed in chapter 1 and section 2.1. Two blend systems, transparent PI(BPDA/PDA)/PI(PMDA/PDA) and cloudy PI(BPDA/PDA)/PI(PMDA/ODA) were mainly treated. For the former blend, the fluorescence intensity rapidly decreases with the addition of non-fluorescent PI(PMDA/PDA) into fluorescent PI(BPDA/PDA), while for the latter blend the intensity increases first then decreases with the addition of non-fluorescent PI(PMDA/ODA), showing that the CT fluorescence is strongly affected by the miscibility of the blends. In order to know the relation between the CT fluorescence changes and the miscibility, dynamic mechanical analysis (DMA) and phase-contrast microscopy were also carried out. For the binary blend of PI(BPDA/PDA) with PI(PMDA/PDA;ODA) random copolymer, the blend films become transparent and the fluorescence intensity decreases with increase in PDA content in the copolyimide. This is interpreted as the result in which the CTC formation in PI(BPDA/PDA)

rich-phase was hindered by the non-fluorescent copolyimide. The dependence of the miscibility on casting temperature (T_{cast}) at the stage of PAA was studied. It is clearly shown that the miscibility is strongly affected by T_{cast}. As T_{cast} increases from 40 to 120 or 130 ℃ the domain size reduces and finally the blend films become transparent. The dynamic mechanical spectra for the blends cast at higher temperatures show that the blends are miscible. On the other hand, the CT fluorescence intensity decreases drastically with increasing T_{cast}. These results led to the conclusion that the decrease in the fluorescence intensity reflects sensitively the increase in the degree of mixing for the PI/PI blends composed of fluorescent and non-fluorescent PIs.

Main concern in this thesis is to observe the molecular aggregation of aromatic PIs which affects strongly some physical properties by using the intrinsic intermolecular CT fluorescence. Another interest is the influence of CT interactions in PIs to physical properties (photoconductivity is affected strongly by CT interactions). The author believes that knowledge obtained from this study are will be used for the molecular design and structure control of aromatic PIs.

LIST OF PUBLICATIONS

1. "Molecular Aggregation and Fluorescence Spectra of Aromatic Polyimides"
   M.Hasegawa, M.Kochi, I.Mita and R.Yokota, Eur.Polym.J., 25, 349 (1989).
   (Section 1.1)
2. "Charge-Transfer Emission Spectra of Aromatic Polyimides"
   M.Hasegawa, M.Kochi, I.Mita and R.Yokota, J.Polm.Sci.: C, 27, 263 (1989).
   (Section 1.1)

2. "Excitation Energy Transfer in Slid Polyimide and Electronic Spectra of Model Compounds of Polyimide"
   M.Hasegawa, T.Yamashita, Q.Jin, K.Horie, M.Kochi, R.Yokota and I.Mita,
   in preparation. (Section 1.2)

3. "Isothermal Imidization of an Aromatic Polyimide Precursor Studied by Fluorescence Spectroscopy"
   M.Hasegawa, H.Arai, I.Mita and R.Yokota, Polym.J., 22, 875 (1990).
   (Section 2.1)

4. "On Amide Exchange Reaction of Polyimide Precursor"
   M.Hasegawa, Y.Shindo, T.Sugimura, R.Yokota, K.Horie and I.Mita,
   J.Polym.Sci.: A, submitted. (Section 2.2)

5. "Miscibility of Polyimide/Polyimide Blends and CT Fluorescence Spectra"
   M.Hasegawa, M.Kochi, I.Mita and R.Yokota, Polymer, in press.
   (Chapter 3)

6. "Compatibility of PI/PI Blends and CT Fluorescence Spectra"
   M.Hasegawa, M.Kochi, I.Mita and R.Yokota, Proceedings of "Polymer for Microelectronics", Elsevier, 1990. (Chapter 3)

ACKNOWLEDGEMENT

The author would like to thank Professor Itaru Mita for his constant guidance in all phases of this work.

The author thanks Professor Kazuyuki Horie, Dr.Masakatsu Kochi, and Dr.Rikio Yokota for their helpful comments on experimental techniques. The author learned methodology and philosophy in study from them.

Gratitude is also extended to Dr.Yoichi Shindo and Dr.Tokuko Sugimura for providing a position at Toho University to me by consuming significant effort.

Thanks are given to Dr.Takuya Naito and Dr.Takashi Yamashita for their stimulative and useful comments and to collaborators, Ms.Hisae Arai and Ms.Nobuko Sato for their industrious and active works and also to Dr.Tomiki Ikeda of Tokyo Institute of Technology, Mr.Yasuhiro Fujita of Hitachi Kasei Polymer, and Mr.Miura of Institute of Space and Astronautical Science for their experimental supports.

The author is grateful to his collaborators in Mita, Horie lab. for their friendship. I think that free and modest atmosphere in our laboratory make possible to have carried out this work.

Finally, the author would like to thank his wife, Nana Hasegawa for her constant encouragement and economical support.

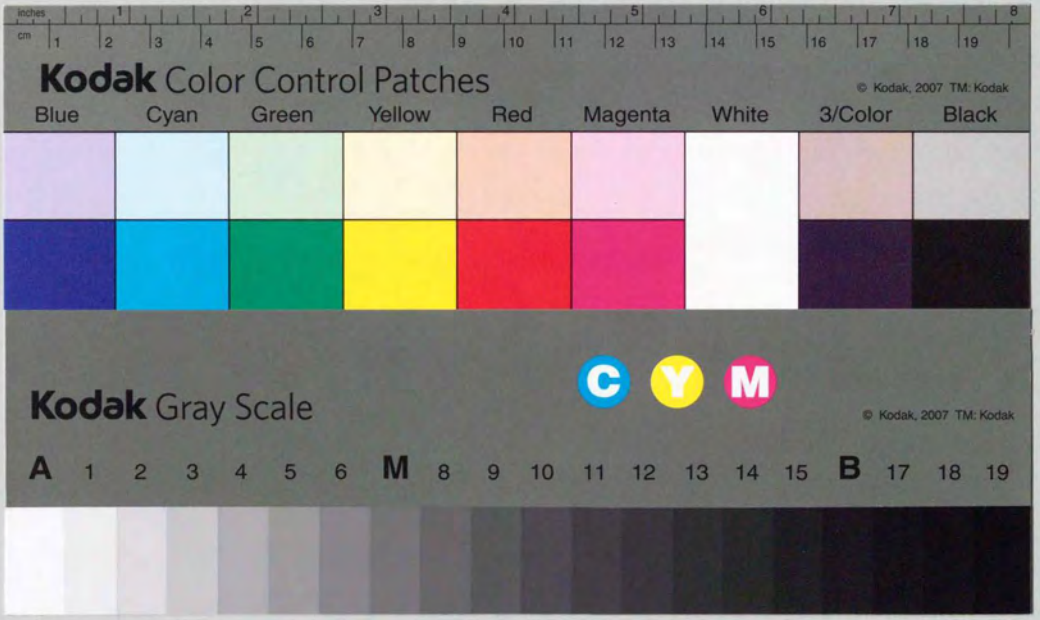
inches
cm
Kodak Color Control Patches
© Kodak, 2007 TM: Kodak
Blue
Cyan
Green
Yellow
Red
Magenta
White
3/Color
Black
Kodak Gray Scale
C
Y
M
© Kodak, 2007 TM: Kodak
A 1 2 3 4 5 6 M 8 9 10 11 12 13 14 15 B 17 18 19